Title
Frontal and Basal Ganglia Contributions to Memory and Attention

Author
Voytek, Bradley

Publication Date
2010

Peer reviewed|Thesis/dissertation

Frontal and Basal Ganglia Contributions to Memory and Attention

by

Bradley Thomas Voytek

A dissertation submitted in partial satisfaction of the requirements for the degree of

Doctor of Philosophy

in

Neuroscience

in the

Graduate Division

of the

University of California, Berkeley

Committee in charge:

Professor Robert T. Knight, Chair
Professor Richard B. Ivry
Professor Michael Silver
Professor Stephen P. Hinshaw

Spring 2010

Frontal and Basal Ganglia Contributions to Memory and Attention

by

Bradley Thomas Voytek

Abstract

Frontal and Basal Ganglia Contributions to Memory and Attention

by

Bradley Thomas Voytek

Doctor of Philosophy

in Neuroscience

University of California, Berkeley

Professor Robert T. Knight, Chair

Herein I research the role of the basal ganglia and prefrontal cortex in visual working memory and attention by examining patients with focal, unilateral lesions to these brain regions. By combining patient-based behavioral research with scalp electroencephalography (EEG) I study the specific deficits caused by focal frontal brain lesions and explore the effects that such lesions have on diverse cortical network functioning related to working memory and attention. Furthermore, I investigate the role that neuroplasticity plays in compensating for damage to the prefrontal cortex as relates to working memory and attention.

By examining the localization of cognitive functions in the brain and how these seemingly fixed locations may reflect flexible neural networks that can change in response to brain damage, I show how the intact homologous prefrontal cortex compensates for the damaged hemisphere in patients with unilateral prefrontal lesions when these patients are cognitively challenged. I then expand on this notion of cognitive compensation by demonstrating that behavioral performance is reduced when we block the fidelity of visual information transferred from the damaged to the intact hemisphere. Finally, in a methodological analysis of a unique patient cohort, I address the advantages and limitations of scalp EEG.

Defining specific brain regions by function does not necessarily inform us about how cognitive functions arise or change and adapt during development and in response to brain injury or disease. Rather, I argue that we must adopt a dynamic view of cognition wherein cortical regions are but nodes in fluctuating, malleable networks that give rise to the complexities of human behavior.

Table of Contents

Acknowledgements

Neuroscience is unlike the other physical sciences. Ours is a field that bridges the scientific method with the human experience: we do not just stand upon the shoulders of giants; we stand also in a field with countless forgotten individuals. Although Galen, Willis, Penfield, Sacks and others are giants in the truest sense, the patients they studied and worked with are the real knowledge-givers. Our understanding of the functional localization and relationships between cognition, emotion, development, and perception are heavily informed by our observations of and conversations with the people who have experienced some form of neuropathy. Without these people our field would not be what it is today, and this thesis would not exist. Thus, I foremost dedicate the philosophy of this thesis to both the giants and the patients of my field: it is for them—and because of them—that this work could be accomplished.

First and foremost, thank you Jessica for your apparently endless understanding, love, and compassion for your sometimes crazy and overworked husband. We have walked together into our futures. You have walked before me when I needed you, behind me when I didn't, but beside me, always, just as we vowed. For more than 7 years you have assisted me in every way: emotionally, academically, and ridiculously. No language exists to communicate my feelings for what you mean to me.

Thank you to everyone who provided me with conversations on the science, translation, and ontology of my work. While there are dozens of individuals that to whom I am grateful, I must give specific thanks to "Paco" Francisco Barceló, Aurelie Bidet-Caulet, Sonia Bishop, Maya Cano, Ryan Canolty, Wes Clapp, Cat Dam, Matar Davis, Roby Duncan, Erik Edwards, Adeen Flinker, Josh Hoffman, Christina Karns, Sara LaHue, Brian Miller, Kai Miller, Torgeir Moberget, Lavi Secundo, Amitai Shenhav, Avgusta Shestyuk, Timothy

Verstynen, and Ed Vogel. Also, thank you to my friends who have stuck by my side and helped keep me happy and amused: Sarah Cate Boone, Josh Burkett, Paul Byers, Curtis Chambers, Tsiao-Mei Misha Cheung, Matt deWit, David Higgins, Sheila Katz, Bryan Pearson, BW Mike Robrock, Erica Warp, Richard Warp, Andrea Weinstein, and many, many others.

My friends and family have been amazing in supporting me these past 6 years and for understanding that sometimes it's okay to trade poor pay for the right to work on my passions. I get paid to think (about thinking!) and that's an extremely amazing thing.

Thank you to my committee—Rich Ivry and Michael Silver—for your patience, advice, and the occasional useful interrogation, and to Kati Markowitz for her amazing and (usually) tireless organization and assistance.

Bob Knight, you have been the ideal mentor for me. Thank you so very much for your guidance and mentorship: you have been a unique advisor and I couldn't have asked for a more interesting and fun 6 years. You've got an amazing lab and I'm going to be sad to leave.

The true heart of this work, however, is dedicated to my grandfather, Fiske W. Isler, III. His experience with Parkinson's disease and my experience in watching him decline during that time is what ultimately led me to neuroscience and, more specifically, to my interest in translational research. I miss you very much, and I'm sorry that your twilight years were so difficult. But thank you for opening the door for me to understand what it means to be human.

Chapter 1

Introduction

1.1 Background and Significance

How do we maintain a stable percept of the world in the face of the powerful drive for neuroplasticity in both health and disease? This dichotomy forms one of the most fundamental unanswered questions of neuroscience concerns the balance between the dynamic, plastic underpinnings of our neurobiology with the relative stability of our cognition. The brain undergoes massive changes in size, morphology, and connectivity during normal development (Gogtay, et al., 2004) and aging (Sowell et al., 2003) as well as in response to brain injury (Alsott et al., 2009; Carmichael 2003), yet we can maintain a relatively stable sense of cognition and self as we grow older. Almost every human brain, each with trillions of neurons and glia, develops similarly enough despite the wide variation in environment and experience that neuroscientists can discuss such general phenomena as "memory" and "attention". However, within the bounds of this stability there exists a wide range of variability and capacity for change.

The aim of this thesis is to investigate the neuroanatomical and behavioral origins of working memory and attention and to examine the role that neuroplasticity plays in compensation after brain damage. Because I make extensive use of scalp electroencephalography (EEG) in these projects I conclude with an analysis of the scalp EEG signal in a group of patients who had undergone a surgical hemicraniectomy—a

procedure that involves the long-term removal of part of the calvaria of the skull. In order to examine the neuroanatomical underpinnings of working memory and attention I specifically worked with patients with unilateral prefrontal cortical (PFC) or basal ganglia (BG) lesions. I sought to dissociate the contributions of these brain regions to executive cognitive functions and document the role of compensatory neuroplasticity in patients with PFC lesions. By making use of scalp EEG I could further scrutinize the role that the PFC and BG play in working memory and attention networks that include interactions with posterior visual extrastriate regions of the neocortex. Furthermore, I could examine the time-course of compensatory processes and investigate functional communication between cortical networks.

The ultimate goal of these studies—and the reason why I choose to work with people with brain damage—is to make use of the information learned from this group of subjects to benefit future patients who have experienced neuropathology. Ideally what we have learned here can be incorporated into the greater medical realm to help guide treatment and inform translational research.

1.2 Lesion Studies of Human Cognition

Localization of cortical function poses a major problem in modern neuroscience (Brett, Johnsrude, & Owen, 2002). First is the problem of comparing localization data across methodologies and across subjects; rectifying findings from various neuroimaging methodologies—each with their own limitations and underlying assumptions—with computational, lesion, and animal studies. This is a daunting prospect for any investigator. Second is the inherent morphological variability across subjects; currently, any claims to cortical functional specificity are probabilistic claims in that—barring direct cortical stimulation mapping—one cannot guarantee that a specific cortical region plays a specific functional role. For example, direct cortical stimulation mapping suggests frontal, temporal, and parietal sites are all involved in language functions, yet the cytoarchitectonic localization of these sites differ a great deal across subjects (Sanai, Mirzadeh, & Berger, 2008). These problems are not just theoretical or didactic issues: neurosurgeons performing cortical tissue resections must use intraoperative cortical stimulation mapping to ensure that the cortical tissue to be removed is not "eloquent" (language or motor) cortex. Such stimulations are performed while the patient is awake and performing cognitive and behavioral tasks. During this testing period the surgeon electrically stimulates different brain regions to monitor speech arrest or motor engagement. This method is still used today precisely because of the wide variability in functional localization and cortical morphology across subjects.

Although the functional localization story appears bleak at the level of a single individual, cerebral regions of functional localization are clearly observed when averaged across a group of subjects with neuroimaging techniques such as functional magnetic resonance imaging (fMRI) and positron emission tomography (PET). Most studies rely upon the idea of cognitive subtraction, originally established in reaction time studies by Franciscus Donders (Donders, 1869). The underlying assumption in these studies is that activity in different brain networks alters in a task-dependent manner that becomes evident after averaging many event-related responses and comparing those against a baseline condition. Deviations from this baseline reflect a relationship to the change in neuronal processing

demands required to perform the task of interest. Although both the cognitive subtraction method (Friston et al., 1996) and assumptions regarding baseline activity (Gusnard & Raichle, 2001) have their own problems, these methods provide details of functional localization that can then be tested and corroborated using other methodologies, including lesion studies. However such functional localization studies are just a starting point and the current effort to map a human connectome (Sporns, Tononi, & Kötter, 2005) will provide researchers with the roadmap necessary in the effort to examine changes in large-scale cortical network activity during cognition.

While functional neuroimaging techniques such as fMRI and PET have greatly advanced our understanding of regional specificity, the lesion method provides the strongest case in the argument for causality; i.e., brain region *A* can almost be guaranteed to play an important role in function *X* if a lesion to *A* impairs function *X*. Research on humans with focal brain lesions has heavily informed our understanding of which brain regions contribute to specific behavioral, sensory, and cognitive functions (Rorden & Karnath, 2004). For example, because PFC lesions lead to working memory deficits, the PFC can be said to play an important, necessary role within working memory related networks. Research using scalp EEG has shown that unilateral PFC lesions cause lateralized deficits in top-down modulation of visual attention (Barceló, Suwazano, & Knight, 2000; Yago et al., 2004), which makes EEG a powerful tool for investigating the temporal dynamics of the effects of a defined brain lesion on cognitive networks.

1.3 Function Recovery and Compensation

While the underlying notion of brain damage disrupting function is fairly obvious—damaging parts of a machine prevent the machine from working optimally—the specific effects of brain damage are neither obvious nor always predictable. This fuzziness in predictability is further confounded by the fact that the brain is not a static machine, but rather a fluctuating (plastic), self-repairing organ (Cramer, 2008). There are several factors that prohibit accurate prediction of which deficits will manifest after a given brain lesion because we are still uncertain with regards to the accuracy of regional localization of function. Furthermore, the probability distribution of functional localization across subjects is broad, especially across cortical association areas (Sanai, Mirzadeh, & Berger, 2008). However association cortex is related to many behavioral processes and thus the importance of distributed cortical networks in behavior and subsequent recovery cannot be ignored. Predicting the course of recovery from brain damage is further confounded by a lack of understanding about the extent and time course of recovery possible across different regions of the central nervous system.

Brain damage has an immense personal and societal cost yet the neural mechanisms underlying recovery are poorly understood. Damage to the human PFC results in attention (Barceló, Suwazano, & Knight, 2000) and memory deficits (Tsuchida & Fellows, 2009) with variable levels of recovery observed in individual patients. However, unlike damage to primary motor or sensory cortices which results in overt deficits such as hemiparesis or hemianopsia, long-term deficits in working memory and attention after unilateral PFC damage are often less dramatic. This basic clinical observation suggests that cognitive processes supported by frontal association cortex are more plastic and likely to recover

(though our measurements of cognitive functions may also be less precise and reliable than for primary sensory or motor functions). EEG and fMRI studies report that neurological patients who have recovered from motor, language, or attention deficits show increases in activity in homologous cortical regions in the non-lesioned hemisphere and in perilesion cortex (Ward et al., 2007; Johansen-Berg et al., 2002; Blasi et al., 2002; Corbetta et al., 2005; He et al., 2007; Nudo, 2007; Chao & Knight, 1998; Rosahl & Knight, 1995). However, cognitive compensation after PFC damage is less understood.

Neural plasticity is critical for functional recovery after brain damage with improvement possible even 20 years after the initial injury (Bach-y-Rita, 1990). There are several theories of recovery of function, including: cortical compensation by perilesion and intact homologous brain regions (Wundt, 1902) or subcortical (Van Vleet et al., 2003) structures; diaschisis reversal (von Monakow, 1969); unmasking (Lytton et al., 1999); distributed cortical representations (Jackson, 1958); and axonal sprouting and neurogenesis (Carmichael et al., 2001). Many of these theories predate neuroimaging and were based on clinical observations of patients with brain damage. These early theories of recovery logically concluded that recovery must be mediated by intact, undamaged brain regions (Kolb, 1992). Given the number of brain regions needed to support visual attention and working memory, it is not unreasonable, given the variety of recovery theories, to hypothesize that recovery could be supported by the any part of the intact network. However, the PFC plays an important role in cognitive networks by biasing information flow to favor positive behavioral outcomes (Miller & Cohen, 2001) and may play a privileged role in cognitive compensation. We examine the role of the intact PFC in compensation by recording scalp EEG from patients performing a cognitively demanding visual working memory task. We then extend these results by preventing the flow of visual information from the damaged to the intact hemisphere, thus demonstrating that we can reduce the compensatory efficacy of the intact PFC.

1.4 Non-invasive Electrophysiology

Because scalp EEG plays such a prominent role in my thesis—and because my future work will incorporate subdural electrophysiological recordings from the human brain—I conducted an experiment to characterize the differences between the two signals. That is, how does the skull interfere with the electrophysiological signals I record at the level of the scalp? Scalp EEG was first reported by Hans Berger in 1925 from a 17-year-old boy with electrodes placed over a large surgical skull defect (Berger, 1929; Millett, 2001). These initial recordings were faint due to technical limitations, but for several years EEG was only performed on patients with fissures or surgical holes in their skulls (Millett, 2001; Cobb, Guiloff, & Cast, 1979). As Berger improved his EEG recording technology he was able to acquire EEG from scalp electrodes over the intact skull and recordings from patients with skull defects diminished.

Despite its contributions to human cognitive neuroscience, scalp EEG has well-known limitations (Luck, 2005; Nunez & Srinivasan, 2005). Scalp EEG has poor spatial localization and is susceptible to contamination from noise sources such as muscle activity that limit reliable acquisition of high-frequency neural activity. Further, the spectral

amplitude of EEG signals is reduced as a function of frequency resulting in substantial reductions in higher frequency power at scalp electrodes distant from the cortical surface.

EEG in subjects with skull defects has been previously reported as the "breach rhythm" (Cobb, Guiloff, & Cast, 1979; Cobb & Sears, 1960). These studies showed that breach rhythm signals were higher in overall power compared to normal scalp EEG in agreement with our findings. These earlier studies examined the effects of the skull on scalp electrical recordings showing that the skull acts as a spatial filter smoothing underlying signals (Cobb & Sears, 1960) and averaging electrical potentials from an extended patch of cortex (DeLucchi, Garoutte, & Aird, 1962). Because of the improved signal quality and spatial localization, many researchers are now recording EEG signals from electrodes implanted directly on the cortical surface of patients undergoing brain surgery, a technique known as electrocorticography (ECoG). These ECoG signals have improved power, increased bandwidth extending into the γ_H (>60 Hz) range, and improved spatial localization compared to scalp EEG. Practically, researchers are making use of the improved signal from invasive recordings to drive brain-machine interface (BMI) devices to assist people with paralysis (Hochberg et al., 2006; Miller et al., 2007).

Intracranial and scalp EEG and MEG research indicates that task-relevant γ_H oscillations are generated in each of these tasks (Ball et al., 2008; Crone et al., 1998b; Dalal et al., 2008; Edwards et al., 2005). It is important to emphasize that these high-frequency oscillations are emerging as important markers for a variety of cognitive and behavioral functions. Recent evidence from human intracranial electrocorticography (ECoG) shows that the amplitude of ongoing high gamma (80-150 Hz) oscillations is modulated by the phase of low frequency theta (4-8 Hz) (Mormann et al., 2005, Canolty et al., 2006) and alpha (8-12 Hz) (Osipova et al., 2008) oscillations within and between (Bruns & Eckhorn, 2004) electrodes. Such cross-frequency coupling is intriguing given current hypotheses about the functional roles of different brain rhythms. Low frequency oscillations may coordinate long-range communication between different brain regions (von Stein & Sarnthein, 2000) whereas high frequency high gamma activity is more spatially restricted and reflects local cortical processing (Crone et al., 1998; Fries et al., 2007; Canolty et al., 2007). High gamma amplitude is correlated with both local neuronal spiking activity (Mukamel et al., 2005) and the fMRI BOLD signal (Logothetis et al., 2001; Mukamel et al., 2005). Phase-amplitude coupling may reflect the means through which multiple overlapping long-range networks can communicate by statistically biasing the extracellular membrane potential in local cortical regions such that neurons will be more likely to fire during particular phases of low frequency oscillations (Haider & McCormick, 2009; Klausberger et al., 2003). Such a selection mechanism would support complex behaviors such as top-down attentional modulation in a physiologically plausible manner, and thus scalp indices of low-frequency oscillations may reflect underlying cortical activity.

Power in human EEG drops off as a function of distance and is inversely proportional to frequency in a 1/*f*-like relationship (Bédard, Kröger, & Destexhe, 2006; Freeman, 2004; Pritchard, 1992), making high-frequency γ_H signals difficult to record at the surface of the scalp (but see Lenz et al. (2008) and Ball et al. (2008)). Furthermore, γ_H activity recorded at the scalp is susceptible to noise from scalp (Fu, Daly, & Cavuşoğlu, 2006; Goncharova et al., 2003), facial (Whitham et al., 2008), and eye movement (Yuval-Greenberg et al., 2008) muscles. These noise sources, coupled with the well-known localization issues

due to the inverse problem, limit neurocognitive scalp EEG research. These issues have been verified in many experimental and computational models of the interaction between the skull and EEG (Abraham & Marsan, 1958; Cooper et al., 1965; Geisler & Gerstein, 1961; Williams & Parsons-Smith, 1950), and have shaped the way human EEG research has been performed for the past several decades.

While MEG, implanted electrodes, and intraoperative intracranial electrophysiology overcome some of these limitations, they are sensitive to other confounding issues. Scalp MEG requires subjects to sit with their heads motionless in rooms shielded from electromagnetic noise and the MEG is less sensitive to radial dipole sources in the crowns of gyri (Cohen & Cuffin, 1991). Intraoperative electrophysiology during neurosurgical procedures is not only invasive but it is limited by cognitive and EEG changes associated with abnormal neural tissue, pharmacological manipulations during anesthesia, and the small number of patients available for study. In this thesis I provide the first systematic quantification of the effects of the skull on behavioral EEG that could help bridge findings from human intracranial and extracranial electrophysiology.

Chapter 2

Prefrontal Cortex and Basal Ganglia Contributions to Visual Working Memory

Abstract

Visual working memory (VWM) is a remarkable skill dependent on the brain's ability to construct and hold an internal representation of the world for later comparison to an external stimulus. Prefrontal cortex (PFC) and basal ganglia (BG) interact within a larger cortical and subcortical network supporting VWM. We used scalp electroencephalography in a group of patients with unilateral PFC or BG lesions to show that these regions play complementary but dissociable roles in VWM. PFC patients show behavioral and electrophysiological deficits manifested by attenuation of both extrastriate attention and VWM-related neural activity only for stimuli presented to the contralesional visual field. In contrast, patients with BG lesions show behavioral and electrophysiological VWM deficits independent of the hemifield of stimulus presentation but have intact extrastriate attention activity. The results support a model wherein the PFC is critical for top-down intrahemispheric modulation of attention and VWM with the BG involved in global VWM processes.

2.1 Introduction

Even a seemingly simple action such as determining whether a banana is ripe requires us to compare real world visual information—such as the color of a banana in your hand—to

your memory of the yellowness of a ripe banana. This relies in part on visual working memory (VWM), a remarkable ability wherein we construct and hold an internal model of a real-world visual stimulus that we then later compare against another stimulus. In essence we construct and hold a model of the visual world and compare that model against subsequent inputs from the external world. VWM relies upon an intact and functioning prefrontal cortex (PFC) and patients with damage to this region, such as from stroke, have VWM impairments (Curtis & D'Esposito, 2004; Müller & Knight, 2006). However cognitive processes do not localize to specific brain regions *per se* as a behavior as complex as VWM recruits a distributed network of cortical and subcortical structures (Bressler, 1995; Knight, 2007; Friedman & Goldman-Rakic, 1994; Gazzaley, Rissman, & D'Esposito, 2004; Curtis & D'Esposito, 2003) including the basal ganglia (BG) (McNab & Klingberg, 2008; Levy et al., 1994) and visual extrastriate regions (Vogel & Machizawa, 2004; Todd & Marois 2004; Bledowski, Rahm, & Rowe, 2009).

Most computational models of VWM rely upon intercommunication between the PFC and the striatum such that memories are maintained via recurrent activation in frontostriatal loops (Ashby et al., 2005; O'Reilly & Frank 2006, Hazy, Frank, & O'Reilly, 2006). *In vivo*, working memory maintenance is associated with sustained delay-period activity in the PFC (Fuster & Alexander, 1971; Curtis & D'Esposito, 2003) and BG (Histed, Pasupathy, & Miller, 2009), though the BG are thought to play a role in gating information into the PFC to allow it to update representations where necessary (Moustafa, Sherman, & Frank, 2008). While neurons in both visual extrastriate and the PFC maintain working memory representations during delay periods, PFC neurons encode more information about the stimuli and are more impervious to distractors than extrastriate neurons (Miller, Erickson, & Desimone, 1996). Animal research shows that the BG rapidly learn task-relevant rules and may send relevant, pre-processed information to the PFC for subsequent selection and further processing (Pasupathy & Miller, 2005). Anatomically, the BG are situated in an ideal position to mediate cognitive behavior modulated via reinforcement learning (Schultz 2002; Williams & Eskandar, 2006). Each striatum receives inputs from many cortical regions including the PFC and visual extrastriate cortex (e.g., Draganski et al., 2008; McGeorge & Faull, 1989) and these inputs converge with dopaminergic afferents from the substantia nigra (Redgrave & Gurney, 2006). The striatum appears to be organized through parallel interconnected loops (Draganski et al., 2008; Haber, 2003; Yeterian & Pandya, 1991) with frontal cortical regions (including the PFC) via the globus pallidus, thalamus, and subthalamic nucleus. From a neuroanatomical perspective, each striatum receives PFC input bilaterally from both hemispheres (Dunnet, Meldrum, & Muir, 2005; McGeorge & Faull, 1989) and thus both basal ganglia have connections to both PFC hemispheres. Patients with BG pathology such as from stroke or Parkinson's Disease have deficits in a variety of cognitive learning and switching tasks (Cools, Ivry, & D'Esposito, 2006; Ell, Marchant, & Ivry, 2006; Frank, Seeberger, & O'Reilly, 2004; Graybiel, 2005; Packard & Knowlton, 2002) similar to the profile observed in patients with lateral PFC lesions (see Stuss & Knight, 2002).

The BG deficits are proposed to be due to a general deficit in the manipulation of internally represented stimuli (see Lewis et al., 2004). Human neuroimaging shows that activity in the BG and PFC is associated with individual differences in working memory capacity and that BG activity is specifically associated with filtering out irrelevant distracting information (McNab & Klingberg, 2008), consistent with gating models of BG function and

stimulus manipulation. Scalp EEG studies show that extrastriate activity increases with the number of items held in working memory up to an individual's VWM capacity limit and that this activity correlates with individual differences in VWM capacity (Vogel & Machizawa, 2004). Although sustained PFC activity is associated with working memory maintenance, the role of attention in working memory—both to external stimuli and internal representations of the same—cannot be ignored (Postle et al., 2004; Awh, Vogel, & Oh, 2006; Kimberg & Farah, 1993). This attention/working memory interrelationship has lead to theories of PFC function that highlight the role of the PFC in information integration (Miller & Cohen, 2001), with interactions between the PFC and BG necessary to build models of complex rules and behavior from discrete components (Miller & Buschman, 2007).

Lesion studies in human and non-human primates have provided the strongest evidence for a causal relationship between anatomy and function (Müller & Knight, 2006; Rorden & Karnath, 2004). For example, because PFC lesions lead to working memory deficits, the PFC can be said to play an important, necessary role in working memory. Research has shown that unilateral PFC lesions cause lateralized deficits in top-down modulation of visual attention (Barceló, Suwazano, & Knight, 2000). These deficits manifest as errors in target detection specifically to targets that appear in the contralesional hemifield, suggesting that top-down cognitive functions of the PFC are at least partly constrained on a within-hemisphere basis.

Based on these observations we hypothesized that the BG plays a visual field independent role in working memory updating and rule acquisition. Conversely we predicted that the PFC has an executive role in working memory maintenance, attentional control, and top-down facilitation of visual extrastriate cortices on a within-hemisphere basis. To test the relationship of the PFC and the BG to VWM, we examined two groups of patients with unilateral PFC or BG lesions (**Fig. 2.1**) performing a lateralized VWM task (**Fig. 2.2a**) while recording scalp electroencephalography (EEG). By making use of a lateralized visual design we can take advantage of the inherent contralateral organization of the mammalian visual system wherein visual input from the right visual field enters the left visual cortex and vice versa. For example, in **Fig. 2.2b** we illustrate how a patient with a left PFC lesion viewing a stimulus in the left visual hemifield would receive the visual input into the intact cerebral hemisphere, whereas that same patient viewing a right hemifield stimulus would receive the information in the damaged hemisphere, thus emphasizing behavioral deficits. By combining a lateralized VWM design with scalp electrophysiology in patients with unilateral brain lesions we can dissociate the role of the PFC and BG in VWM maintenance and separately examine the role of each region in top-down modulation of extrastriate activity.

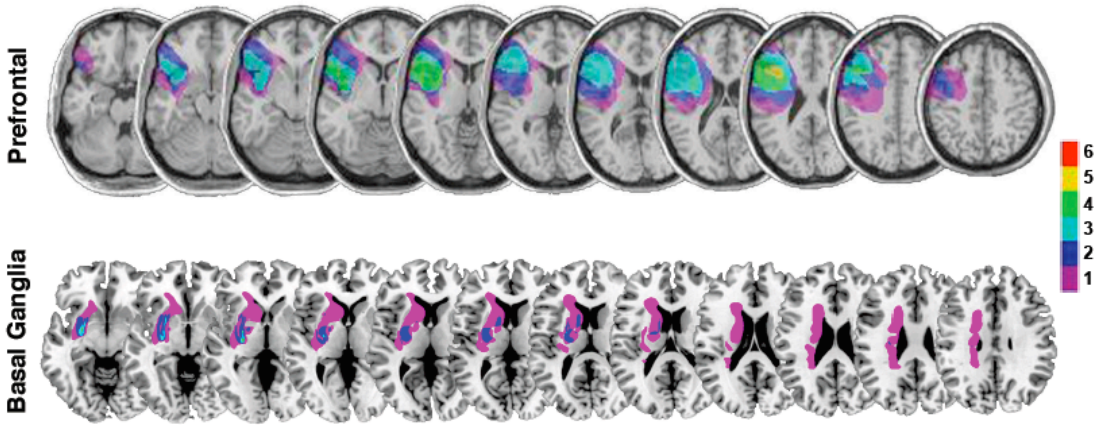

Figure 2.1 Patient lesion reconstruction. Structural MRI slices illustrating the lesion overlap across the two patient groups. For the PFC group (n = 6) maximal lesion overlap (>50%) was in Brodmann areas 6, 8, 9, and 46 and encompassed portions of the middle and superior frontal gyri. For the BG group (n = 6) maximal lesion overlap was in the putamen and encompassed the head and body of the caudate as well as the globus pallidus. All lesions are normalized to the left hemisphere for comparison, however two patients in each group had right hemisphere lesions. Software reconstructions were performed using MRIcro (Rorden & Brett, 2000).

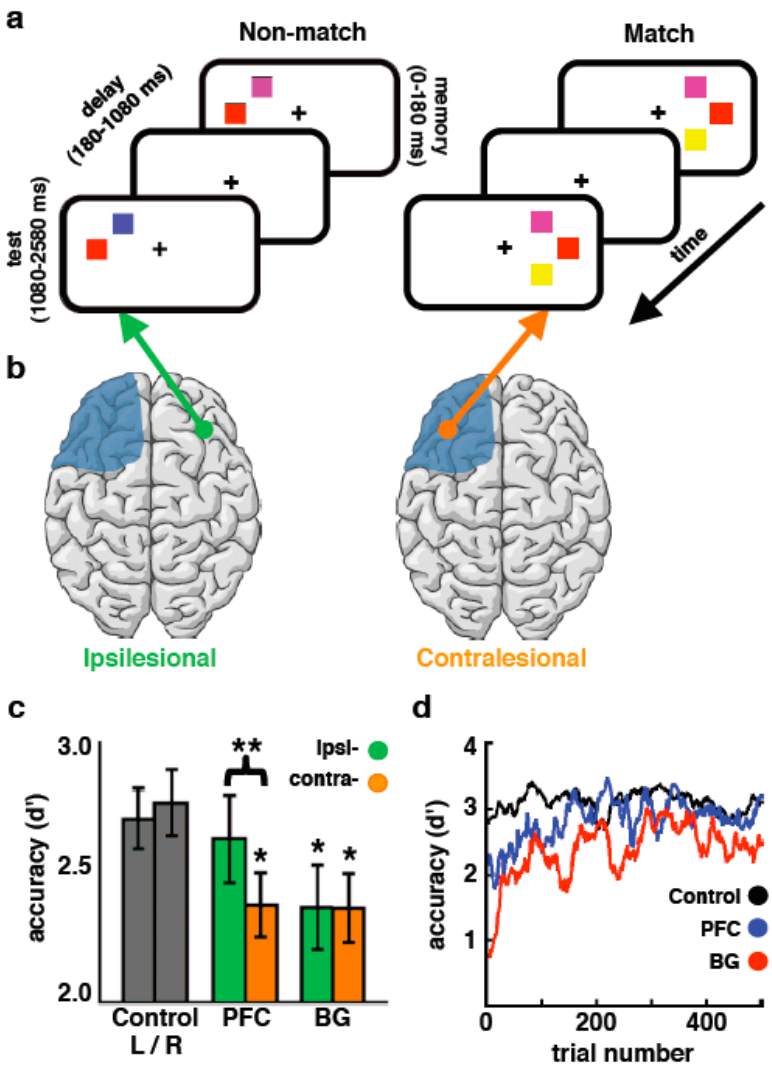

Figure 2.2 Behavioral paradigm and performance. (**a**) For each trial, subjects were presented with a brief memory array (180 ms) of one, two, or three colored squares in either the left or right visual hemifield. After a 900 ms delay the same number of squares was presented in the same spatial location and the subject manually responded to indicate whether the squares in the test array were the same color as those in the memory array. (**b**) For a patient with a left unilateral PFC lesion as illustrated here, stimuli that appear in the left visual hemifield are "ipsilesional" and the visual information selectively enters the intact cerebral hemisphere, whereas stimuli that appear in the right visual hemifield are "contralesional" and selectively enter the damaged hemisphere. (**c**) Patients with unilateral PFC lesions performed as well as controls when stimuli were presented ipsilesionally but were impaired for contralesional stimuli. In contrast, patients with unilateral BG lesions performed more poorly overall, regardless of the hemifield of stimulus presentation. (*$p < 0.05$ compared to controls, **$p < 0.0005$, error bars represent s.e.m.). (**d**) Control subjects and PFC patients perform equally well across trials. BG patients are significantly impaired in early trials and their behavior reached an asymptote at later trials.

2.2 Methods

2.2.1 Data Collection

All subjects gave informed consent approved by the University of California, Berkeley Committee for Protection of Human Subjects and the Department of Veterans Affairs Northern California Health Care System Human Research Protection Program. Controls were matched to patients by age and education. Because there were neither age nor education differences between PFC and BG groups ($p > 0.5$ both comparisons) we compared the results of each group separately to the combined group of 12 controls. For both patient groups testing took place at least 6 months after the date of the stroke; lesion etiology was either cerebrovascular accident or hypertensive bleed. A neurologist (R.T.K.) inspected patient MRIs to ensure that no white matter hyperintensities were observed in either patient group.

Subjects were tested in a sound-attenuated EEG recording room at the University of California, Berkeley. EEG data were collected using a 64+8 channel BioSemi ActiveTwo amplifier (Metting van Rijn et al., 1990) sampled at 1024 Hz. Horizontal eye movements (HEOG) were recorded at both external canthi and vertical eye movements (VEOG) were monitored with a left inferior eye electrode and a fronto-polar electrode. Subjects were instructed to maintain central fixation and to respond using the thumb of their unaffected ipsilesional hand. All data were referenced offline to the average potential of two earlobe electrodes and analyzed in MATLAB® (R2009b, Natick, MA) using custom scripts and the EEGLAB toolbox (Delorme & Makeig, 2004) and SPSS® (Rel. 18, Chicago: SPSS Inc.). Only trials in which subjects later response correctly were included in EEG analyses.

2.2.2 Behavioral Task

Subjects were presented with a memory array consisting of a set of one, two, or three colored squares (180 ms presentation; equiprobable presentation of each set size to either the left or right visual hemifield). After a 900 ms delay, a test array of the same number of colored squares appeared in the same spatial location. Subjects were instructed to manually respond to indicate whether or not the test array was the same color as the initial (memory) array. Behavioral accuracy was assessed by normalizing percent correct responses for each subject using a d' measure of sensitivity which takes into account false alarm rate to correct for guessing. To test the effects of learning on behavioral performance we calculated a sliding window d' measure across blocks of 25 trials moving in one-trial steps for the first 500 trials looking at overall behavioral performance regardless of memory load or hemifield of stimulus presentation. To avoid mathematical constraints in the calculation of d', we applied a standard correction procedure wherein, for any subjects with a 100% hit rate or 0% false alarm rate, performance was adjusted such that $1/(2N)$ false alarms were added or $1/(2N)$ hits subtracted where necessary.

2.2.3 Data Analysis

All statistical analyses on behavior and ERP were first assessed using repeated-measures ANOVAs with group membership (control, PFC, or BG) as the between-subjects factor and memory load and hemifield of stimulus presentation (left/ipsilesional vs.

right/contralesional) as the within-subjects factors. Comparisons between control and patient results were such that responses to left-hemifield stimuli in controls were compared against ipsilesional responses in patients and right-hemifield stimuli were compared to contralesional responses. To test the effects of learning on behavioral performance we calculated a sliding window d' measure across blocks of 25 trials moving in one-trial steps looking at overall behavioral performance regardless of memory load or hemifield of stimulus presentation. For analyses on learning we ran a repeated measures ANOVA with trial number as the within-subjects factor using the mean d' in the first 100 trials in four bins of 25 trials each. For *post hoc* analyses, significant effects were reported using one-way independent (between groups) or paired-samples (within group) *t*-tests with the assumption that controls performed better than patients, that patients were impaired for ipsilesional stimuli, and that greater memory load lead to decreased behavior and increased electrophysiological responses. For overall comparisons collapsing across loads or hemifields of presentation we used all of the data for those conditions in the *post hoc t*-tests.

ERP analyses were performed on bandpass filtered (0.1-20 Hz) data resampled to 256 Hz using a 100 ms pre-stimulus baseline. Blinks and saccades were identified on raw VEOG and HEOG channels respectively and verified with scalp topographies. Events with incorrect or no response, blinks, or saccades were removed from all analyses except where otherwise stated. CDA values were calculated as the mean amplitude difference from 300-900 ms between extrastriate electrodes contralateral to the stimulus and electrodes ipsilateral to the stimulus. Thus, for controls, for a right hemifield stimulus, CDA was calculated as the average of left minus right extrastriate activity from 300-900 ms. For patients, CDA was calculated in the same manner but was analyzed relative to the lesion such that for patients with left hemisphere lesions CDA for right hemifield stimuli was classified as contralesional and CDA for left hemifield stimuli was classified as ipsilesional. Patient behavioral data we classified in the same manner. N1 amplitude was calculated as the minimum amplitude over the extrastriate cortex contralateral to the hemifield of stimulus presentation from 100-200 ms post stimulus onset.

We examined correlation between CDA and behavior across time by correlating each subject's accuracy for each memory load with their respective CDA amplitude at that load. This was done on the average CDA amplitude across a 100 ms sliding window from 300-900 ms. To compare differences in correlation between EEG and behavior between groups and hemifields we performed χ^2 tests for equality of correlation coefficients using the correlation coefficients from the 300-900 ms range.

2.3 Results

2.3.1 Behavior

In a three-way ANOVA including all three groups we found a main effect of load on accuracy such that all groups were less accurate with increasing memory load ($F_{2,42} = 344.45$, $p < 0.0005$). There was also a three-way interaction between group, memory load, and hemifield of presentation ($F_{4,42} = 12.47$, $p < 0.0005$). We performed multiple ANOVAs comparing performance between and within the patient groups to examine the nature of this three-way interaction. Behavioral results are summarized by the group X hemifield effect in **Fig. 2.2c** ($F_{2,21} = 10.17$, $p = 0.001$; see **Table 2.1** for all results).

In a comparison between controls and PFC patients there was a three-way interaction ($F_{2,32} = 14.41$, $p < 0.0005$) driven by a hemifield X memory load ($F_{2,32} = 14.64$, $p < 0.0005$) and hemifield X group interaction ($F_{1,16} = 16.17$, $p = 0.001$). To examine the nature of these hemifield effects we performed separate planned ANOVAs for controls and the PFC group. The PFC patients showed a significant hemifield X load interaction ($F_{1,5} = 37.46$, $p = 0.002$) as well as a main effect of hemifield ($F_{1,5} = 29.21$, $p = 0.003$) wherein they were less accurate overall for contralesional stimuli ($t_{17} = 3.94$, $p < 0.0005$). We ran a series of *post hoc t*-tests to examine hemifield differences within the PFC group for each load; we found that for loads one and two PFC patients were impaired for contralesional stimuli but accuracy converged at three-item memory loads (one item: $t_5 = 5.26$, $p = 0.002$; two items: $t_5 = 3.12$, $p = 0.013$; three items: $t_5 = 1.21$, $p = 0.14$). Within the control group we found no such hemifield X load interaction ($F_{1,11} = 1.24$, $p = 0.29$) nor a main effect of hemifield ($F_{1,11} = 1.47$, $p = 0.25$). These results suggest that the hemifield X group interaction were driven by deficits in the PFC group in response to contralesional stimuli. This was confirmed in an analysis comparing accuracy by hemifield between groups wherein PFC patients were impaired for contralesional stimuli compared to controls ($t_{52} = 1.99$, $p = 0.026$).

In comparing controls and BG patients we also found a three-way interaction ($F_{2,32} = 5.40$, $p = 0.010$) driven by a hemifield X memory load interaction ($F_{2,32} = 30.82$, $p < 0.0005$). In separate planned ANOVAs for controls and the BG group, neither group showed a main effect of hemifield (controls: $F_{1,11} = 1.47$, $p = 0.25$, BG: $F_{1,5} < 1.0$) however the BG group showed a hemifield X load interaction ($F_{2,10} = 20.77$, $p < 0.0005$). This interaction was non-linear (linear: $F_{1,5} = 1.76$, $p = 0.242$; quadratic: $F_{1,5} = 61.14$, $p < 0.0005$) due to equal performance for ipsilesional stimuli at one- and two-item loads (one v. two: $t_5 < 1.0$, $p = 0.38$) and rapidly declining at three items (two v. three: $t_5 = 10.81$, $p < 0.0005$) compared to a steady decline in performance for contralesional stimuli (one v. two: $t_5 = 4.32$, $p = 0.004$; two v. three: $t_5 = 17.52$, $p < 0.0005$). Overall, however, BG patients performed worse than controls ($t_{106} = 2.67$, $p = 0.005$).

Research suggests that the BG are critical in learning behavioral requirements (Pasupathy, & Miller, 2009; Frank, Seeberger, & O'Reilly, 2004; Poldrack et al., 2001; Seger & Cincotta, 2006). Therefore we examined the temporal evolution of behavioral performance across the first 100 trials (see **Methods**). In comparing controls to PFC patients, there was a main effect of trial on performance ($F_{3,48} = 3.14$, $p = 0.034$) and a main effect of group ($F_{1,16} = 15.88$, $p = 0.001$), but no group X trial number interaction, which suggests that both groups improved across the first 100 trials and that the PFC group performed worse than controls. In contrast, when we compared the BG group to controls we found a significant group X trial number interaction ($F_{3,48} = 3.64$, $p = 0.019$). Although both the BG and control groups showed a main effect wherein behavior improved across trials (BG: $F_{3,15} = 5.13$, $p = 0.012$; controls: $F_{3,33} = 2.95$, $p = 0.047$), only the BG group showed a significant deficit in the first few trials (see **Fig. 2.2d**, trials 1-25 compared to 26-51, $t_5 = 6.13$, $p = 0.001$; $p > 0.05$ for all other pair-wise comparisons between successive trial bins for both BG and control groups). It is important to note that although the behavioral deficits in the BG group were exaggerated during the first 25 trials, they continued to perform worse in all time bins examined ($p < 0.05$ for all other binned analyses).

2.3.2 Electrophysiology

We examined the effects of PFC and BG lesions on delay period EEG activity. We replicated previous findings (Vogel & Machizawa, 2004; Vogel, McCollough, & Machizawa, 2005) that the amplitude of contralateral delay activity (CDA, see **Methods**) increases with memory load in a three-way ANOVA including all three groups ($F_{2,42} = 18.84$, $p < 0.0005$); visual inspection of the CDA time courses (**Fig. 2.3**) showed that patient CDA amplitudes for contralesional stimuli are abnormal. In the three-way ANOVA, there was a significant quadratic three-way interaction between group, memory load, and hemifield of presentation ($F_{2,21} = 3.74$, $p = 0.041$), likely driven by the non-linear effects of the lesion leading to the pathological patient contralesional CDA in the patients. This was reflected in a significant group X hemifield effect ($F_{2,21} = 6.65$, $p = 0.006$; see **Table 2.1** for all results).

In comparing PFC patients to controls there was a significant group X hemifield interaction ($F_{1,16} = 7.45$, $p = 0.015$), though neither group showed a significant effect of hemifield in separate ANOVAs of each group (controls: $F_{1,11} = 2.95$, $p = 0.11$; PFC: $F_{1,5} = 3.21$, $p = 0.13$). This interaction was driven by a crossover effect wherein CDA amplitude is reduced in the PFC group for ipsilesional stimuli ($t_{52} = -3.16$, $p = 0.001$) but higher for contralesional stimuli ($t_{52} = 4.06$, $p < 0.0005$). In separate planned contrasts we wanted to examine the effects of hemifield of presentation on CDA amplitude within the patient groups separately for ipsilesional and contralesional stimuli. As a comparison, when this analysis is done in the control group, effect of load is significant for both hemifields the (left: $F_{2,22} = 7.37$, $p = 0.004$; right: $F_{2,22} = 6.44$, $p = 0.006$). In the PFC group there was a significant effect of load for ipsilesional stimuli ($F_{2,10} = 4.17$, $p = 0.048$), driven by an effect wherein CDA amplitude increases from one to two items ($t_5 = 4.52$, $p = 0.003$) but not from two to three items ($t_5 = -0.42$, $p = 0.69$) similar to pattern seen in control subjects (one to two: $t_{11} = 4.06$, $p < 0.0005$; two to three: $t_{11} = 1.20$, $p = 0.13$). As predicted due to the loss of top-down facilitation, for contralesional stimuli there is no effect of load ($F_{2,10} < 1.0$) in the PFC group.

In an analysis comparing CDA between the BG and control groups there was also a significant group X hemifield interaction ($F_{1,16} = 13.20$, $p = 0.002$), though neither group showed a significant effect of hemifield in separate ANOVAs of each group (controls: $F_{1,11} = 2.95$, $p = 0.11$; BG: $F_{1,5} = 3.39$, $p = 0.13$). Just as with the comparison between controls and PFC patients, this interaction appears to be driven by a crossover effect wherein CDA amplitude is reduced in the BG group for ipsilesional stimuli ($t_{52} = -5.76$, $p < 0.0005$) but higher for contralesional stimuli ($t_{52} = 4.04$, $p < 0.0005$). In contrast to PFC patients, in an analysis of hemifield of presentation on CDA amplitude within the BG group there was no effect of load for either ipsilesional or contralesional stimuli (ipsilesional: $F_{1,5} = 1.52$, $p = 0.27$; contralesional: $F_{1,5} < 1.0$).

On visual inspection of the CDA time-series, the CDA begins with a rapid increase in amplitude that then sustains in the control group. In an analysis of this early rise in activity (peak amplitude 300-400 ms) we find that the group X hemifield interaction disappears in both patient groups. That is, there is no group X hemifield interaction between controls and the PFC group ($F_{1,16} < 1.0$) or between controls and the BG group ($F_{1,16} < 1.0$). This suggests that early maintenance-related activity is normal, but that it degrades throughout the delay period as the loss of top-down facilitation of extrastriate cortex leads to failures in working memory maintenance.

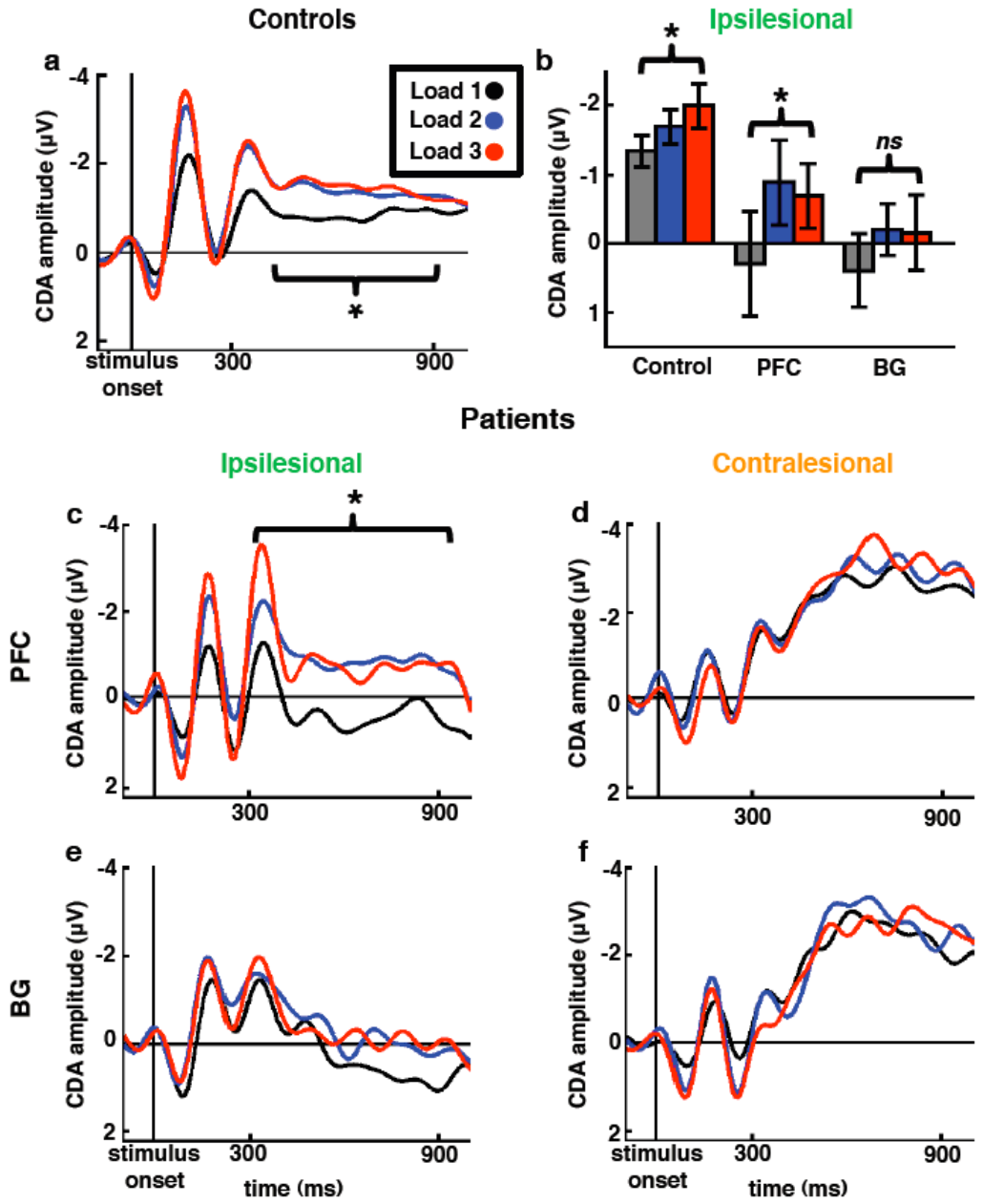

Figure 2.3 Electrophysiological analyses. (**a**) Controls show a significant effect of memory load on CDA where increasing memory loads lead to larger CDA amplitude (*main effect of load, $p < 0.0005$). (**b**) Summary of CDA findings for ipsilesional stimuli in the two patient groups (shown in detail in **c**-**f**) and for left hemifield stimuli for controls. For ipsilesional stimuli (**c**, **e**) both controls and the PFC group show a significant effect of memory load on CDA (*$p < 0.05$, error bars represent s.e.m.) that is not seen in the BG group (*ns*, not significant). For contralesional stimuli (**d**, **f**) the relationship between CDA and load is abolished in both patient groups. (**c**) The PFC patient group shows a significant effect of memory load on CDA for ipsilesional stimuli suggesting that top-down mediated memory maintenance is partially dissociable on a within-hemisphere basis.

In order to examine the behavioral relevance of our electrophysiological findings we performed a sliding-window correlation analysis at each time point between instantaneous CDA amplitude for each subject at each load with that subject's behavioral performance at the same load. As can be seen in **Fig. 2.4a**, for control subjects instantaneous CDA amplitude and behavior are significantly correlated from approximately 250-950 ms post stimulus onset, which corroborates the *a priori* selection of the 300-900 ms time window based upon previous studies (e.g., Vogel & Machizawa, 2004). This same analysis was performed separately for each group and each hemifield of stimulus presentation (see **Fig. 2.4b**). For ipsilesional stimuli in the PFC group there was no difference in the CDA/behavioral correlation compared to controls ($\chi^2 = 0.78$, $p = 0.38$); however, for contralesional stimuli correlations were significantly lower ($\chi^2 = 3.42$, $p = 0.027$). Within the BG group correlations were attenuated for both hemifields (ipsilesional: $\chi^2 = 32.74$, $p < 0.0005$; contralesional: $\chi^2 = 8.68$, $p = 0.003$). These results recapitulate the CDA and behavioral findings and demonstrate a strong relationship between delay-period electrophysiology and later behavioral outcomes.

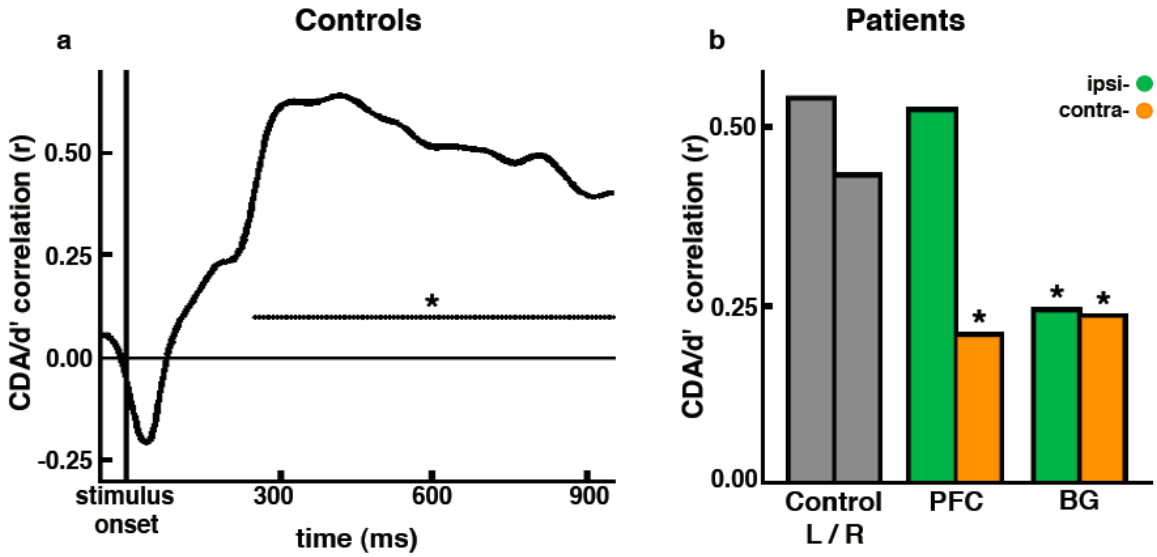

Figure 2.4 Correlations between electrophysiology and behavior. (**a**) CDA activity during the delay period correlates with behavioral accuracy in controls. Here we show the correlation between accuracy and CDA for each memory load for each subject across time. Every time point with a dot indicates a significant electrophysiology/behavior correlation. There is a significant correlation between behavior and CDA during the time-window of interest (300-900 ms) (*$p < 0.05$ at each time point). (**b**) Median correlation coefficients from 300-900 ms. The electrophysiology/behavior correlation analyses reflect our previous results wherein the PFC group shows a deficit only for contralesional stimuli whereas the BG group shows an overall deficit (*$p < 0.05$ chi-squares tests for equality of correlation coefficients, significant deficit compared to controls).

In a final analysis, we sought to examine the effects of lesions on attention. Because of the relatively rapid nature of our task and the brief presentation time we hypothesized that the observed behavioral deficits in the patient groups could be partly due to the effects of the lesion on attentional control. We used the posterior contralateral visual N1 as the surrogate event related potential (ERP) for visual attention (Fu et al., 2008). In a three-way ANOVA including all three groups we found a main effect of load on N1 amplitude such that increasing perceptual load lead to more negative N1 amplitude ($F_{2,42}$ = 23.54, p < 0.0005). There was also a three-way interaction between group, load, and hemifield of presentation ($F_{4,42}$ = 5.63, p = 0.001; see **Table 2.1** for all results). N1 results are summarized by the group X hemifield effect in **Fig. 2.5**. In separate analyses comparing controls with PFC patients and controls with BG patients we also observed significant three-way interactions in both comparisons (PFC: $F_{2,32}$ = 8.89, p = 0.001; BG: $F_{2,32}$ = 5.78, p = 0.007). The control versus BG interaction was mediated by a group X load interaction ($F_{2,32}$ = 8.01, p = 0.002) that was mediated by group differences for one-item arrays wherein BG patients had lower N1 amplitudes (t_{34} = -2.06, p = 0.024). These differences disappeared for higher loads (two-items: t_{34} = 0.24, p = 0.41; three-items: t_{34} = 0.75, p = 0.23). In a *post hoc* analysis of the control versus PFC interaction we examined the *a priori* hypothesis that PFC patients would have attention deficits in response to contralesional stimuli. Looking across all memory loads there was no significant difference in N1 amplitude between groups for ipsilesional stimuli (t_{52} = 0.20, p = 0.43) however N1 amplitude was attenuated in the PFC group for contralesional stimuli (t_{52} = -2.86, p = 0.003). As a comparison, there were no differences between controls and BG patients for either hemifield (ipsilesional: t_{52} = 0.22, p = 0.42; contralesional: t_{52} = -0.73, p = 0.24).

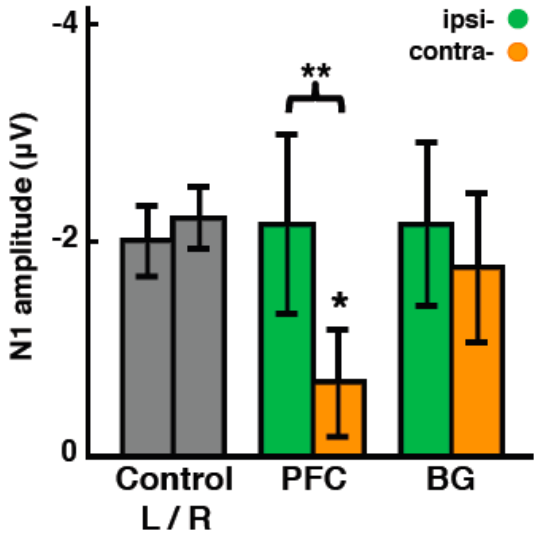

Figure 2.5 Attention-modulated ERPs. N1 amplitudes from the contralateral visual cortex in response to the memory array. In the PFC group there is a significant effect of hemisphere (**p = 0.023) where N1 amplitudes are attenuated for contralesional stimuli and lower than control amplitudes (*p = 0.003). The BG group shows no such deficit, supporting the idea that poor performance in the BG group is mediated by failures in working memory rather than problems in attending to relevant stimuli. These results suggest that top-down attention deficits, in conjunction with maintenance deficits, might be conjointly affecting behavioral performance in the PFC group. (Error bars represent s.e.m.).

Table 2.1
Summary of results, mean (SEM)

	Control		**PFC**		**BG**	
Memory Load	*Left*	*Right*	*Ipsilesional*	*Contralesional*	*Ipsilesional*	*Contralesional*
1-item						
d'	3.23 (0.18)	3.32 (0.22)	3.46 (0.04)	2.91 (0.08)	2.76 (0.20)	2.85 (0.15)
CDA	-1.34 (0.23)	-0.31 (0.35)	0.29 (0.76)	-2.42 (0.72)	0.39 (0.53)	-2.18 (0.42)
N1	-2.16 (0.47)	-1.29 (0.29)	-0.60 (1.21)	-0.08 (0.76)	-0.55 (1.18)	-0.24 (0.93)
2-items						
d'	2.89 (0.13)	2.81 (0.16)	2.64 (0.08)	2.47 (0.08)	2.74 (0.20)	2.41 (0.16)
CDA	-1.69 (0.25)	-1.03 (0.42)	-0.89 (0.62)	-2.57 (0.84)	-0.20 (0.38)	-2.29 (0.23)
N1	-1.70 (0.53)	-2.11 (0.44)	-2.60 (1.30)	-1.29 (0.84)	-2.03 (1.30)	-2.13 (1.12)
3-items						
d'	2.00 (0.09)	2.17 (0.11)	1.79 (0.04)	1.74 (0.06)	1.58 (0.11)	1.82 (0.14)
CDA	-2.00 (0.32)	-0.97 (0.48)	-0.70 (0.47)	-2.74 (0.67)	-0.16 (0.54)	-2.26 (0.33)
N1	-2.13 (0.70)	-3.23 (0.57)	-3.24 (1.76)	-0.68 (1.04)	-3.86 (1.28)	-2.88 (1.42)

2.4 Discussion

These results highlight the distinct roles of the PFC and BG in working memory maintenance. We tested two separate groups of patients with either unilateral PFC or unilateral BG lesions, and age-matched controls, while they performed a lateralized VWM task. By making use of a lateralized VWM design with scalp EEG we were able to take advantage of the anatomical separation of visual inputs into the neocortex by visual hemifield and examine the effects of lesions on top-down working memory maintenance. This multiple methodological design allowed us to assess behavioral and electrophysiological responses on a within- and between-subjects basis. That is, because patients' lesions were unilateral we could assess differences in response to contralesional stimuli versus ipsilesional stimuli. Previous studies have shown this to be an effective means in highlighting top-down attention deficits associated with PFC lesions (Barceló, Suwazano, & Knight, 2000; Yago et al., 2004).

We found that patients with unilateral PFC lesions performed just as well as controls for ipsilesional stimuli and that accuracy dropped only when stimuli were lateralized to the contralesional hemifield. When we examined the evolution of performance over time and found that PFC patients performed as well in the first few trials as they did in later trials. This mimicked the results of normal control subjects. In contrast to PFC patients, the BG group performed worse than controls regardless of the hemifield of stimulus presentation. Furthermore, BG patients performed worse during the initial 25 trials than they did in later trials. This was despite the fact that subjects were all able to explicitly restate the rules and requirements of the task when questioned before the experiment began.

Previous EEG research using a paradigm similar to ours has shown that delay-period CDA activity increases in magnitude with increasing memory load up to a subject's working memory capacity (Vogel & Machizawa, 2004; Vogel, McCollough, & Machizawa, 2005). We replicated this scaling effect for our relatively low working memory load in our control group and extended this work to show that individuals' CDA amplitudes at each load correlate with their later behavioral performance. These results suggest that CDA accurately indexes behavioral performance. Within our PFC group we found similar CDA effects for ipsilesional stimuli only. That is, the PFC group, as in controls, showed an increase in CDA from one- to two-item loads. CDA amplitude in response to ipsilesional stimuli also correlated with later behavioral performance. Similar to their behavioral performance, patients with unilateral PFC lesions showed no scaling of CDA amplitude in response to contralesional stimuli, nor did CDA amplitude correlate with later behavioral outcomes.

In contrast to the BG patients and controls, we found that PFC patients had attenuated attention-dependent N1 amplitudes within the lesioned hemisphere only for contralesional stimuli. Previous studies have shown that posterior visual association cortex N1 amplitude is modulated by voluntary attention (Fu et al., 2008). Combined with the impaired CDA to contralesional stimuli, these electrophysiological results suggest that PFC lesions lead to overall executive functioning deficit within the damaged hemisphere. That is,

PFC damage results in a loss of top-down facilitation of visual extrastriate cortex during the working memory delay period resulting in attention and working memory maintenance deficits leading to poorer behavioral performance. Although we observed a strong brain/behavior correlation in this experiment using a simple delayed match-to-sample task, previous research using more complicated designs (e.g., moving stimuli) has found that the best predictor of behavioral performance is the difference in CDA amplitudes between high and low memory loads rather than the actual amplitudes themselves (Drew & Vogel, 2008). Notably, both patient groups showed a pronounced negative shift for all contralesional stimuli that was independent of VWM load; this abnormal extrastriate negativity may reflect a dysregulation of intrahemispheric inputs from the PFC that are normally present to facilitate VWM processes.

Contrary to our findings in the PFC group, patients with unilateral BG lesions showed no load-dependant scaling of CDA amplitudes for either ipsilesional or contralesional stimuli. This was despite the fact that N1 amplitudes within the BG group were intact, even in the lesioned hemisphere. So although patients with basal ganglia neuropathology show deficits in attentional set shifting and general cognitive flexibility (Moustafa, Sherman, & Frank, 2008; Cools, Ivry, & D'Esposito, 2006) the basal ganglia do not appear to play a critical role in the rapid allocation of visual attention. Rather our BG patients show intact electrophysiology related to attentional allocation whereas our PFC group have attentional impairments for contralesional stimuli. This suggests that the BG play a visual field independent role in working memory maintenance, but are not involved in top-down facilitation of visual extrastriate cortex attentional processes. This also adds further support to the specificity of the PFC in intrahemispheric control of top-down visual attention in the visual extrastriate cortex. These overall behavioral and working memory maintenance impairments in the BG group cannot be explained by a general effect of larger lesion volumes, as overall lesion volumes were significantly smaller in the BG group compared to PFC patients ($p < 0.0005$). The fact that BG patients are especially impaired during the first 25 trials supports the hypothesis that the BG are critical for rule-based learning and implementation (Ell, Marchant, & Ivry, 2006).

We hypothesize that unilateral BG lesions lead to a failure to update working memory representations, which in turn causes a degradation in the fidelity of the VWM representation in fronto-extrastriate networks. The deficits may also be due in part to a failure to filter out irrelevant information (McNab & Klingberg, 2008). Even though our protocol had no explicit distractors, the BG play an important role in filtering out irrelevant information, and thus the stimulus information that is to be reinforced may be degrading over time due to increased ambient noise from the visual world. While several studies have implicated the BG in updating or shifting the focus of attention (Bledowski, Rahm, & Rowe, 2009; Ravizza & Ivry, 2001), here we show that the BG are not associated with deficits in early top-down attentional processes as demonstrated by their intact N1 electrophysiology.

This pattern of results suggests that the PFC plays a broader role in executive functioning including both top-down attentional control and working memory maintenance whereas the BG are more directly related to working memory maintenance processes. Several studies have reported VWM deficits after lateral PFC damage (Müller & Knight, 2006; Stuss & Knight, 2002). In contrast, here we show that BG lesions lead to a VWM behavioral impairment associated with maintenance deficits despite intact attention

mechanisms. It is important to note that, although patients performed worse than controls in our study, the N1 and CDA deficits we report were from our examination of correct trials only. Thus, despite their pathological electrophysiological responses, patients performed the task well, albeit with impairments. This suggests that there are other mechanisms related to correct behavioral outcomes, possibly including functional reorganization (see **Chapters 3** & **4**), whereby the unilaterality of the lesions allows other intact cortical structures to compensate for the damaged regions.

Chapter 3

Dynamic Neuroplasticity after Human Prefrontal Cortex Damage

Abstract

Memory and attention deficits are common after prefrontal cortex (PFC) damage, yet people generally recover some function over time. Recovery is thought to be dependent upon undamaged brain regions but the temporal dynamics underlying cognitive recovery are poorly understood. Here we provide evidence that the intact PFC compensates for damage in the lesioned PFC on a trial-by-trial basis dependent on cognitive load. The extent of this rapid functional compensation is indexed by transient increases in electrophysiological measures of attention and memory in the intact PFC, detectable within a second after stimulus presentation and only when the lesioned hemisphere is challenged. These observations provide evidence supporting a dynamic and flexible model of compensatory neural plasticity.

3.1 Introduction

To examine the nature of cognitive compensation in patients with unilateral prefrontal (PFC) damage we conducted two scalp electrophysiology (EEG) experiments on patients with unilateral PFC lesions in the chronic phase at least one year post-injury. In Experiment

1, six patients with unilateral PFC lesions (**Fig. 3.1A**) and age-matched controls performed a lateralized visual working memory task (Vogel & Machizawa, 2004). In Experiment 2 eight patients with unilateral PFC lesions (**Fig. 3.1B**) and age-matched controls performed a lateralized visual attention task (Yago et al., 2004). Previous research on patients with unilateral PFC lesions has demonstrated that patients show behavioral deficits in response to contralesional stimuli in a visual attention paradigm (Barceló, Suwazano, & Knight, 2000; Yago et al., 2004). These deficits are associated with a loss of top-down facilitation of visual cortical regions as indexed using scalp EEG. These findings suggest that the separation of visual information by hemifield can emphasize deficits. By making use of two lateralized visual tasks we aimed to take advantage of this lesion by visual field of presentation phenomena. The design of randomly presenting stimuli to either the intact or damaged hemisphere allowed us to rapidly and flexibly challenge the damaged PFC on a trial-by-trials basis. This technique allows us to make use of a within-subjects design wherein our patients partially serve as their own controls such that we can examine differences within subjects in response to contralesional versus ipsilesional stimuli.

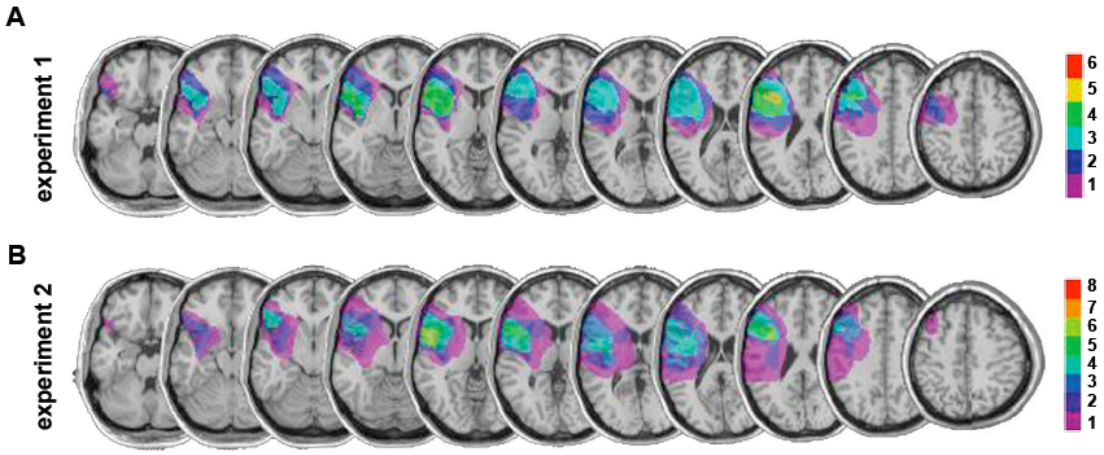

Figure 3.1 Patient MRIs. Horizontal MRI slices showing the group-averaged reconstruction of the extent of lesion overlap of the PFC damage in patients from (A) Experiment 1 (n = 6) and (B) Experiment 2 (n = 8). All lesions are normalized to the left hemisphere for comparison. Maximal lesion overlap (>50%) was observed in Brodmann areas 6, 8, 9, and 46 and encompassed portions of the middle and superior frontal gyri. Software reconstructions of the lateral perspective of lesions, determination of lesion volumes, and putative cytoarchitectonic areas damaged were performed using MRIcro (Rorden & Brett, 2000). Note that one of the six subjects from Experiment 1 also participated in Experiment 2.

We hypothesized that cognitive recovery in patients with unilateral PFC damage would be supported by flexible and dynamic compensatory contributions from the intact PFC. That is the plasticity of frontal association cortex would allow the intact PFC to dynamically compensate for the damaged hemisphere. In this model, activity in the intact PFC would increase specifically in response to demands placed on the damaged hemisphere.

That is, when behaviorally relevant stimuli are specifically presented to the damaged hemisphere the intact PFC would become more active, in a load-dependent manner, to compensate for the deficits due to the lesion. This is in contrast to a fixed recovery model that might predict that frontal activity would increase with memory or attention load regardless of the hemifield of presentation (see **Fig. 3.2** for hypothetical models). Here we show, in two separate patient groups performing two separate PFC-dependent tasks, rapid trial-by-trial increases in neural activity over the intact frontal cortex only when the damaged PFC is challenged. These observations of sub-second dynamic neural activity highlight the role of the intact hemisphere in supporting recovery of function and would not be detected using imaging methods with lower temporal resolution.

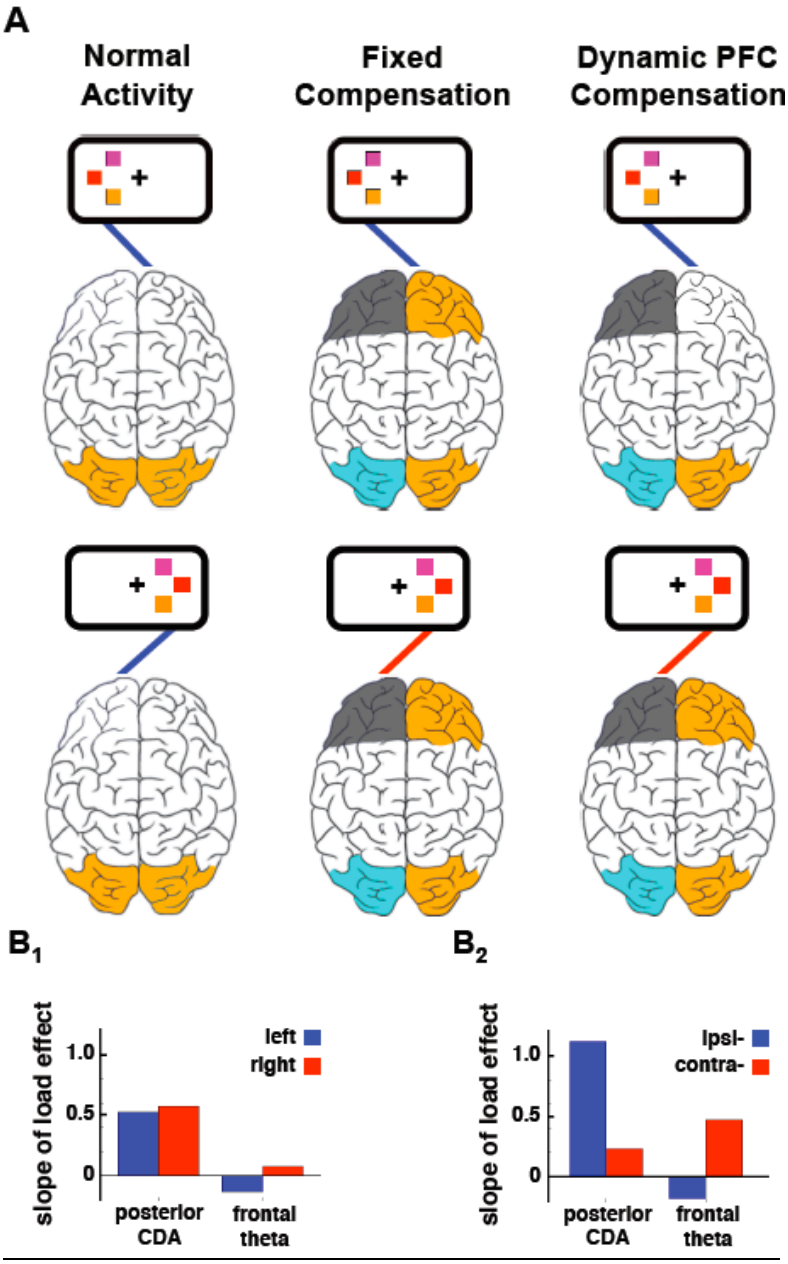

Figure 3.2 Experiment 1: Hypothetical models of posterior and frontal activity compared to real data.

(A): We illustrate the two possible models of EEG activation related to recovery. Relative activity increases are illustrated in orange and decreases in cyan. Unilateral PFC lesions are represented in grey.

In the Normal Activity model, as memory load increases from one to three items, posterior CDA increases parametrically with little delay-period frontal activity and no substantial EEG

activity differences between left and right hemifield stimuli. Observations in healthy controls adhere to this model (B_1).

In the Fixed Compensation model, patients with unilateral PFC lesions show relatively normal CDA for ipsilesional stimuli but show deficits in CDA to contralesional stimuli due to a loss of top-down facilitation. In this model, activity in the intact PFC increases in response to all stimuli due to an overall increase in task difficulty as a result of the unilateral lesion. This model also conceptually encompasses a less specific network recovery wherein activity changes related to behavioral outcomes are not detectable using scalp EEG.

In the Dynamic PFC Compensation model, CDA behaves similarly to that in the Fixed model. In contrast to the Fixed model, however, CDA deficits in response to contralesional stimuli are dynamically compensated for by the intact PFC. This model is dynamic in the sense that the intact PFC does not respond when stimuli are presented to the intact hemifield but rather only when the opposite, damaged hemifield is challenged. In response, the intact PFC assists the damaged hemifield in a load-dependent manner, with increasing activity with increasing demand. Observations from our PFC patients best fit this model (B_2).

3.2 Methods

3.2.1 Subjects

All subjects gave informed consent approved by the University of California, Berkeley Committee for Protection of Human Subjects and the Department of Veterans Affairs Northern California Health Care System Human Research Protection Program. In Experiment 1 we tested six patients (three male) with unilateral PFC damage due to stroke (two right hemisphere, average lesion volume 59 cm^3). Age for the patients (mean 57 years) and education (mean 15 years) were matched by our six controls such that each control was within $\pm$5 years of age and $\pm$3 years of education to their matched patient ($p > 0.05$, between groups for age and education). PFC subjects were in the chronic stroke phase (5-12 years post-stroke at the time of study). Details for subjects included in Experiment 2 are reported in a previous manuscript (Yago et al., 2004).

3.2.2 Data Collection

Subjects were tested in a sound-attenuated EEG recording room. In Experiment 1, EEG was collected using a 64+8 channel BioSemi ActiveTwo amplifier (Metting van Rijn, Peper, & Grimbergen, 1990) sampled at 1024 Hz. In Experiment 2, EEG was collected from 32 scalp electrodes and sampled at 512 Hz. Horizontal eye movements (HEOG) were recorded at both external canthi; vertical eye movements (VEOG) were monitored with a left inferior eye electrode and superior eye or fronto-polar electrode. In both experiments, subjects were instructed to maintain central fixation and responded using the thumb of their ipsilesional hand. All data were referenced offline to the average potential of two earlobe electrodes and analyzed in MATLAB® (R2008b, Natick, MA) using custom scripts and the EEGLAB toolbox (Delorme and Makeig, 2004) and SPSS® (Rel. 16, Chicago: SPSS Inc.). Electrodes in

patients with right hemisphere lesions (n = 2 for each experiment) were swapped across the midline allowing us to plot scalp topographies wherein lesions are normalized to the left hemisphere.

3.2.3 Behavioral Tasks

The behavioral paradigm used in Experiment 1 was slightly modified from the procedures used in Vogel and Machizawa (2004). We modified this design such that subjects were visually presented with one, two, or three colored squares. These squares were presented for 180 ms and only appeared in one visual hemifield at a time. After a 900 ms delay, a test array of the same number of colored squares appeared in the same spatial location. Subjects were instructed to manually respond to indicate whether or not the test array was the same color as the initial memory array. Every subject completed 8-10 blocks of 60 trials each resulting in 80-100 trials per subject per condition (2 visual hemifields x 3 memory loads for 6 total conditions). All other features of the task (color template, eccentricity, stimulus size, etc.) are identical to Vogel and Machizawa (2004). Behavioral accuracy was assessed by normalizing percent correct responses for each subject using a d' measure of sensitivity.

The behavioral paradigm used for Experiment 2 has been described in detail previously (Yago et al., 2004), but in brief, subjects were rapidly presented (107 ms presentation; 200, 800, or 1000 ms interstimulus interval) with a series of non-target standard stimuli (p = 0.7), target stimuli (p = 0.2), or neutral novel stimuli (p = 0.1) to either the left or right visual field (p = 0.5 for each hemifield). On separate blocks of trials, subjects manually responded to targets presented only to the left or only to the right visual hemifield. For both experiments PFC patients responded with their ipsilesional hand to reduce the influence of motor deficits on responses.

3.2.4 EEG Analyses

ERP analyses were performed on bandpass filtered (0.1-30 Hz) data resampled to 256 Hz using a 100 ms pre-stimulus baseline. Blinks and saccades were identified on raw VEOG and HEOG channels respectively and verified with scalp topographies. Events with incorrect or no response, blinks, or saccades were removed from all analyses except where otherwise stated. For time-frequency analyses, the absolute value of the Hilbert transform of bandpass filtered raw EEG was used to extract frequency band analytic amplitudes (frequency-domain Gaussian kernel multiplication; Gaussian standard deviation was 10% of the center frequency resulting in full width half maximum of 0.2355 of the center frequency). These frequency band analytic time series were then subjected to normal event-related analyses.

In Experiment 1, in patients, there was no load dependence on HEOG ($F_{2, 10} < 1.0$) or VEOG ($F_{2, 10} = 1.40$, $p = 0.29$) activity. There were no differences for three-item arrays between patients and controls for HEOG ($p = 0.43$) or VEOG ($p = 0.25$) activity, or in patients for three-item ipsilesional versus contralesional HEOG ($p = 0.94$) or VEOG ($p = 0.52$). To test the specificity of the theta compensatory effect we examined broadband ERP, alpha (8-12 Hz), and beta (12-18 Hz) frontal delay activity over intact PFC in Experiment 1 in a series of *post hoc* analyses. Patients showed no set-by-laterality interactions for frontal ERP or for alpha or beta frequencies ($F_{1,5} < 1.0$ for all analyses), nor was there an effect of load over intact cortex for contralesional stimuli for ERP ($F_{1,5} < 1.0$), alpha ($F_{1,5} < 1.0$), or beta ($F_{1,5} = 1.25$, $p = 0.32$) bands during the time window of interest.

In Experiment 2 there were no differences between patients and controls in VEOG (p = 0.88) or HEOG (p = 0.59) activity (mean activity during late frontal activity time windows; two-sample t-tests). We examined theta, alpha, and beta activity in patients over intact cortex for Experiment 2. There was no attention effect of laterality on compensatory measures of oscillatory activity over the intact PFC during the frontal positivity time window for theta, alpha, or beta bands ($F_{1,7} < 1.0$ for all analyses).

Because there was an imbalance in the number of patients with right hemisphere versus left hemisphere lesions in each group there is some concern that the effects of interest may be driven by differences in hemispheric function rather than specifically reflecting compensation for the lesioned cortex. While we did not have enough power to examine left/right hemispheric lesion differences among our patient groups, we do not see any trend toward differences among patients with left or right hemisphere lesions. In Experiment 1 the four patients with left hemisphere lesions show intact frontal theta increases from one- to three-item arrays of -0.15, 0.40, 0.63, and 0.94 μV and the two patients with right hemisphere lesions show increases of 0.57 and 0.44 μV. In Experiment 2 the six patients with left hemisphere lesions show ERP increases for contralesion stimuli over ipsilesion stimuli of 2.00, 2.04, 2.83, 2.17, 4.31, and 1.57 μV and the two patients with right hemisphere lesions show increases of 4.00 and 0.92 μV.

3.2.5 Resampling Statistics

Because patients had many more correct than incorrect trials, in order to more accurately calculate the significance of any mean amplitude difference between correct and incorrect trials we calculated the real mean difference (d) between correct (c) and incorrect (i) trials for Experiment 1 theta (d = 1.33μV) and Experiment 2 ERP amplitude (d = 7.73 μV). For each experiment separately we pooled all correct and incorrect trial compensatory amplitudes for patients and then randomly selected n_c and n_i amplitudes. We then calculated a difference between these surrogate data and repeated this process 10,000 times. For each experiment this provided a distribution of surrogate mean differences from the actual data from which we could calculate the probability (z-score) and one-tailed significance (p-value) of finding such an amplitude difference if the correct and incorrect labels were uninformative.

3.3 Results

In Experiment 1 we used a lateralized visual working memory task that allowed us to parametrically manipulate the memory load (i.e., 1, 2, or 3 visual objects) delivered to either cerebral hemisphere. As expected, both groups showed a main effect of memory load on behavioral accuracy (d') such that accuracy decreased with increasing memory load (repeated measures ANOVA, main effect of set size, ($F_{2,20}$ = 210.41, $p < 0.0005$, see **Fig. 3.3**). There was a three-way interaction between group, memory load, and hemifield of stimulus presentation ($F_{2,20}$ = 11.85, $p < 0.0005$). A series of *post hoc* analyses examining the effect of group on accuracy suggest that this three-way interaction is driven by an interaction between hemisphere and group ($F_{1,10}$ = 17.31, p = 0.002) rather than memory load and group ($F_{2,20} <$ 1.0). Controls show no interaction between memory load and hemifield ($F_{2,10}$ = 3.12, p = 0.14), nor a main effect of hemifield on accuracy ($F_{1,5}$ = 3.28, p = 0.080). In contrast, PFC patients show a strong effect of hemifield on accuracy ($F_{1,5}$ = 29.21, p = 0.003), as well as a

strong load by hemifield interaction ($F_{2,10}$ = 15.65, P = 0.001). This interaction is driven by decreased performance for contralesional stimuli at memory loads one (one-tailed paired samples t-tests, p = 0.002) and two (p = 0.013) with performance equalizing between hemifields at three-item loads (p = 0.14).

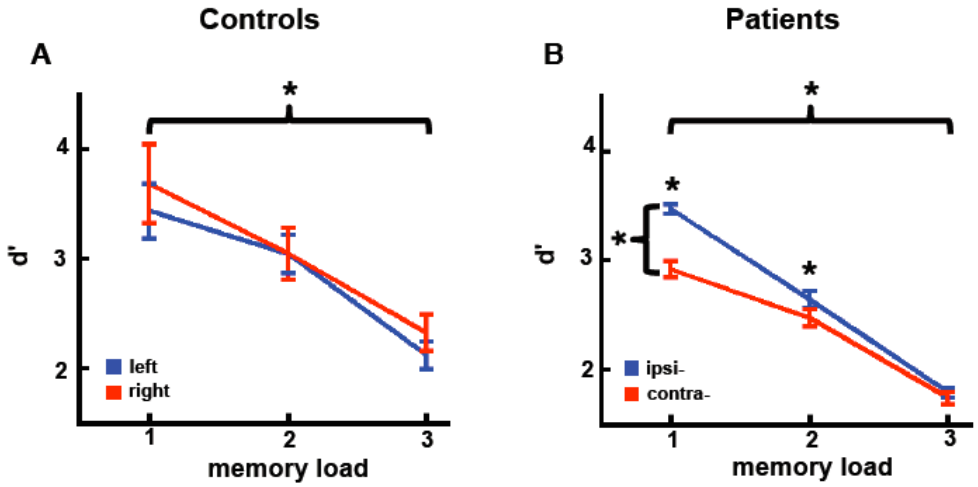

Figure 3.3. Experiment 1: Behavioral Performance. Behavioral accuracy (d') decreases with increasing memory load for both groups. (A) Control subjects perform equally well regardless of hemifield of stimulus presentation. (B) In contrast, patients perform worse for contralesional stimuli, but as well as controls for ipsilesional stimuli. PFC patient deficits manifest as poorer performance for contralesional stimulus at memory loads of one and two items, but performance converges at three items. Error bars denote SEM. *p < 0.05.

This task elicits a lateralized neural event-related potential (ERP) during the delay period. This contralateral delay activity (CDA) is focused over extrastriate cortex and is modulated by the number of items that are currently being maintained in working memory (Vogel & Machizawa, 2004; Vogel, McCollough, & Machizawa, 2005). For controls, we replicated the finding that CDA amplitude increases as memory load increases ($F_{2,10}$ = 9.75, p = 0.004) and that CDA amplitude was equivalent for each hemisphere (set-by-laterality interaction: ($F_{2,10}$ < 1.0; **Fig. 3.4A**$_{1,2}$). However, while the PFC patients showed a similar load increase in CDA amplitude for ipsilesional stimuli ($F_{2,10}$ = 4.77, p = 0.035), this load effect was absent when the memory array was presented contralateral to the lesioned hemisphere (contralesional hemifield, **Fig. 3.4B**$_{1,2}$; $F_{2,10}$ < 1.0). Notably, patient CDA amplitude for contralesional stimuli are of larger amplitude despite their lack of memory load specificity. In a two-way *post hoc* analysis comparing control CDA for right hemifield stimuli to patient CDA for contralesional stimuli we found a main effect of group that corroborates this observation ($F_{1,10}$ = 7.43, P = 0.021), though there was no interaction between group and load ($F_{2,20}$ = 1.30, P = 0.29). Although amplitudes are larger in patients, absolute CDA amplitude is a poor predictor of behavioral performance; rather, it is the slope of the CDA load effect that tracks behavior (Drew & Vogel, 2008; Vogel & Machizawa, 2004).

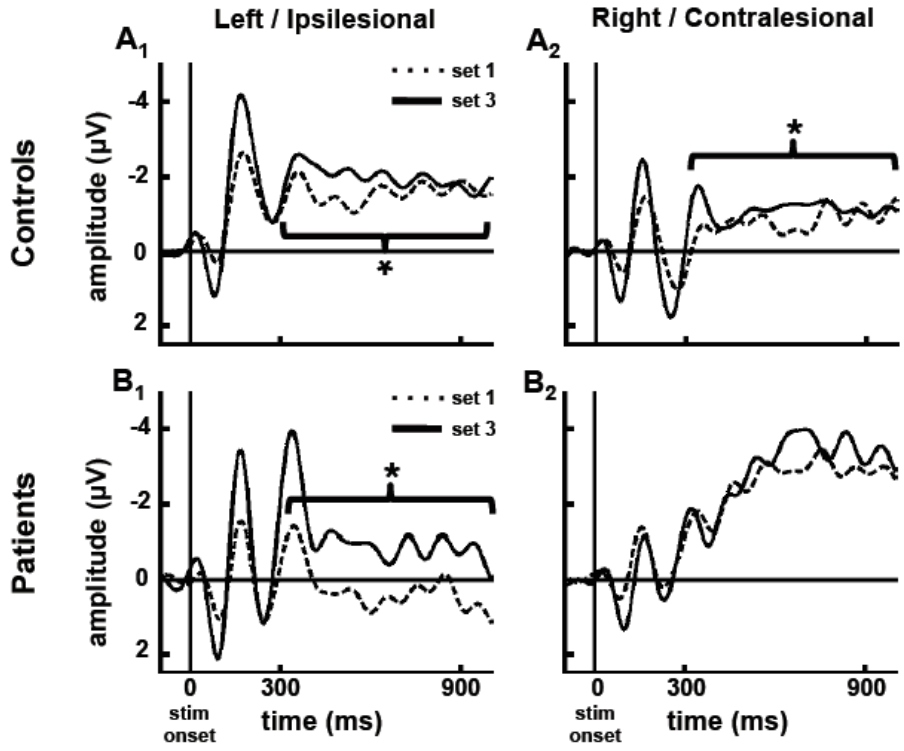

Figure 3.4. Experiment 1: Posterior Contralateral Delay Activity. (A_1, A_2) CDA magnitude in controls increases with number of items held in working memory. (B_1, B_2) In contrast, CDA for patients increases with memory load only for ipsilesional stimuli. Contralesional CDA does not index memory load, consistent with the idea that PFC lesions result in top-down working memory deficits. *$p < 0.05$.

Working memory paradigms generate increased frontal theta (4-8 Hz) oscillatory EEG activity (Bastiaansen et al., 2002; Raghavachari et al., 2001), and here we focus our frontal analyses on the theta band during the memory delay period (see **Methods** for other band analyses which were non-informative). While controls showed negligible frontal theta activity over either hemisphere, patients showed sustained frontal theta activity (600-900 ms) only over their intact hemisphere. This frontal theta activity increased as a function of memory load for contralesional stimuli (**Figs. 3.5A$_1$** and **3.5A$_2$**; $F_{1,5} = 10.45$, $p = 0.023$), but was absent for ipsilesional stimuli ($F_{1,5} < 1.0$), resulting in an interaction in the PFC group between set size and visual field for sustained frontal theta over the intact PFC (**Fig. 3.5A$_2$**; $F_{1,5} = 12.07$, $p = 0.018$) that was not seen in controls (**Figs. 3.5B$_1$** and **3.5B$_2$**; $F_{2,10} < 1.0$) nor over the lesioned cortex (**Fig. 3.6**; $F_{2,10} = 1.05$, $p = 0.39$). This pattern of results cannot be accounted for by eye movement differences between groups or conditions (see **Methods**).

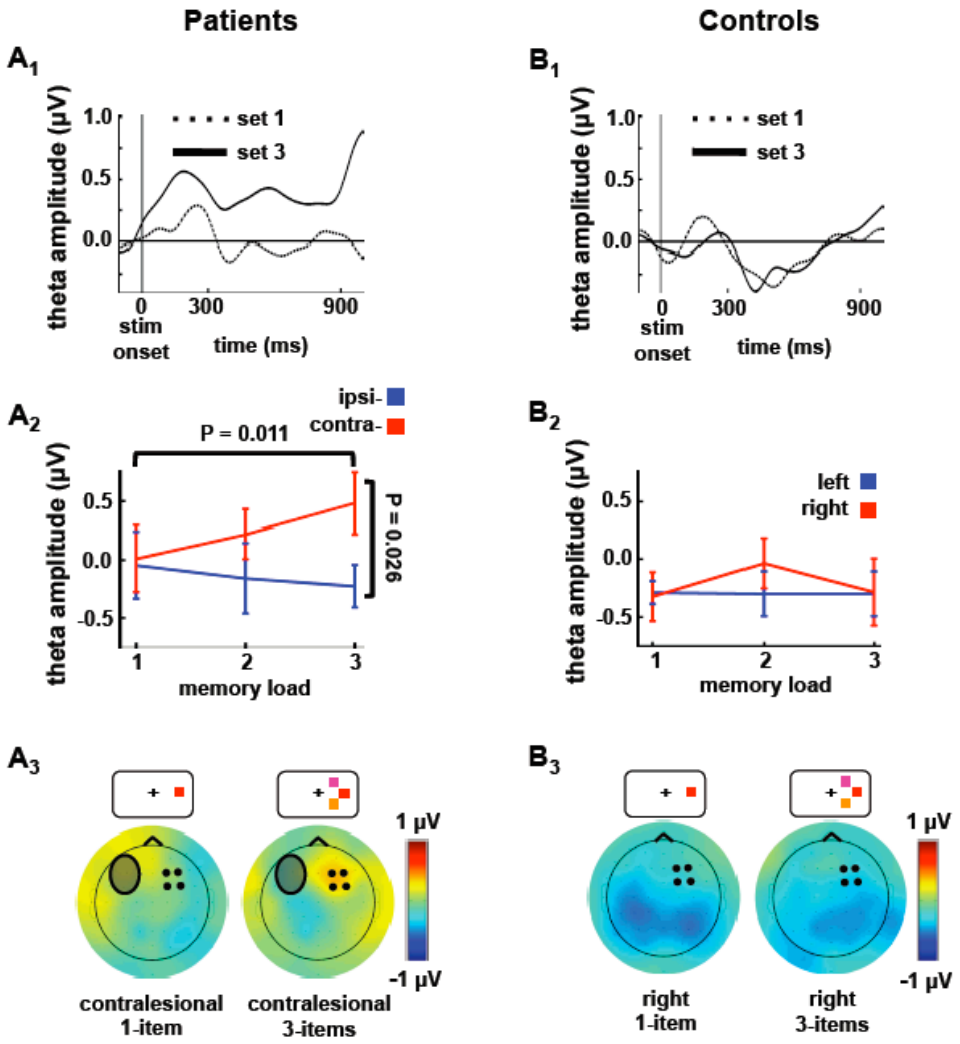

Figure 3.5. Experiment 1: Frontal Load-Dependent Compensation During Visual Working Memory. (A_1-A_3) Patient and (B_1-B_3) age-matched control data showing load dependence of frontal theta activity. (A_1, B_1) Frontal theta waveforms are measured from the intact frontal region represented by the black dots in the scalp topographies in (A_3) and (B_3) and show theta amplitudes for one- (dashed lines) and three-item (solid lines) memory arrays over the frontal sites. (A_1) Time course of the sustained frontal theta load dependence measured over the intact frontal cortex when the lesioned hemisphere is challenged.

(A_2, B_2): Frontal theta amplitude and standard error by memory load and hemifield of stimulus presentation. (A_2) Compensatory theta in patients is largest over intact frontal sites and increases with memory load in response to contralesional stimuli. (B_2) In age-matched controls there is no frontal theta activity difference between one- and three-item or left and right memory arrays. Error bars denote SEM.

(A_3, B_3): Scalp topographies of the difference in theta for contralesion minus ipsilesion (right minus left) activity for three-item memory loads. (A_3) The scalp topography highlights the increased theta in response to contralesional memory load. The shaded oval represents the relative scalp location of the patients' lesions. (B_3) There are no load-dependent activity changes over frontal sites in controls.

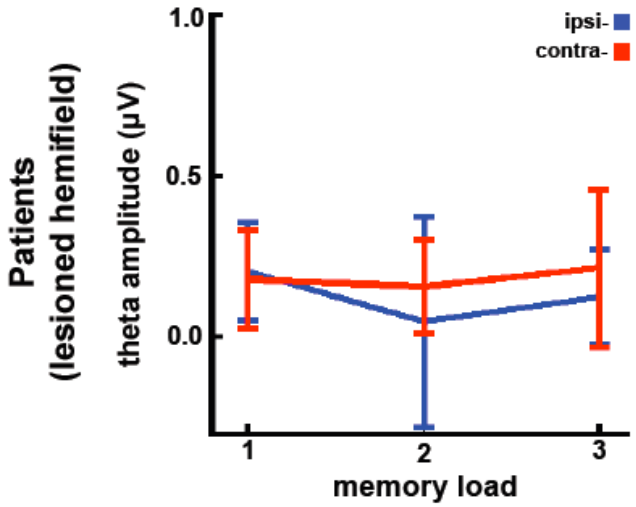

Figure 3.6. Experiment 1: Frontal Theta Activity over Lesioned Cortex. Theta activity over the lesioned PFC is neither affected by memory load nor by hemifield of stimulus presentation, consistent with control data. Error bars denote SEM.

Our hypothesis that intact frontal theta increases are related to memory function necessitate that information from the visual cortex from the lesioned hemisphere crosses to the intact hemisphere for processing by the intact PFC. To examine such information flow we looked at correlations between early visual ERPs (N1 amplitude from 100-200ms) between visual hemispheres. Consistent with the notion that visual information crosses transcallosally between visual hemispheres, N1 amplitude is correlated in both hemispheres in both conditions (Pearson correlation across all trials, all subjects; ipsilesional: $r = 0.62$, $p < 0.0005$; contralesional: $r = 0.68$, $p < 0.0005$). In contrast, for contralesional stimuli only, N1 magnitude of the intact hemisphere and intact frontal theta amplitude are also correlated, partialling out the effects of N1 magnitude of the damaged hemisphere (contralesional: $\rho = 0.076$, $p = 0.003$; ipsilesional: $\rho = 0.007$, $p = 0.40$) across trials (**Fig. 3.7**). Intact frontal theta and N1 magnitude from the damaged hemisphere are uncorrelated partialling out the effects of N1 magnitude from the intact hemisphere (contralesional: $\rho = 0.019$, $p = 0.24$; ipsilesional: $\rho = 0.019$, $p = 0.24$). These findings suggest that the degree of compensatory frontal theta activity is contingent upon the fidelity of the visual information that crosses from the damaged to the intact hemisphere. Although correlation analyses alone cannot directly address information flow *per se*, the timing of the two electrophysiological processes (100-200 ms for N1, 600-900 ms for frontal theta) support our directionality arguments. Importantly, frontal compensatory theta activity in response to contralesional stimuli was

larger for correct trials when compared to incorrect trials, (**Fig. 3.9A**; p = 0.038 for 3-item load) supporting the contention that theta activity is related to correct performance, is thus likely non-pathological, and indexes second to second functional compensation.

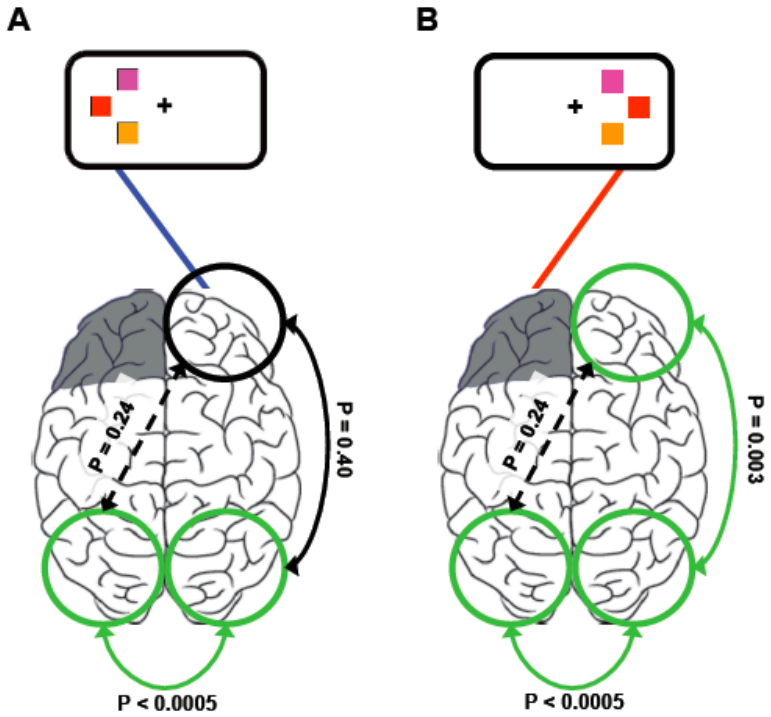

Figure 3.7. Experiment 1: Posterior visual activity is correlated with compensatory frontal theta. (A, B): Consistent with information crossing transcallosally from the visual cortex contralateral to the stimulus over to the opposite hemisphere, N1 amplitude between the ipsi- and contralesional visual cortices is highly correlated across all trials. Unilateral PFC lesions are represented in grey.

(A): In response to ipsilesional stimuli, N1 amplitude between both visual cortices is highly correlated, however there is no correlation between N1 magnitude and frontal theta across trials.

(B): Similar to ipsilesional stimuli, in response to contralesional stimuli, N1 amplitudes are highly correlated between visual cortices. In contrast however, later compensatory frontal theta amplitude is correlated with N1 magnitude only within the intact hemisphere. These results suggest that early visual components are related to later compensatory frontal theta activity consistent with the hypothesis that information enters the visual cortex of the damaged hemisphere and crosses to the intact hemisphere for processing to support working memory.

To test whether the observed compensatory neural activity over the intact frontal cortex generalizes across PFC-dependent cognitive functions, we analyzed data from a lateralized visual attention experiment conducted in patients with unilateral PFC lesions

(Yago et al., 2004) (**Fig. 3.1B**). Subjects viewed a rapid stream of stimuli presented to the left or right visual fields while attending to one hemifield and responding to infrequent targets embedded within a stream of frequent non-target stimuli (see **Methods** for details). Patients were impaired in detecting contralesional targets (repeated measures ANOVA, group-by-hemifield of presentation interaction on arcsine transformed percent correct, ($F_{1, 17} = 7.62$, $P = 0.013$); controls, 95.7% and 94.7% correct for left and right targets, ($p = 0.65$); patients 94.7% and 87.9% correct for ipsi- and contralesion targets, respectively, ($p = 0.027$); one-tailed paired-samples t-tests). However, even though the task placed heavy demands on sustained attention, performance in both hemifields was well above chance (one-sample *t*-tests for both hemifields, $p < 0.0005$). As in experiment 1, preserved behavioral performance was evident despite the fact that the PFC lesion markedly reduced neural responses over visual cortices ipsilateral to the PFC lesion during correct trials (Barceló, Suwazano, & Knight, 2000; Yago et al., 2004).

In contrast to controls, the patients' P1 (60 - 160 ms) and P3 (450 - 650 ms) components of the extrastriate ERP were attenuated in the lesioned hemisphere in response to contralesional targets (P1: $p = 0.003$; P3: $p = 0.009$); all between-group comparisons are one-tailed independent sample *t*-tests) replicating the pattern of attenuated extrastriate activity observed in Experiment 1. Similar decrements have been shown in fMRI studies of aphasic patients with PFC lesions during word learning wherein visual cortical activity in the hemisphere ipsilateral to the lesion was decreased relative to controls (Blasi et al., 2002). A different pattern emerged in the frontal neurophysiological data. The PFC group showed no target-related electrophysiological differences over the intact frontal cortex compared to controls (**Fig. 3.8A**, left panel; $p = 0.63$) in response to ipsilesional stimuli. However, a late frontal positivity (450-650 ms) increased in amplitude in the intact hemisphere in patients in response to contralesional stimuli compared to controls (**Fig. 3.8A**, right panel and **Fig. 3.8B**; $p = 0.003$). Just as in Experiment 1, this enhanced electrophysiological activity in patients in response to contralesional targets was absent on error trials (**Fig. 3.9B**; $p < 0.0005$). There were no differences in intact frontal oscillatory activity in this target detection task (see **Methods**).

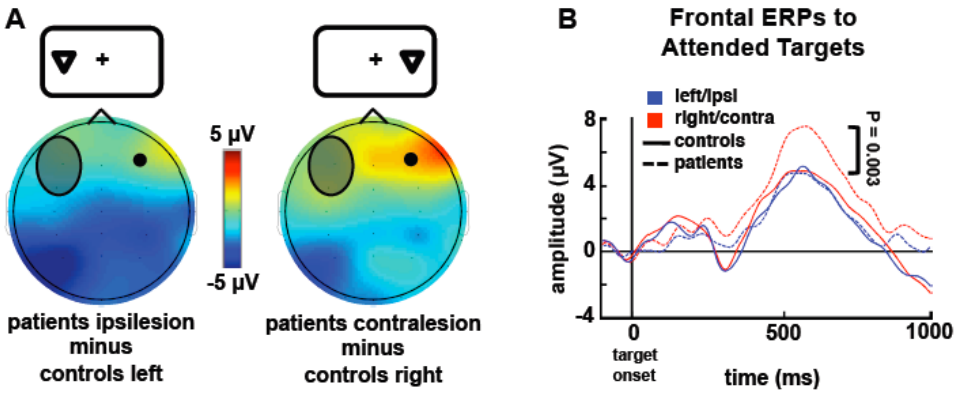

Figure 3.8. Experiment 2: Frontal Load-Dependent Compensation During Visual Attention. (A): Late frontal positivity (450-650 ms) in patients is enhanced over the intact PFC and attenuated over the extrastriate in the damaged hemisphere compared to controls in response to attended targets presented contralateral to the side of the lesion.

Topographies show average frontal positivity differences—patient minus control difference waves—in response to left/ipsilesional (left panel) or right/contralesional (right panel) targets. The shaded oval represents the relative scalp location of the patients' lesions.

(B): Frontal ERPs show the time course of activity over the intact PFC in comparison to controls. The dashed blue line represents the response to ipsilesion target stimuli. The dashed red line shows the enhanced activity over intact PFC when stimuli are delivered contralesionally. The ERP waveforms are measured from the intact frontal region represented by the black circle in (A). Error bars denote SEM.

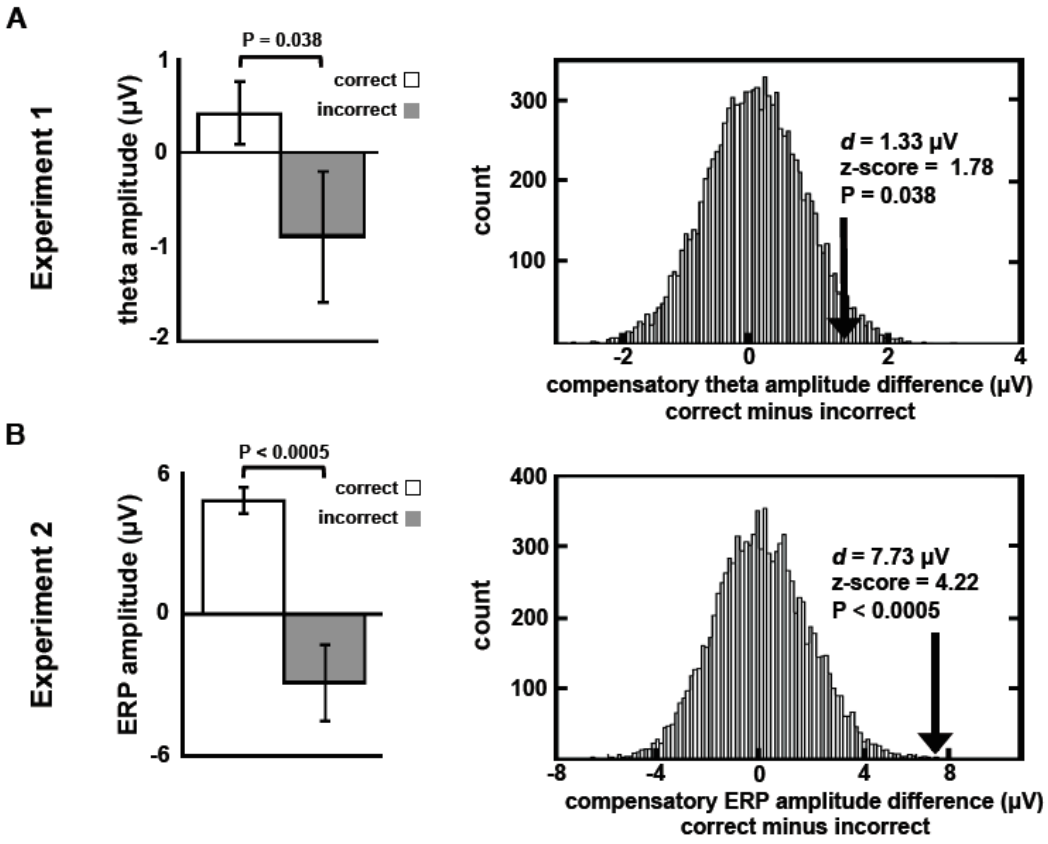

Figure 3.9. Compensatory Activity and Standard Error During Correct Versus Incorrect Trials. Left panels show means for correct and incorrect trials, right panels show distributions of differences from resampling statistics (see **Methods**). (A) Sustained frontal theta amplitudes over intact PFC in patients are larger during correct trials than during incorrect trials in response to three-item contralesional stimuli. Error bars denote SEM. (B) Frontal ERP amplitudes over intact cortex in patients in response to correctly identified contralesional targets are larger than for incorrect trials.

3.4 Discussion

Our results provide evidence that the intact, non-lesioned hemisphere dynamically compensates for the damaged PFC when the damaged hemisphere is challenged with either memory or attentional loads. In a recent paper examining alterations in cortical activity related with normal, healthy aging (Davis et al., 2008), two criteria were established as necessary for cortical activity differences in older adults to be more likely to be regarded as "compensatory". First, novel activity increases not seen in normal controls must be associated with correct behavioral outcomes. Second, deficits in processing by one region must be associated with increases in activity in the "compensatory" region. Consistent with the first criterion, increases in activity over the intact PFC are enhanced on correct trials in both of our experiments. With regards to the second criterion, by nature of our experimental designs as well as our patient selection, when we preferentially challenge the damaged hemisphere our PFC patients have inherent processing deficits due to unilateral PFC damage, and associated top-down cognitive deficits are reflected by decreased electrophysiological responses in the posterior visual cortex. The fact that we observe increased activity over the intact PFC which correlated with posterior visual activity specifically when the damaged hemisphere is challenged satisfies the second criterion.

Thus, we suggest that the observed neural pattern supports a mechanism of compensation whereby the intact hemisphere plays a dynamic and flexible role in mediating the cognitive functions impaired by unilateral PFC injury. In both experiments PFC damage resulted in marked attenuation of neural activity in the extrastriate cortex ipsilateral to PFC damage, yet the patients performed well above chance even when stimuli were delivered to the impaired field. Our findings account for this behavioral/electrophysiological discrepancy by providing evidence that the intact frontal cortex is assuming control of the task on a sub-second time scale. That is, although patients show attenuated responses in ipsilesional visual cortex, these decreases are accompanied by rapid increases in activity over intact frontal cortex (**Fig. 3.2B**).

The electrophysiological increases we observed over the intact frontal cortex varied with load and predicted behavior as evidenced by their increased neural activity during correct compared to incorrect task performance. We did not observe any such electrophysiological changes when stimuli were presented ipsilesionally. This supports and extends findings in motor recovery where selective disruption of the intact motor cortex using transcranial magnetic stimulation increases simple reaction times (Johansen-Berg et al., 2002). Here we expand the findings of motor recovery and demonstrate a dynamic compensation model that contrasts with a fixed compensation model. By using lateralized memory and attention tasks to alternately challenge the damaged or intact cerebral hemispheres we highlight intrahemispheric electrophysiological deficits in top-down visual working memory and attention processing. Furthermore, by taking advantage of the temporal resolution of EEG we show that neural compensation occurs rapidly as task demands increase compensatory requirements.

In Experiment 1, theta power over intact frontal cortex increased with memory load when the damaged hemisphere was challenged. Frontal theta amplitude has been previously shown to be modulated by memory load and is proposed to represent active maintenance of the visual stimuli by prefrontal cortex (Jensen & Tesche, 2002). In Experiment 2, late frontal activity, linked to attentional allocation, increased over the intact cortex in response to

targets presented only to the damaged hemisphere. If these effects were purely modulated by task difficulty we would expect load-dependent increases in frontal activity in either the control group or in response to ipsilesional stimuli. Neither pattern was observed.

Although we found robust, lateralized theta delay period activity in Experiment 1 in PFC patients when the damaged hemisphere was challenged, we note that we observed no frontal theta activity in normal controls. Several scalp and intracranial EEG studies have found that frontal theta activity increases with memory load (Raghavachari et al., 2001; Onton, Delorme, & Makeig, 2005). In scalp EEG this usually manifests as a midline frontal theta increase. Notably, these studies most often make use of a Sternberg or *n*-back paradigm in which multiple items are presented in succession, or in delayed match to sample paradigms similar to ours but across longer (3-10 sec) delays. Single-unit, intracranial electrophysiology, and fMRI studies also show similar PFC delay-period activity, however these studies often also make use of successive visual presentation and/or longer delays. Sternberg and *n*-back paradigms with successive item presentation may require more fronto-striatal resources to filter out irrelevant distractors (McNab & Klingberg, 2008) and may not directly reflect only simple visual template maintenance.

The fact that we observe frontal theta activity in our patient group across a relatively short delay and with a relatively low memory load may reflect a shift in the threshold at which large groups of PFC neurons are recruited to perform the task. That is, the fronto-parietal network involved in maintaining a template of the visual stimulus during the delay period may be less prefrontally dependent in normal controls across a short delay, with fewer prefrontal neurons participating in active stimulus maintenance. However, in patients with unilateral PFC lesions, the frontoparietal network in the intact hemisphere behaves normally for ipsilesional stimuli; that is, at short delays and low loads the PFC is relatively inactive at a level observable in scalp EEG. However, that same network in the intact hemisphere becomes active at a much lower time/load threshold in response to contralesional stimuli, reflecting a dynamic compensatory process to assist the damaged hemisphere. Also of note is the fact that the compensatory activity we observe in our patients in Experiment 2 is relatively late and may reflect post-decision processes. While this may be true in the context of a single-trial, over the course of an entire task post- decision processes related to the increased frontal EEG activity may lead to improved performance. This design requires subjects to maintain an internal representation of the target stimulus across the entire task, and these late potentials may reflect a reinforcement of the template. While we cannot directly support this assertion, the fact that intact frontal activity is associated with correct performance is in agreement with the argument that this activity reflects a compensatory mechanism.

Models of anatomical connectivity changes in response to unilateral PFC lesions show that fronto-parietal connectivity is drastically reduced within the damaged hemisphere, as is fronto-frontal connectivity between the damaged and intact hemispheres (Alstott et al., 2009). Thus, in order for subjects to correctly perform our lateralized visual working memory task, the most likely route through which the necessary information can be processed and maintained during the delay period is across the posterior corpus callosum. That is, at an early stage post-stimulus onset, visual information must cross from visual cortex in the damaged hemisphere to the intact hemisphere for processing by the intact PFC. This idea is corroborated by our finding that early visual potentials are correlated across

hemispheres, and that these early potentials correlate with later frontal theta amplitude within the intact hemisphere only when the damaged hemisphere is challenged (**Fig. 3.7**).
We propose that the visual information delivered to the contralesional hemisphere is transferred trans-callosally to the intact hemisphere where the intact PFC assumes task control as needed on a trial-by-trial basis. Support for this contention is provided by studies in non-human primates revealing that top-down PFC control over visual cortex during memory retrieval relies on callosal information transfer (Hasegawa et al., 1998; Tomita et al., 1999). Our results show that the neural changes observed in movement recovery after motor cortex damage (Johansen-Berg et al., 2002; Ward et al., 2007) expand to cognitive domains and apply to a dynamic model of memory and attention compensation by the intact, undamaged cortex. We demonstrate that brain recovery can manifest itself as transient changes in information processing occurring on a sub-second timescale after the injured brain has been challenged to perform, supporting a dynamic and flexible model of neural plasticity.

Chapter 4

Role of Callosal Transfer in Prefrontal Dependent Object-Spatial Integration

Abstract

Recovery after brain damage is mediated in part by homologous regions in the non-damaged hemisphere. We tested the role of interhemispheric information transfer in cognitive compensation by examining ten patients with unilateral prefrontal cortex (PFC) lesions who performed a lateralized visual object-spatial integration task designed to alternately challenge the intact or damaged hemispheres. We employed a visual mask to selectively interfere with processing of task-relevant visual information by the intact cortex. We show that unilateral PFC lesions impair object-spatial integration and demonstrate exacerbation of this impairment by interfering with callosal transfer of visual information. Specifically, PFC patients were further impaired in object-spatial integration when a visual mask was presented during the time when visual information was being transferred from the damaged to the intact hemisphere. These results highlight both the critical role of PFC in object-spatial integration and the key role of callosal transfer in cognitive compensation after unilateral PFC damage.

4.1 Introduction

The ability to navigate a complex visual world relies upon knowing both what and where an object is located. This capacity makes the difference between recognizing the red brake light on the motorcycle right in front of you from the red stoplight far ahead. Distinct ventral "what" and dorsal "where" pathways support object identification and location, yet we seamlessly integrate object form and location information into a unified percept (Smith et al., 1995; Ungerleider & Haxby, 1994). Determining how and where this integration takes place is a fundamental problem in visual cognition; a candidate area supporting this process is the prefrontal cortex (PFC), which shares reciprocal connections with both the ventral and dorsal processing streams (Romanski et al., 1999) and maintains separate object and spatial domains (Wilson, Scalaidhe, & Goldman-Rakic, 1993). Human electrophysiological and fMRI studies, as well as animal single-unit studies, support the notion that the lateral PFC is a conjunction area for visual information and location (Gronau, Neta, & Bar, 2008; Rao, Rainer, & Miller, 1997; Simon-Thomas et al., 2003; Tomita et al., 1999). Interestingly, Simon-Thomas et al., observed a performance boost during object-spatial integration compared to separate two-item object or two-item spatial tasks, suggesting that object and spatial information are processed in parallel, rather than serially.

In our study we sought to examine two distinct hypotheses. First, given previous neuroimaging and single-unit findings related to object-spatial integration, the PFC appears to be a critical integration region for separate object-spatial information streams. To address whether human PFC is critical for object-spatial integration we tested ten patients with unilateral PFC lesions (**Fig. 4.1**) and age-matched controls who performed a speeded, lateralized visual object-spatial recognition task (**Fig. 4.2**). By examining patients with unilateral brain lesions we can extend the results of neuroimaging and single-unit research to address the causal role of the PFC in object-spatial integration with the hypothesis that, if the PFC is a critical component of the object-spatial integration network, patients with unilateral PFC lesions will be behaviorally impaired relative to control subjects.

Previous studies with patients with unilateral PFC lesions (Barceló, Suwazano, & Knight, 2000; Yago et al., 2004) have demonstrated a main effect of visual hemifield on performance wherein behavioral deficits are observed in PFC patients when stimuli presented in the contralesional visual hemifield. However, these behavioral deficits are relatively subtle given the severity of the top-down extrastriate electrophysiological deficits in the hemisphere of the PFC damage that is routinely observed in these patients. Research into functional compensation and recovery suggests that, over time, individuals often regain some degree of previously lost functions. Motor (Johansen-Berg et al., 2002; Ward et al., 2007), language (Blasi et al., 2002), and attention (Corbetta et al., 2005; He et al., 2007) recovery are associated with task-dependent increases in functionally and anatomically homologous brain regions in the non-damaged hemisphere (Nudo, 2007).

These previous findings suggest that interhemispheric transfer of task-relevant information would be a critical component of compensatory support by the intact hemisphere. Thus, we designed our experiment to test the second hypothesis that transcallosal transfer of visual information is crucial for cognitive compensation. We employed a lateralized visual stimulus design to emphasize the behavioral deficits in PFC patients in response to contralesional stimuli. We then incorporated a visual mask into our design to specifically test the hypothesis that the intact PFC would compensate for the

damaged hemisphere when the damaged hemisphere was challenged by a contralesional stimulus. In this model, visual information presented to the lesioned hemisphere would be transferred to the non-lesioned hemisphere via the corpus callosum (Tomita et al., 1999) whereby the non-lesioned hemisphere would assume task control and assists in stimulus processing.

To test the hypothesis that the intact hemisphere compensates for unilateral PFC damage, we included in our design a visual mask presented to the hemifield opposite the task stimulus during two time windows: an early mask presented in conjunction with the task stimulus (0-500 ms after stimulus onset) or later during the delay period (500-1000 ms). This mask was used to manipulate the fidelity of information transfer between the hemispheres where the early mask would reduce the fidelity of the relevant information that crosses into the opposite hemisphere, whereas the late mask served to control for the effects of distraction while allowing visual information to transfer between hemispheres more completely. We hypothesized that patients with unilateral PFC lesions have an impaired object-spatial integration network and would be impaired compared to controls. Importantly, we also hypothesized that patients would show a further performance decrement for contralesional stimuli only when we interfered with transcallosal information transfer by the use of an early visual mask.

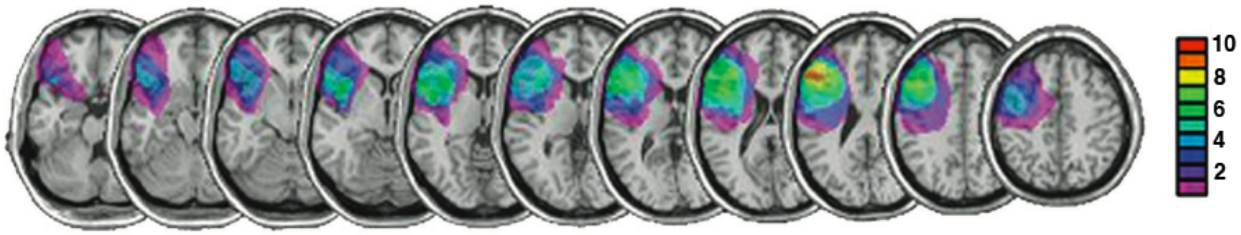

Figure 4.1. Patient MRIs. Overlay of the average damaged area in the PFC lesion group (n = 10). MRI reconstructions were obtained using MRIcro (Rorden and Brett, 2000). Patients with right hemisphere lesions (n = 2) were transcribed to the left hemisphere for display purposes. The color bar indicates the number of patients with a lesion in a specific region. The area of greatest lesion overlap across the patients occurs in Brodmann areas 9 and 46, centered in the middle frontal gyrus.

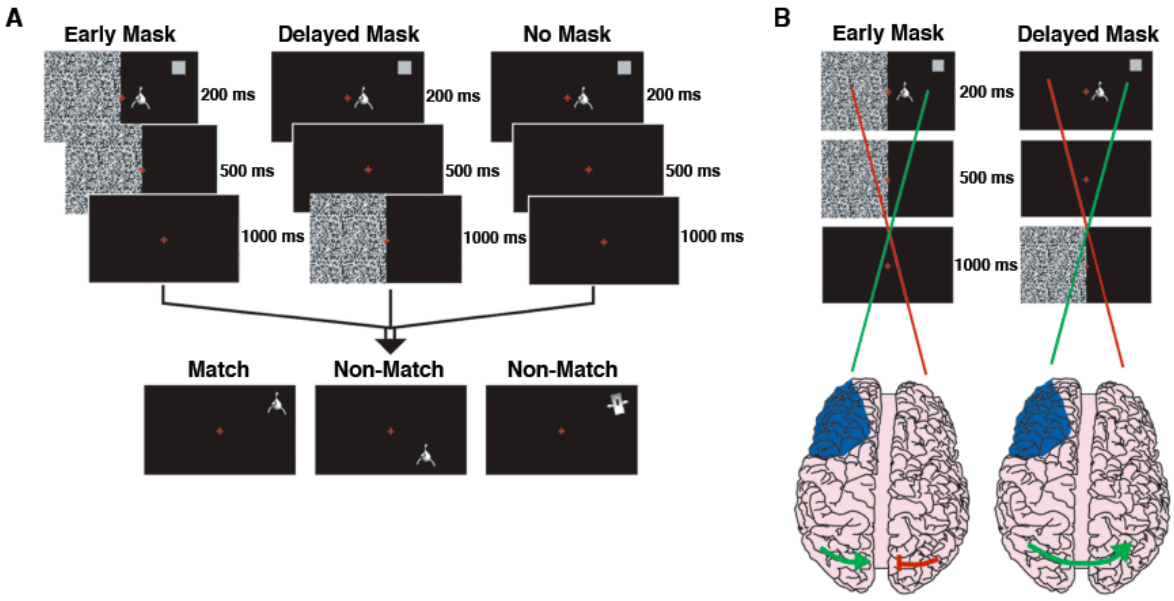

Figure 4.2. Behavioral Paradigm. (**A**) In all three conditions (early mask, delayed mask, and no mask) subjects were presented with an unidentifiable, non-verbalizable, black and white object and a gray location cue (see Materials and Methods for details). (**B**) Schematic of the main hypothesis. In the early mask condition the mask adds noise during the processing of the visual object and spatial cue by the non-lesioned hemisphere, disrupting transcallosal transfer of visual information (disconnected green/red line over visual cortex). In the delayed mask condition, however, task-relevant visual information crosses the corpus callosum allowing the non-lesioned hemisphere to assist in object-spatial recognition (intact green line over visual cortex). Blue shading illustrates the location of the subjects' lesions.

4.2 Methods

Ten patients with unilateral damage to the lateral PFC (8 left and 2 right lesions, aged 43-76; see **Fig. 4.1**) and eleven age-matched controls (aged 42-74) were tested. All subjects consented to participate in the study and were recompensed. All patients were at one year post stroke at the time of testing. The research was approved by the UC Berkeley Committee for the Protection of Human Subjects. Subjects were tested individually on a desktop computer in a dark, soundproof booth. They sat ~90 cm from the computer monitor. E-prime (Psychology Software Tools, Inc., Pittsburgh, PA) was used for stimulus presentation and data analysis was performed using SPSS® (Rel. 16, Chicago: SPSS Inc.).

During the tasks subjects fixated on a red cross in the center of a computer screen. An experimenter visually monitored eye movements to ensure that subjects maintained fixation and minimized saccades during the task. Trials where subjects made saccades were excluded from analyses. An unidentifiable object (see Simon-Thomas et al., 2003) was presented 3 degrees from the fixation cross and paired with a location cue which appeared in one of seven different locations on the screen in the same hemifield (200 ms duration to minimize saccadic eye movement, i.e., foveating to the stimuli). Stimuli consisted of a the

gray location cue (~4.0 x 4.0 cm), five different unidentifiable, non-verbalizable, black and white objects (~5.0 x 5.0 cm), and a static white noise visual mask flashing at a rate of 16 Hz. After a 1000 ms delay subjects decided whether the test object was the same as the initial object and whether it appeared in the same spatial location as the initial cue (integration effect) by pressing one of two buttons on a computer keyboard. If a response was not made the next trial would begin after 2000 ms. Trials were randomized to either the left or the right visual field with equiprobability. There were three mask conditions: early mask, delayed mask, and no mask. In the early mask condition the noise mask was presented for 500 ms in the field opposite to the concurrently delivered object-spatial stimuli to reduce the fidelity of interhemispheric transfer of the visual stimuli to the intact hemisphere. In the delayed mask condition the mask was presented for 500 ms following a 500 ms delay after the stimulus onset. This condition served as a control for the potential distracting effects of the mask. In the no mask condition patients were presented with only the object and location cues. During the test phase, if the test object was the same as the original object and appeared at the initial location of the cue, the trial was a match. If either the object or the location was different, the trial was a non-match.

Accuracy was quantified using a d' statistic, which considers both correct responses and false alarms to overcome the problem of response bias (Green & Swets, 1966). Statistical comparisons were run using multiple repeated measures ANOVA on reaction time and accuracy separately with mask (early mask vs. delayed mask), hemisphere of presentation (ipsilesional/left vs. contralesional/right), and response condition (match vs. non-match) as within-subjects factors and group (control vs. PFC) as the between-subjects factor. Our experiment was designed specifically to examine the hypothesis that an early mask would affect behavior for contralesional, rather than ipsilesional stimuli in the PFC patient group. Accordingly, we examined the effect of hemisphere of presentation on behavior within the patient group in a planned mask X hemisphere contrast. All pair-wise t-tests were performed for each group separately to examine the effect of hemifield of stimulus presentation on behavior for a total of 8 total pair-wise comparisons (2 group, 2 task, and 2 response condition); a conservative Bonferroni correction was applied giving an adjusted alpha of 0.00625.

4.3 Results

There was a main effect of group on accuracy wherein the PFC patients performed worse than controls ($F_{1,19} = 11.85$, $p = 0.003$) (**Fig. 4.3A**). There was no main effect of response condition, mask, or hemisphere, nor any interaction between these variables, on accuracy for either group ($p > 0.05$ all comparisons). Notably the PFC group performed well above chance levels in all conditions (*post hoc* one sample t-tests for each response condition, mask, and hemisphere trial type; $p < 0.005$ for each comparison). This suggests that, although unilateral PFC lesions cause behavioral impairments, unilateral lesions are not sufficient to abolish object-spatial integration.

Similar to the accuracy results, overall reaction times were slower in the PFC group (main effect of group, $F_{1,19} = 13.99$, $p = 0.001$) (**Fig. 4.3B**). There was also an overall main effect of response type ($F_{1,19} = 7.75$, $p = 0.012$) wherein subjects were slower to respond during non-match trials. These results suggest that participants required more time to

process and evaluate non-match stimuli before responding. Within the control group there was no effect of mask or hemisphere. In contrast to control subjects, PFC patients demonstrated a main effect of hemisphere of lesion on reaction time ($F_{1,9}$ = 13.63, p = 0.005). The effect of hemisphere was driven by reaction time differences during match trials in the predicted condition and direction. That is, PFC patients had slowed reaction times for contralesional stimuli only when processing by the intact hemisphere was disrupted using an early mask when information would normally be transferred between the visual hemispheres (t_9 = 5.50, p < 0.0005) (**Fig. 4.3C** and **Table 1**). This disruption manifested as an average of a 65 ms response time deficit within the PFC group for masked stimuli presented to the contralesional hemisphere compared to those presented to the ipsilesional hemisphere.

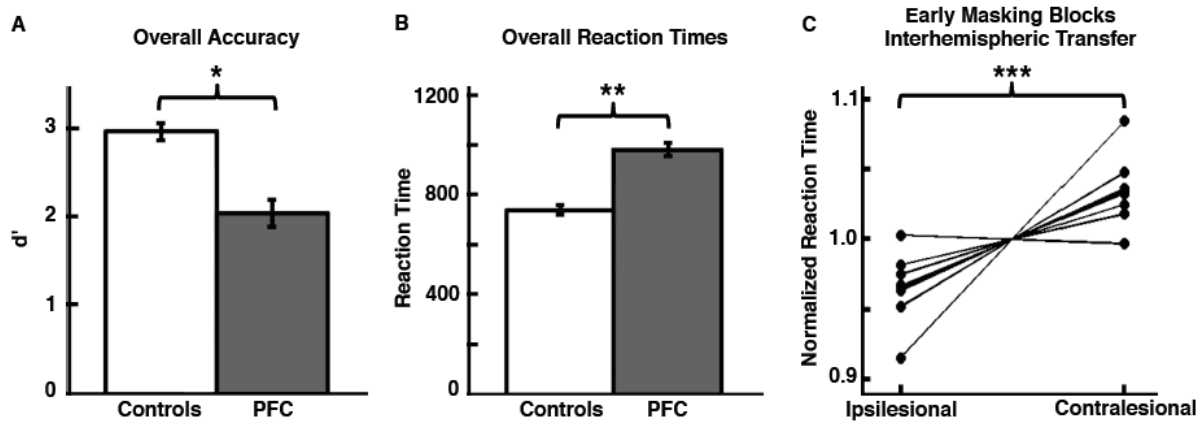

Figure 4.3. Behavioral Results. (**A**) Patients showed an overall impairment in object-spatial integration resulting in decreased stimulus sensitivity (d') across all trials and conditions.

(**B**) Similarly, patients showed an overall response impairment resulting in increased reaction times across all trials and conditions. (**C**) Plots of individual PFC patient reaction times for ipsilesional (left) and contralesional (right) hemifield stimuli in the early mask condition illustrating the behavioral effect of the mask. Nine out of the ten participants show a hemispheric cost. Reaction times are normalized by mean reaction time for each subject to highlight the direction of the effect while preserving relative effect size.

Error bars indicate SEM. (*), significant difference with p = 0.003; (**), significant difference with p = 0.002; (***), significant difference with p = 0.001.

Table 4.1
Summary of reaction times

	Control, M (SEM)		PFC, M (SEM)	
	Left	Right	Ipsilesional	Contralesional
No Mask				
Match	714 (45)	712 (37)	929 (47)	958 (42)
Non-match	774 (46)	762 (44)	1038 (65)	1055 (63)
Delay Mask				
Match	726 (42)	731 (38)	910 (45)	946 (56)
Non-match	748 (42)	752 (41)	1008 (69)	1046 (65)
Early Mask				
Match	713 (40)	733 (39)	904 (43)	969 (39)*
Non-match	755 (40)	764 (44)	1028 (76)	1047 (64)

Note: M, mean; SEM, standard error of the mean. Hemispheric differences: *$p < 0.0005$.

4.4 Discussion

The goal of this study was to investigate the role of the intact PFC in supporting correct object-spatial integration in patients with unilateral PFC damage. During the integration phase, initially separate object and location information is fluidly combined into a single unified percept within a few hundred milliseconds. Primate studies have shown that the PFC exhibits differential neural firing patterns to "what", "where", and "what-where" combined information (Rao, Rainer, & Miller, 1997; Wilson, Scalaidhe, & Goldman-Rakic, 1993). Human electrophysiology and fMRI studies have demonstrated that the PFC might act as a conjunction area for object-spatial integration (Simon-Thomas et al., 2003; Gronau, Neta, & Bar, 2008). We show that humans with unilateral PFC lesions have impaired ability to integrate object and spatial information. Despite these impairments, subjects still performed well above chance levels. So although PFC lesions impair object-spatial integration, a unilateral lesion is not sufficient to abolish this cognitive ability.

We posited that the intact, non-lesioned PFC assisted the damaged hemisphere to support object-spatial integration. We found that the PFC patients show an effect of hemisphere of presentation wherein they were slower to respond to contralesional stimuli only when we interfered with the transfer of visual information between the two visual cortices with a visual mask presented to the intact hemisphere. This deficit emerged only when the mask was presented in conjunction with the task-relevant stimuli during the time window when visual information usually transfers between the two hemispheres (i.e., within 500 ms after stimulus onset). This effect cannot be explained simply by the distracting effect of the early mask as we controlled for this possibility by including a delayed mask condition where the mask was presented for the same amount of time as in the early mask condition. In the delayed mask condition the mask did not appear until 500 ms after the onset of the object-spatial stimuli, well after the information would have transferred from the damaged to

intact hemisphere. Furthermore, reaction times were slower in both groups for non-match compared to match trials. This suggests that subjects required more time to evaluate object-spatial information when the object was not located in the cued spatial region. One plausible explanation for this effect would be that, during object-spatial disjunctions, subjects had to perform and an extra processing step to recognize the disjunction.

It is important to note that we observed an overall behavioral deficit in object-spatial integration in patients with unilateral PFC lesions. These deficits manifested both as an overall decrement in accuracy as well as increased reaction times. The enhanced deficits caused by the visual mask manifested as increased reaction times during the match trials. These data provide neuropsychological evidence that the lateral PFC is a key node for the integration of object form and location. They also support the notion that callosal transfer to the non-lesioned hemisphere contributes to the patients' abilities allowing them to conduct goal-directed behaviors successfully, even after suffering unilateral brain damage. Research on macaques suggests that the posterior corpus callosum is necessary for interhemispheric transfer of visual information but once the information is transferred, long-term retrieval is mediated by prefrontal cortical communication and is not affected by a posterior corpus callosum split (Hasegawa et al., 1998). Here we show how a lateralized visual paradigm can be used to assess the role of the PFC in object-spatial integration. Furthermore, we show that masking the intact visual cortex impairs performance in patients with unilateral PFC lesions, supporting the contention that intact homologous brain regions support cognitive functions after brain damage.

Chapter 5

Hemicraniectomy: A New Model for Human Electrophysiology with High Spatio-Temporal Resolution

Abstract

Human electrophysiological research is generally restricted to scalp electroencephalography (EEG), magnetoencephalography, and intracranial electrophysiology. Here we examine a unique patient cohort that has undergone decompressive hemicraniectomy, a surgical procedure wherein a portion of the calvaria is removed for several months during which time the scalp overlies the brain without intervening bone. We quantify the differences in signals between electrodes over areas with no underlying skull and scalp EEG electrodes over the intact skull in the same subjects. Signals over the hemicraniectomy have enhanced amplitude and greater task-related power at higher frequencies (60-115 Hz) compared to signals over skull. We also provide evidence of a metric for trial-by-trial electromyography/EEG coupling that is effective over the hemicraniectomy but not intact skull at frequencies >60 Hz. Taken together these results provide evidence that the hemicraniectomy model provides a means for studying neural dynamics in humans with enhanced spatial and temporal resolution.

5.1 Introduction

Although early research on patients with skull defects was successful and lead to the discovery of the EEG, there has not been a systematic, within-subjects comparison of task-relevant EEG signals between electrodes placed over a large skull opening and those placed over the skull in human behavioral EEG. To address this issue we examined three human participants who had undergone a surgical procedure wherein a portion of their skull was surgically removed for several months. This procedure, known as a decompressive hemicraniectomy, is an increasingly common, potentially life-saving neurosurgical procedure performed to reduce damage from an uncontrolled elevation in intracranial pressure (ICP) that frequently occurs following severe traumatic brain injury (TBI) and large-volume ischemic stroke. Many studies have shown that decompressive hemicraniectomy for elevated ICP in TBI and stroke reduces mortality and improves patient outcome (Huang et al., 2008; Hofmeijer et al., 2006; Juttler et al., 2007; Vahedi et al., 2007; Yang et al., 2009). In the subjects included in this analysis, a large portion of the calvaria was removed exposing the central sulcus and Sylvian fissure regions, providing a window devoid of bone over the primary motor and auditory cortices without contamination from underlying muscle activity. Thus, electrodes over the hemicraniectomy site are substantially closer to the underlying neural sources of the EEG. Based on the extant literature on breach rhythms we hypothesized that that data from the electrodes placed over the hemicraniectomy site would show enhanced signal characteristics in comparison to electrodes placed over the intact skull.

In this report we aim to emphasize the improved quality of the electrophysiological signals recorded over the site of hemicraniectomy in order to highlight the utility of these patients for human cognitive neuroscience research. To this end, we compared electrodes over the hemicraniectomy with homologous electrodes over the intact skull. As with any new method, we first examine raw signal differences, with the hypothesis that, absent intervening skull and with electrodes closer to the cortical signal sources, raw time-series amplitudes would be larger, and power across physiological frequency bands (theta, alpha, beta, and low and high gamma) would be greater, and noise in the higher frequencies often contaminated by muscle artifacts would be lower. Furthermore, without spatial smoothing due to influences of skull tissues and/or distance from source, we hypothesized that natural interelectrode correlations will be lower.

In order to test the utility of this method in behavioral human cognitive neuroscience, we examined the effects of the hemicraniectomy on well studied time-frequency and event-related potential (ERP) electrophysiological measures with the hypothesis that task-related potentials will have greater amplitude and enhanced power across a wider frequency range. Because eye-movement artifacts are a common noise source in human behavioral electrophysiological studies, we also examined the effects of the hemicraniectomy on blink amplitudes with the hypothesis consistent with recent simultaneous scalp and intracranial EEG recordings (Ball et al., 2009) that blink amplitudes would be reduced over the hemicraniectomy.

Here we show that signals recorded over the hemicraniectomy have higher spectral power, improved interelectrode spatial independence, reduced artifact susceptibility, and enhanced task-related power at higher frequencies (>60 Hz, high gamma; γ_H) compared to homologous electrodes over intact skull. To demonstrate that the improved signal characteristics may serve a practical purpose, we also introduce a movement-related EEG

interfrequency coupling metric that correlates with arm movement that is maximally effective using broadband γ_H over the site of the hemicraniectomy.

5.2 Methods

5.2.1 Subjects

Because of the novelty of this method we focus and report on the various methodological challenges we faced. We initially recorded EEG from six participants (four males, two females) each of whom underwent surgical hemicraniectomy as a treatment for deteriorating neurological status resulting from increased intracranial pressure due to TBI. All craniectomies were performed at San Francisco General Hospital. At the time of study, each subject was an outpatient with at least four weeks recovery time following their decompressive surgery. All subjects gave informed consent in accordance to our study protocol approved by the University of California, Berkeley and UCSF Committees on Human Research. Subjects were tested in a sound-attenuated EEG recording room at the University of California, Berkeley in an outpatient setting.

Three subjects were eventually excluded from all analyses due to trauma-related complications mitigating the quality of EEG recording. One of these three subjects developed a diffuse extra-axial hygroma—a collection of proteineous cerebral spinal fluid on the outside of the brain—that can be present for several weeks to months post-surgery. This fluid increases the distance between the recording electrodes on the surface of the skin and the underlying brain, introducing noise and reducing signal strength. The two remaining subjects were excluded because of widespread cortical damage affecting both motor and auditory structures. All three of these subjects had reduced amplitude and noisy EEG signals making them unsuitable to test the main hypothesis. The three remaining subjects who form the basis for the current report were cognitively intact with minimal or no cortical damage at the sites of EEG recording, they performed the two behavioral tasks well, and had reliable EEG signals. All three subjects examined in this report had intact scalp over the site of the hemicraniectomy at the time of EEG. None of these subjects had a significant hygroma at the time of testing and none had any damage in motor or auditory cortices.

Subject 1 had a left hemicraniectomy; of the 64 scalp electrodes, 11 frontal to central-parietal electrodes were situated over the hemicraniectomy (electrode name and approximate underlying Brodmann Area [Koessler et al., 2009; Okomoto & Dan, 2005]): F3 (BA8), F5 (BA46), F7 (BA45), FC3 (BA6), FC5 (BA6), FT7 (BA22), C3 (BA1-2-3), C5 (BA1-2-3), T7 (BA21), CP5 (BA40), and TP7 (BA21). Subject 1 sustained a gunshot wound to the left frontal lobe anterior to premotor and motor cortices. His Glasgow Coma Scale (GCS) was 14 on admission. The patient was taken to the operating room for debridement of the gunshot wound and a decompressive hemicraniectomy was performed to prevent further neurological deterioration from increasing intracranial pressure from the initial penetrating brain injury. At the time of EEG testing his memory, attention, and motor function were normal and he did not have any frontal release signs. Of note the patient is currently back to school.

Subject 2 had a right hemicraniectomy and of the 64 scalp electrodes, 10 anterior frontal to central electrodes were over the hemicraniectomy: AF4 (BA9), AF8 (BA10), F4 (BA8), F6 (BA46), F8 (BA45), FC4 (BA6), FC6 (BA6), FT8 (BA22), C4 (BA1-2-3), and C6

(BA1-2-3). Subject 2 had accidentally fallen from three stories and her GCS score was 3 in the field. She had a right subdural hematoma and right anterior temporal and orbitofrontal contusions. There was no evidence of injury to motor, auditory, or parietal cortices. Due to massive increase in intracranial pressure she underwent an emergency decompressive hemicraniectomy. At the time of EEG testing her memory, attention, and motor function were intact. She noted increased anxiety since the injury and was living with her parents.

Subject 3 had a left hemicraniectomy and of the 64 scalp electrodes, 7 anterior frontal to central electrodes were over the hemicraniectomy: AF7 (BA10), F5 (BA46), F7 (BA45), FC5 (BA6), FT7 (BA22), C5 (BA1-2-3), and T7 (BA21). Subject 3 had fallen from two stories and sustained a left subdural hematoma. The patient had a GCS of 6 in the field that declined to a GCS of 3 on arrival to the ER. He underwent an emergency decompressive hemicraniectomy and removal of the subdural hematoma due to his rapid neurological deterioration. At the time of EEG testing he was doing remarkably well and had no evidence of any residual neurological or behavioral deficits.

5.2.2 EEG Recording

EEG data were recorded using a 64+8 channel BioSemi ActiveTwo amplifier (Metting van Rijn et al., 1990). Horizontal eye movements (EOG) were recorded at both external canthi; blinks were monitored with a left inferior eye electrode and fronto-polar electrodes. Electromyography (EMG) was recorded at the flexor digitorum sublimis muscle used during a particular movement block (left or right hand squeeze). All data—hemicraniectomy, skull, EMG, and EOG—were recorded on the same amplifier and were amplified (-3dB at ~819 Hz low-pass, DC coupled), digitized (2048 Hz), and stored for offline analysis. Data were referenced offline to the average potential of two earlobe electrodes and analyzed in MATLAB® (R2008b, Natick, MA) using custom scripts and the EEGLAB toolbox (Delorme & Makeig, 2004). Due to the location and underlying brain exposure resulting from the hemicraniectomy we chose two behavioral tasks during EEG recording known to activate primary motor and auditory cortices in an effort to assess the value of the hemicraniectomy model. The first task was a visually-cued manual gripping task with simultaneously recorded EMG; the second was a binaural auditory oddball task with tone deviant detection.

From a methodological standpoint we encountered several issues directly related to recording EEG over the hemicraniectomy. Our recording system uses prefabricated, fitted caps (BioSemi, http://www.biosemi.com). After preparation with electroconductive gel, electrodes are snapped in place into the cap. Because this cap is elastic, when the cap is pulled over the head the electrodes are pulled away from the hemicraniectomy due to the large concavity left by the missing piece of skull (see subject CT scans, **Fig. 5.1**). On average, across the three subjects, the cortex-to-epidermis distance over the hemicraniectomy was reduced by 53.4% as compared to over the skull ($p < 0.001$; calculated for each subject as extracted from multiple measurements over absent and intact skull).

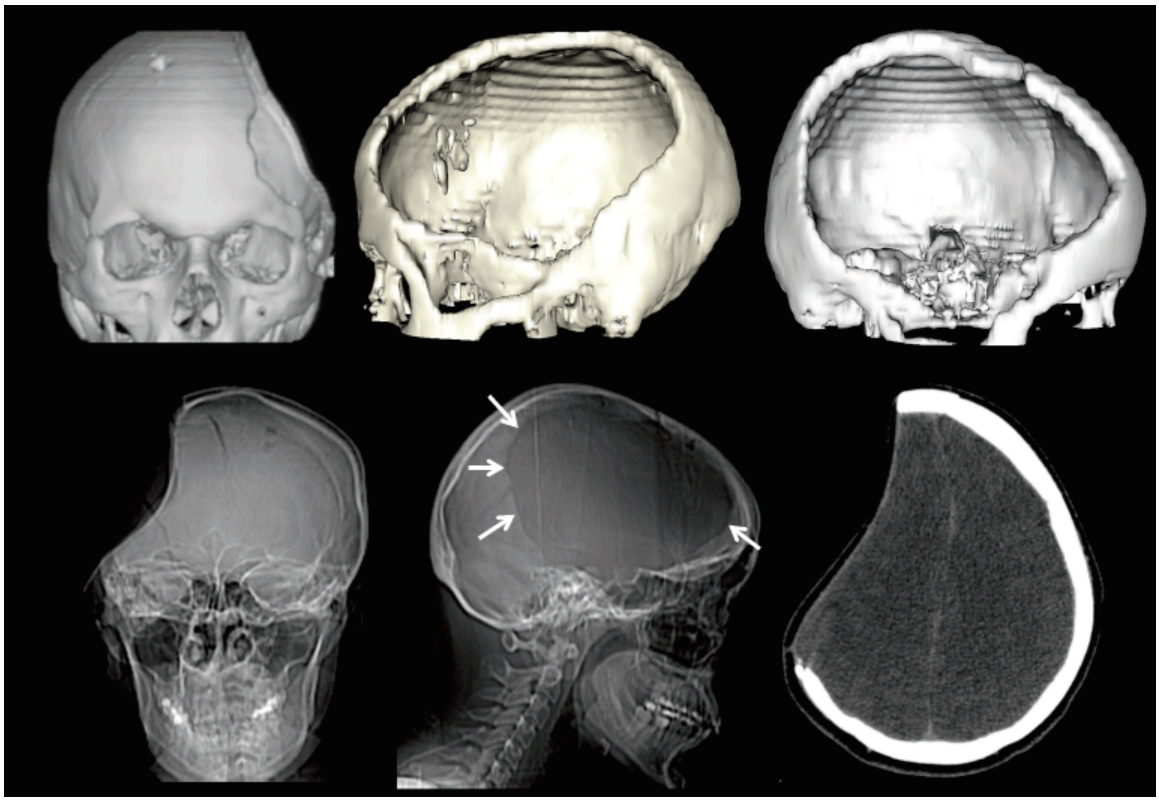

Figure 5.1. Computed tomography (CT) scans of the three subjects demonstrating the extent of the hemicraniectomy. The upper row images were reconstructed using "Surface 3D volume-rendered" multidetector helical CT data. The lower row images include AP and lateral plain radiographs and an axial CT image. Note how the calvarial defect (arrows) includes virtually the entire the frontal bone with relative sparing of the supraorbital rim and paramedian skull. It extends into the parietal bone and squamosal portion of the temporal bone down to just above the ear. The axial CT image demonstrates the characteristic concave deformity seen in many patients prior to cranioplasty. Note the immediate proximity of the skin surface to the underlying normal brain.

In order to get good electrode contact, the method that gave us the best signal stability involved placing a gauze mesh around the head over the electrode cap; this mesh pulled the hemicraniectomy electrodes against the surface of the skin. Snapping electrodes into the cap also proved difficult over the hemicraniectomy site. Without the normal force from the skull pushing back during electrode placement we had to be particularly careful, leading to substantially increased set-up times. Use of a hemostat to hold the cap electrode attachments was a valuable method to safely speed up electrode attachment. Once the electrodes were snapped into place, cotton balls were placed over the hemicraniectomy electrodes, under the gauze mesh, to hold them in place.

5.2.3 Auditory Task

Subjects listened to a sequence of standard ($p = 0.79$) and target ($p = 0.21$) sounds and were instructed to press the space bar on a keyboard after hearing a target. Standard sounds were 50-ms bandpassed noise-bursts (554-740 Hz) while target sounds were 50-ms pure tones of 988 Hz. The inter-trial interval (ITI) between successive sounds was jittered between 700 and 900 ms. All sounds were presented through two speakers positioned in front of the subject on their left and right sides at an intensity level judged comfortable by the patient at the beginning of the experiment (approximately 70 dB).

5.2.4 Motor Task

Subjects were seated in front of a computer monitor while holding a spring grip device in either their left or right hand depending on block. Subjects fixated on a white central cross and were instructed to squeeze the gripper when they saw the "go" cue (whenever the cross flashed green). The ITI was jittered between 1500 and 2000 ms. EMG was recorded as the difference between two electrodes placed approximately 1 cm apart along the flexor *digitorum sublimis* muscle of the gripping hand.

5.2.5 Spontaneous EEG

All root-mean-square (RMS) calculations were performed on bandpass filtered raw EEG data from all three subjects across all conditions across all hemicraniectomy electrodes and their homologous skull electrodes. For the "raw data" analysis, a 0.1-30 Hz passband was used. For each subject, 500 random, one-second data segments were pulled from a random pair of homologous bandpassed hemicraniectomy and skull electrodes and artifact trials were removed as normal; RMS values were then calculated for each segment. A similar method was used for the interelectrode correlation analysis using a passband of 0.1-30 Hz and 500 random one-second data segments per subject. Pearson correlation coefficients were calculated on an all-to-all basis for hemicraniectomy and homologous skull electrodes and binned as a function of interelectrode distance. EMG-contaminated electrodes were classified using three methods outlined in Fu, Daly, & Cavuşoğlu (2006) and Goncharova et al. (2003): 1) Electrodes AF7/8 and FT7/8, which generally sit over frontalis or temporalis muscles; 2) visual inspection for regular "railroad cross-tie" EMG spiking activity; 3) gamma bursting during facial and jaw muscle tensing or biting.

5.2.6 Blinks

In order to calculate the effects of hemicraniectomy on blink amplitude propagation—a common noise source in scalp and intracranial EEG (see Ball et al., 2009)—we time-locked to all naturally occurring blinks across all three subjects by thresholding the product of the inferior and superior eye electrodes, giving a total of 1344 blink trials for the three subjects. In order to identify blinks, we made use of a semi-automatic detection algorithm. First, the inferior and superior EOG channels were point-by-point multiplied, creating a surrogate blink channel with amplified eye-blinks. We also created a surrogate saccade channel by point-by-point multiplication of the left and right horizontal eye channels. Saccades generally have smaller amplitudes and different time-courses than blinks, but both blinks and saccades are easy to visually identify in their surrogate channels. For each subject, we find several canonical blinks in the surrogate blink channel judged by visual inspection of waveforms and

scalp topographies, which look different for blinks than for saccades. We then use the amplitude of the surrogate blink time-series at those canonical trials to set the threshold for the detection algorithm that sweeps through the surrogate channel to indentify time points of putative blinks. Once putative blinks are found we created epochs around those time points and removed non-blink artifacts thorough visual inspection of both the vertical and horizontal surrogate eye channels. For each trial the data were normalized to the maximum value across all electrodes during that trial.

5.2.7 Time-Frequency Analyses

For event related spectral perturbation (ERSP) plots, data were bandpass filtered across 75 pass-bands in 2 Hz increments from 0-150 Hz. We used a Gaussian-shaped filter by performing point-by-point multiplication of a Gaussian with the FFT of the signal. The Gaussian standard deviation was 10% of the center frequency resulting in full width half maximum of 0.2355 of the center frequency. The analytic amplitude (absolute value of the Hilbert transform) for each passband was used to create a grand average time-frequency event-related potential (ERP_{tf}; see Bruns (2004) for comparison of time-frequency decomposition methodologies). After obtaining the real ERP_{tf} for each frequency band, stimulus onset times were randomly shuffled—keeping the real ITIs fixed—and a surrogate passband ERP_{tf} was created using the same window length. 1000 surrogate grand average $ERPs_{tf}$ were created for each passband, giving a probability distribution of amplitude values for each passband from the data itself. From these surrogate ERPs a z-score was calculated at each time point for each passband creating an ERSP across the frequencies of interest.

5.2.8 Auditory Analyses

For ERP analyses, EEG was filtered between 0.1 and 30 Hz and the data were segmented from 100 ms prior to sound onset to 1000 ms after using a 100 ms pre-stimulus baseline. Trials contaminated by blinks or eye movements were removed from analysis. For each subject, for each trial, the extremum value (maximum for P50 and P200, minimum for N100) within the component time window was found; these values were then subjected to statistical analysis. For scalp topographies in **Fig. 5.3A** and **Fig. 5.4B**, the mean amplitude across each component time range was used. ERP component time ranges were 30-80 ms for P50, 70-160 ms for N100, and 150-260 ms for P200. For γ_H- and β-band analyses, the analytic amplitude of band-passed signals were calculated (β: 12-30 Hz, γ_H: 65-115 Hz) and data were then analyzed similar to ERP analysis. For β-band analyses, the minimum value between 300 and 500 ms post-stimulus onset was used to index activity for each trial; for γ_H-band analyses the maximum between 100 and 300 ms was used.

Electrodes for each ERP component were selected based upon whichever hemicraniectomy/skull pair gave the largest mean response for the component of interest across each component's *a priori* time range. For time-frequency analyses, electrode pairs that gave the largest γ_H response were compared (though it is important to note that no skull electrodes showed significant γ_H response to targets or tones). The electrodes pairs used for each component for each subject, as well as the corresponding number of trials (*N*) after artifact rejection are as follows:

- Subject 1 (*N*=143): P50 (C5/6), N100 (C5/6), P200 (T7/8), γ_H/β (CP3/4)

- Subject 2 (N=141): P50 (FC3/4), N100 (FC5/6), P200 (FC3/4)
- Subject 3 (N=144): P50 (C3/4), N100 (FC5/6), P200 (FC3/4), γ_H/β (FC5/6)

Because of the large amount of high-frequency noise in the homologous skull electrode for subject 2, auditory time-frequency analyses were performed on subjects 1 and 3 only.

5.2.9 Motor Analyses

Movement onset and offset were indexed from EMG data conditioned using the Teager-Kaiser Energy Operator [TKEO; see Solnik et al. (2008)] where $x_t = x_t^2 - (x_{t-1})(x_{t+1})$. The first derivative (element-by-element difference) of a logical vector of EMG values surpassing a threshold was calculated giving instantaneous movement onset and offset times. For motor β and γ_H ERP analyses we selected electrode pairs in the same manner as in the auditory ERP analyses, choosing the electrode pairs that gave us the largest β-band amplitude decrease relative to baseline during contralateral hand movement. Hemispheric differences were calculated by finding the minimum (for β-band) or maximum (for γ_H-band) values during the movement. For β-band analyses, the minimum value between 100 and 500 ms post-movement onset was used to index activity for each trial; for γ_H-band analyses the maximum between 0 and 300 ms was used. The electrode pairs used, as well as the N for each contra- or ipsi-craniectomy hand movement, are as follows:

- Subject 1 (C3/4): N = 78 contra-, N = 85 ipsi-craniectomy hand
- Subject 2 (C3/4): N = 64 contra-, N = 66 ipsi-craniectomy hand
- Subject 3 (C5/6): N = 102 contra-, N = 113 ipsi-craniectomy hand

ERSPs were calculated using the same procedure as auditory ERSP analysis, using the same electrode pairs used for ERP_{tf} analyses with a window from 1300 ms before to 500 ms after movement onset and a baseline from 1300-1000 ms before movement onset.

5.2.10 Interfrequency Coupling

Interfrequency coupling indices were calculated using the 10 Hz low-pass filtered γ_H and β analytic amplitudes of bandpassed data for all three subjects using the same electrodes used in the motor task. Bandpass filtered (20-120 Hz) EMG data were smoothed using the TKEO algorithm as above. To calculate the gamma-band index (GBI), the entire β amplitude vector was shifted forward by the median reaction time for each subject, in each condition, and then divided, element-by-element, by the γ amplitude vector of the same electrode to compensate for the relative differences in onset times between bands. Without this shift, GBI/EMG coupling still performs better over hemicraniectomy electrodes than skull ($p < 0.001$, all comparisons) and better than γ_L/β and γ_H alone ($p < 0.001$, both comparisons), but more similar to β alone ($p = 0.18$). Trial-by-trial Pearson correlation coefficients were calculated between the movement index at the electrode contralateral to the movement hand, and the smoothed EMG from that hand, using a window from 500 ms before to 500 ms after movement onset for all subjects.

5.2.11 Statistical Analyses

Significance for all hemicraniectomy versus skull electrode comparisons in the RMS, interelectrode correlation, ERP, ERP_{tf}, EEG/EMG correlation, and blink comparison

analyses were performed using a two-sided Wilcoxon rank sum test. For all scalp topographies (**Fig. 5.3A** and **Fig. 5.4B**), electrodes in subject 2 were digitally swapped across the midline to normalize all electrodes over hemicraniectomy sites to the left hemisphere.

5.3 Results

5.3.1 Spontaneous EEG

RMS activity of the raw time series data was larger at electrodes over the site of hemicraniectomy as compared to homologous skull electrodes ($p < 0.001$). Similarly, RMS activity for all examined frequency bands was larger over the hemicraniectomy compared to the skull ($p < 0.001$ all comparisons; see power spectra in **Fig. 5.2B**). It is important to note that γ_H (65-115 Hz) hemicraniectomy RMS activity was greater only when compared to skull electrodes not contaminated by underlying muscle activity, whereas muscle-contaminated skull electrodes show larger RMS compared to their homologous hemicraniectomy electrodes ($p < 0.001$, **Fig. 5.2B**).

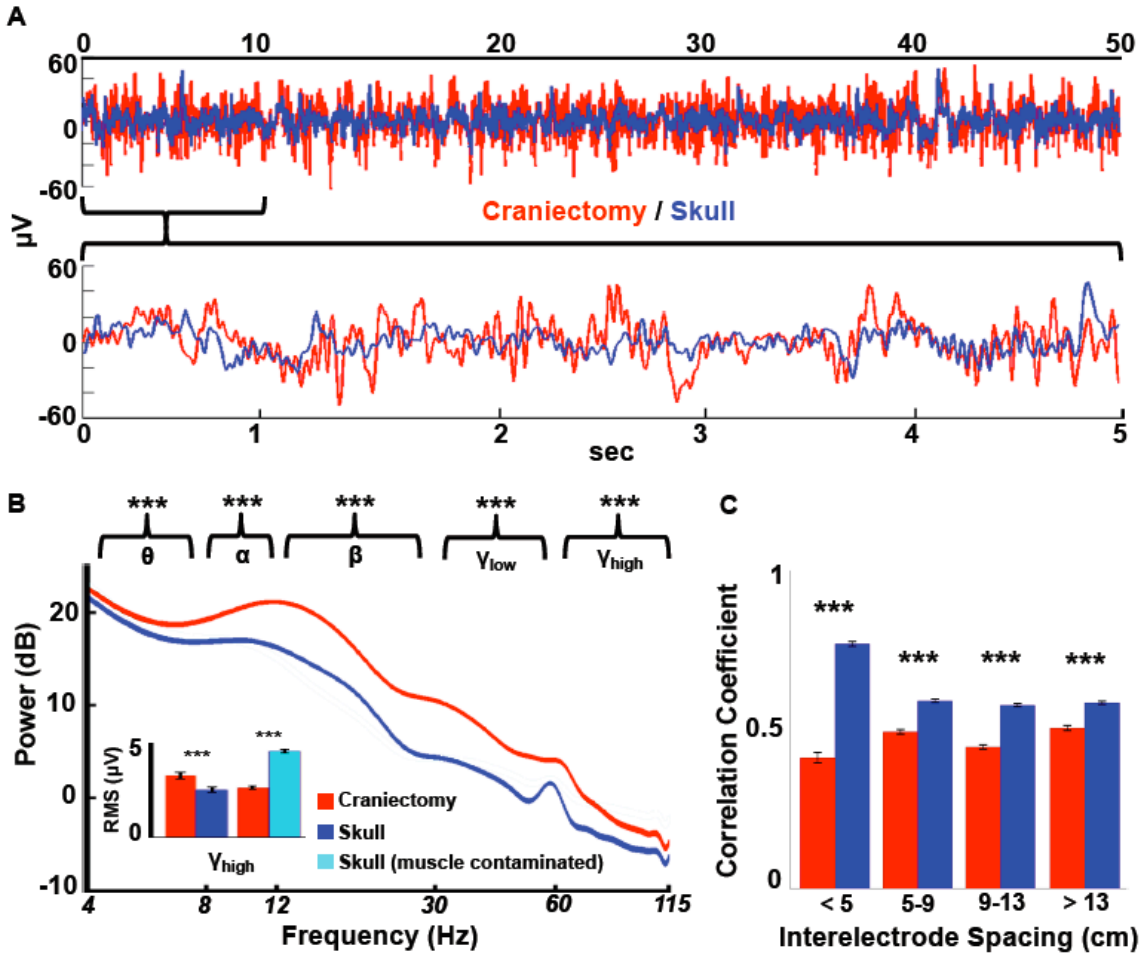

Figure 5.2. Comparison of raw signals. *A*, Time-series data has more power and decreased signal redundancy over the hemicraniectomy (red) as compared to the skull (blue). The top trace shows 50 seconds of raw data from two homologous electrodes from subject 1 (F3/F4); the bottom is zoomed in on the first 5 seconds of the top trace. *B*, Mean power spectra for hemicraniectomy and skull electrodes not contaminated by muscle noise (width of spectrum indicates s.e.m. for each frequency; not 60 Hz contamination). Asterisks above each band grouping indicate root-mean-square (RMS) amplitude for that frequency band is greater for hemicraniectomy electrodes compared to homologous skull electrodes. For γ_H (65-115 Hz) RMS analyses electrodes were divided into two groups: skull electrodes with high muscle noise and those with low (inset; see Supplemental Methods for muscle noise classification methods). γ_H is greater over hemicraniectomy sites compared to skull electrodes only when skull electrodes are not contaminated by muscle noise. *C*, Interelectrode correlations for all hemicraniectomy pairs are lower at all distances compared to homologous skull pairs. ***$p < 0.001$, statistically significant differences; bars are s.e.m.

In order to quantify the extent to which the skull causes spatial smoothing, we examined natural (task-irrelevant) interelectrode time-series correlations in an all-to-all manner for hemicraniectomy electrodes and homologous skull electrodes. Interelectrode correlations were binned into four groups according to interelectrode distance. For all distances, interelectrode correlations were lower over hemicraniectomy sites compared to skull ($p < 0.001$ all comparisons; **Fig. 5.2C**).

Blink artifacts are a common noise source in scalp EEG recordings. Eye movements produce large-amplitude fluctuations that propagate long distances, detectable to some degree even at posterior scalp electrodes. We tested the artifact propagation properties of the skull by time-locking the EEG signal to all naturally-occurring blinks in all three subjects. Extracted blink amplitudes are largest at electrodes closest to the eyes and drop off rapidly as a function of distance. Similar to the interelectrode correlation analysis, blink amplitudes were binned according to distance from the eye. For all electrodes within 13 cm of the eye, blink amplitudes were smaller over the hemicraniectomy hemisphere compared to homologous sites over intact skull ($p < 0.001$ at < 9 cm, $p = 0.042$ between 9-13 cm, **Fig. 5.3**).

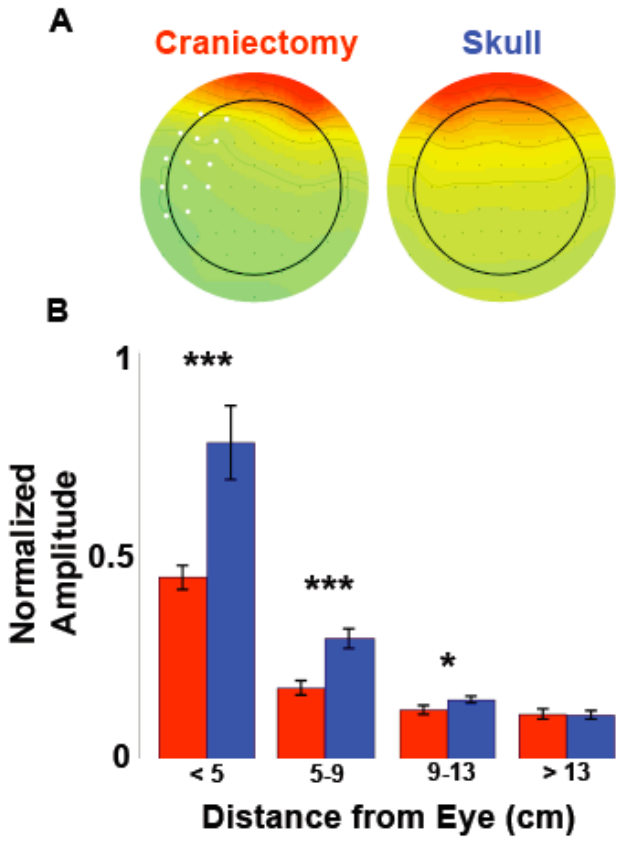

Figure 5.3. Blink artifact propagation. ***A***, Scalp topographies of mean peri-blink amplitude for all three hemicraniectomy subjects compared to three young controls with intact skull, demonstrating the blink amplitude drop over the hemicraniectomy electrodes. Electrodes over the site of hemicraniectomy in any one subject are in white. ***B***, Peri-blink amplitudes as a function of distance from the eye. ***$p < 0.001$, *$p = 0.042$, statistically significant differences; bars are s.e.m.

5.3.2 Auditory Responses

Because different event-related potential (ERP) components had restricted spatial distributions over the hemicraniectomy side (**Fig. 5.4B**), analyses were conducted on a single-electrode basis. ERPs were compared over the pair of homologous electrodes that yielded the largest mean normalized activity across the *a priori* time range of interest for each component. For the oddball task we examined three auditory ERPs evoked by infrequent deviant tones: P50, N100, and P200 (**Fig. 5.4A**). Approximately 12-15ms after tone onset, a focused positivity can be seen lateralized to electrodes over the hemicraniectomy, followed by a frontal negativity and positivity biased toward the craniectomy hemisphere. P50 magnitude was larger in all three participants over the site of the hemicraniectomy ($p < 0.001$ all subjects); N100 amplitude was larger over hemicraniectomy in subjects 1 and 3 ($p < 0.001$ both subjects); and P200 magnitude was larger in all three subjects ($p < 0.001$ subjects 1 and 2, $P = 0.033$ subject 3). In this task, subjects were fast at detecting the targets (reaction times

around 250-300 ms). Thus, long-latency target-related ERPs such as the P300 were superimposed by ERPs related to the motor response and were not reliably observed.

Auditory stimulus-locked ERSPs were calculated for 75 equally spaced frequency bands between 0-150 Hz for subjects 1 and 3. Subject 2 was excluded from auditory time-frequency analyses because of strong, high frequency muscle contamination over intact skull electrodes. Target-related γ_H was higher over hemicraniectomy compared to skull ($p = 0.0032$; **Fig. 5.5A,B**). There was also a robust lower-frequency, β-band (12-30 Hz) amplitude decrease to targets compared to standard stimuli over the hemicraniectomy ($p < 0.001$). The magnitude of this decrease was larger over the hemicraniectomy compared to homologous skull electrodes ($p < 0.001$; **Fig. 5.5C,D**).

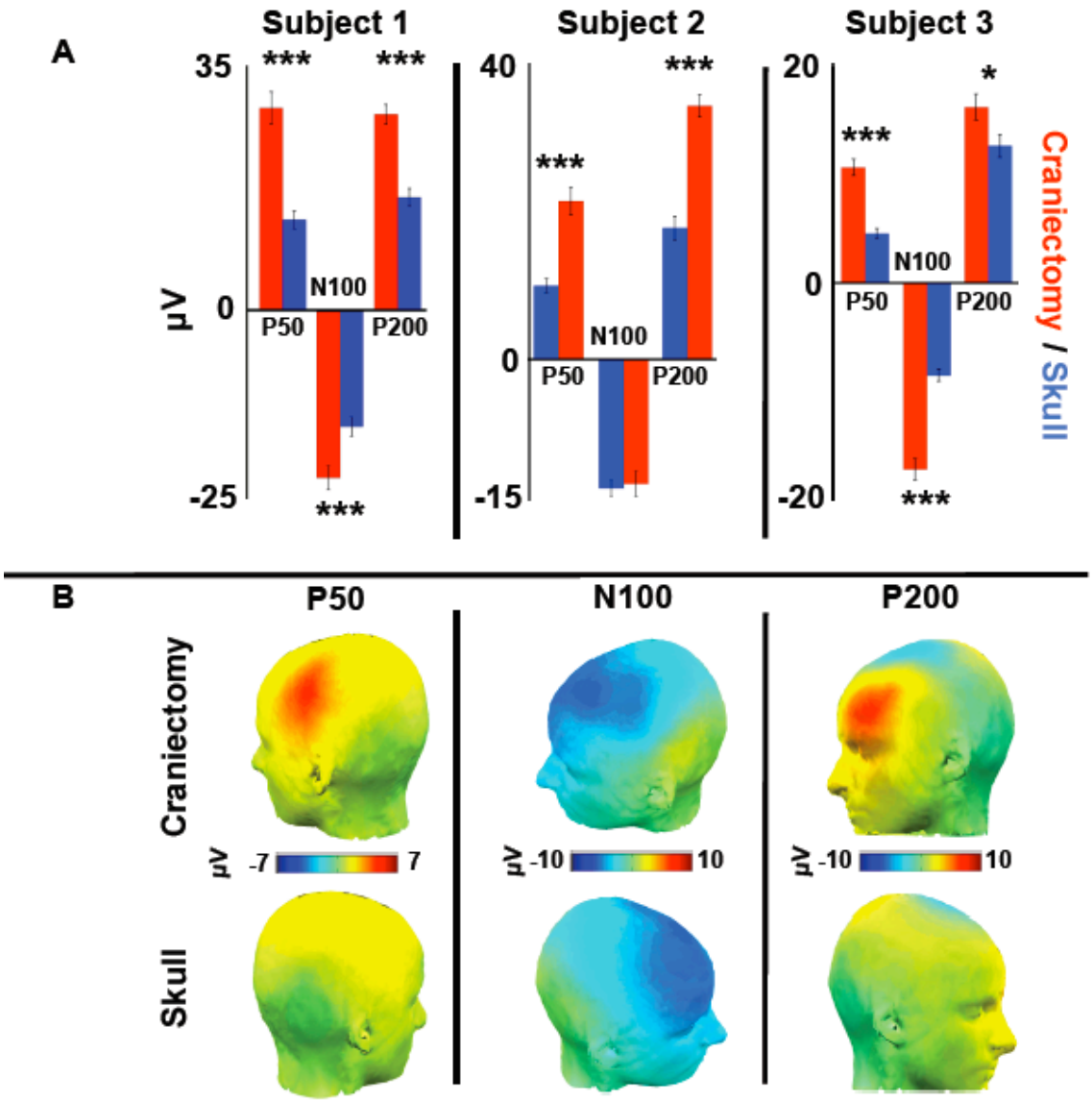

Figure 5.4. Auditory ERPs in response to correctly identified infrequent deviant tones. *A*, Peak ERP amplitudes for components P50, N100, and P200 over hemicraniectomy and homologous skull sites for each subject. *B*, Grand average scalp topographies of mean amplitude across the time range of each ERP for all three subjects. ***$p < 0.001$, *$p = 0.033$, statistically significant differences; bars are s.e.m.

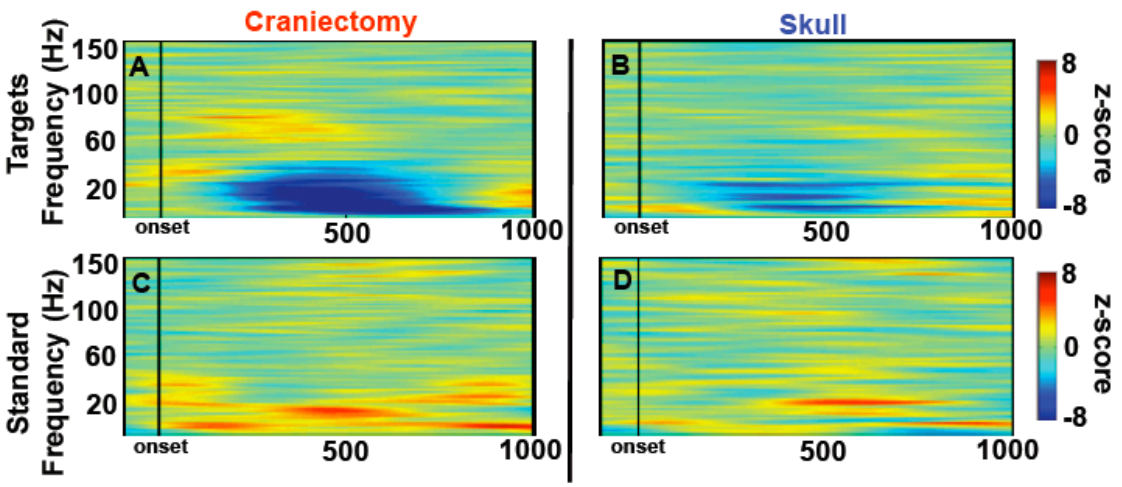

Figure 5.5. Stimulus-locked auditory time-frequency activity. *A*, *B*, Event-related spectral perturbations for subjects 1 and 3 over homologous hemicraniectomy and skull sites showing target-related γ_H over the hemicraniectomy. *C*, *D*, Same as *A* and *B* to non-target auditory stimuli. Note the early cluster of γ_H starting at approximately 100 ms post-stimulus onset is only present over the hemicraniectomy in response to targets.

5.3.3 Motor Time-Frequency Responses

Movement-locked ERSPs were calculated for all three subjects (**Fig. 5.6A,B**). We focused on two specific frequency bands—β and γ_H—in accordance with previous findings (Crone et al., 1998a; Crone et al., 1998b; Dalal et al., 2008; Darvas et al., 2010; Neuper, Wörtz, & Pfurtscheller, 2006). Single-trial analysis of the activity in these bands shows a robust, trial-by-trial event-related profile over the hemicraniectomy (see **Fig. 5.6C-6F**). Across all three subjects, movement-related β and γ_H magnitudes were larger over hemicraniectomy compared to skull ($p < 0.001$ both comparisons; **Fig. 5.6G,H**).

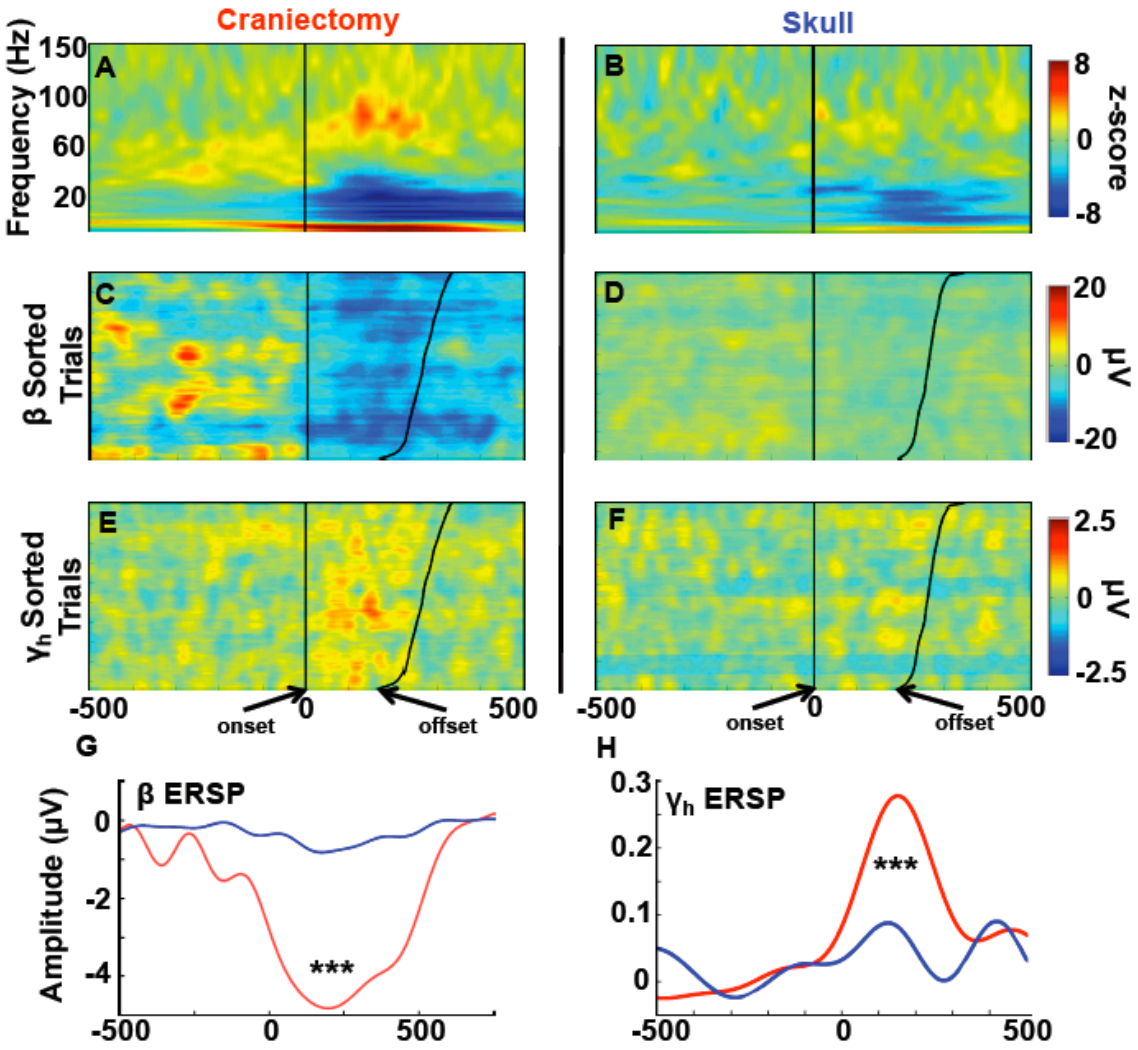

Figure 5.6. Contralateral movement-related time-frequency activity. (Note that figures *A*-*F* are on the same x-axis scale). *A*, *B*, Event-related spectral perturbations for all three subjects over homologous hemicraniectomy and skull sites showing movement-related γ_H over the hemicraniectomy. *C*, *D*, Single trial β (12-30 Hz) and *E*, *F*, γ_H (65-115 Hz) movement-related activity in subject 1 locked to movement onset—sorted by movement offset—illustrating the trial-by-trial power at hemicraniectomy electrode (C3) compared to the homologous skull electrode (C4). *G*, *H*, β and γ_H ERPs for all subjects. Movement-related β and γ_H are greater over hemicraniectomy electrodes as compared to homologous skull sites. ***$p < 0.001$, statistically significant differences; bars are s.e.m.

5.3.4 Interfrequency Coupling in Movement

Research on movement-related scalp EEG, magnetoencephalography (MEG), and intracranial electrocorticography (ECoG) oscillations has shown robust β power decrease (desynchronization) beginning prior to the onset of and extending through the duration of movement (Pfurtscheller & Lopes de Silva, 1999). Several studies have also indicated a relationship between movement-related β-decrease and γ-increase during real and imagined movements (Pfurtscheller & Lopes de Silva, 1999; de Lange et al., 2008). Given the known roles of β-decrease and γ-increase with movement, and the relative robustness of trial-by-trial β and γ_H movement-related activity over the site of hemicraniectomy, we assessed the relationship between these two bands with movement via a GBI that tracked motor behavior in the hemicraniectomy patients.

We examined the relationship between muscle activity (as indexed by EMG) and γ_H/β interfrequency coupling to assess whether this metric provided a better measure of movement than either band alone. We defined the GBI as the division of γ_H by β activity within an electrode; if γ_H increases while β decreases, GBI is larger. We found a robust trial-by-trial correlation between GBI recorded over the hemicraniectomy with the EMG recorded over the active contralateral muscle groups (see example traces in **Fig. 5.7A**). Trial-by-trial GBI/EMG correlations are larger over the site of hemicraniectomy ($p < 0.001$), with the hemicraniectomy GBI performing better than γ_H/EMG or β/EMG correlations ($p < 0.001$ both comparisons; **Fig. 5.7B,C**). To assess whether this index is dependant upon γ_H specifically, and not just γ in general, we calculated the same correlation using a low-gamma (γ_L) band (30-55 Hz) separately. This hemicraniectomy γ_L/β index correlated less with EMG than the high-gamma metric ($p < 0.001$, **Fig. 5.7B**).

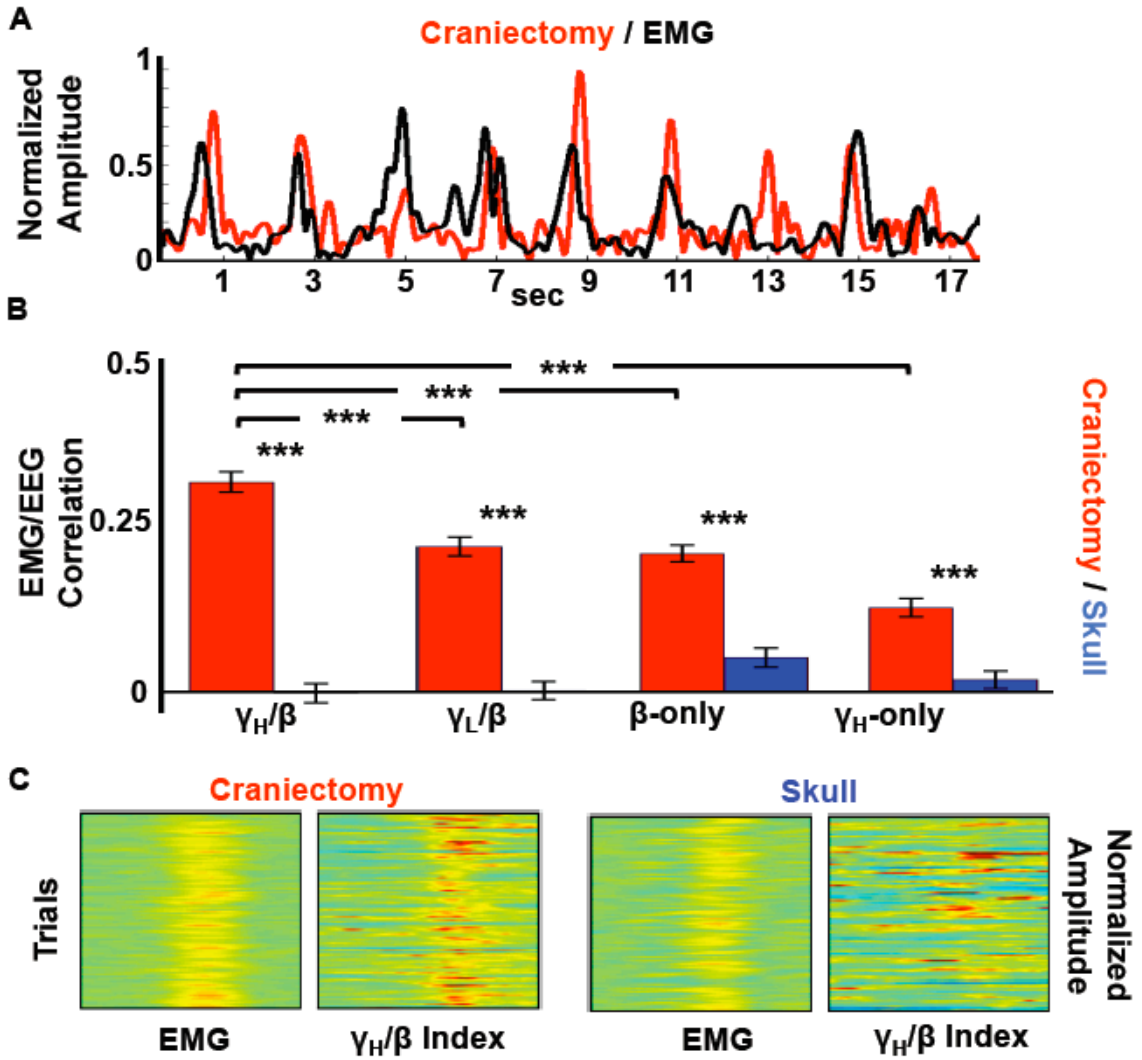

Figure 5.7. EEG/EMG movement correlation. *A*, Example of raw traces of EMG and contralateral γ_H/β index in subject 1 over hemicraniectomy electrode C3. *B*, Average trial-by-trial EMG/EEG correlations for all subjects. For all correlation bands, hemicraniectomy electrodes perform better than skull electrodes. For hemicraniectomy electrodes, γ_H/β correlates higher with movement than γ_L/β, β-only, and γ_H-only. *C*, Single-trial movement-locked EMG and contralateral γ_H/β index in subject 1 over hemicraniectomy (C3) and skull (C4) illustrating trial-by-trial correlation between γ_H/β index and EMG. ***$p < 0.001$, statistically significant differences; bars are s.e.m.

5.4 Discussion

Absent intervening skull, our electrodes were physically closer to the surface of the brain and free from the smoothing effects of bone and non-neural tissue, resulting in larger EEG signal and improved spatial independence. Without a measure of electrode conductivity we cannot rule out the possibility of a systematic bias in conductivity between hemicraniectomy and skull electrodes. Such a bias would result in apparent signal differences. However, there are several aspects of our data that suggest that conductivity differences are not a significant variable. We recorded all electrodes from the same amplifier with comparable skin resistance. The signal-to-noise ratio indicates good signal quality over the hemicraniectomy and we can assume that the effects of noise on interelectrode correlations should be minimized. The hemicraniectomy and skull power spectra have the same basic shape, which suggest that their signals have the same general levels of noise. Finally, because the hemicraniectomy electrodes are closer to the cortex (the signal source), one might predict on a simple amplitude basis that—barring any filtering or smoothing by the skull—neighboring hemicraniectomy electrodes would be more similar. However, we found evidence that the hemicraniectomy electrodes are more independent supporting the notion we were recording from more restricted neural populations.

We found larger task-relevant ERPs and ERSPs with more robust high-frequency activity over the site of hemicraniectomy. Furthermore, movement-related β and γ_H activity are visible at the single-trial level over the hemicraniectomy site. Previous research has demonstrated reliable BMI control in humans using scalp EEG β (Wolpaw & MacFarland, 2004) and intracranial γ_H (Miller et al., 2007; Ball et al. 2008) frequencies. We believe this is the first instance showing that coupling between two different frequencies in a single electrode can also be used as an index for movement. Specifically, this GBI is better correlated with movement than the β or γ_H bands alone. Of note, the scalp γ_H band is compromised by signal strength decrease and muscle noise from a host of sources (eye, facial, scalp, and pharyngeal muscles), so this boost in movement prediction using the GBI is not as evident at the level of the scalp. This GBI adds to the growing literature (Canolty et al., 2006) that information obtained through interfrequency coupling provides a valuable metric to assess neurobehavioral network dynamics that can complement time-series analysis.

The enhanced window to EEG activity provided by a hemicraniectomy may provide an important model to test the accuracy and efficacy of electrophysiological source-localization models and component extraction methods such as principal- and independent-components analysis. Several studies have used EEG and MEG data collected from subjects with smaller skull defects (e.g., burr holes, craniectomy scars) to test a variety of inverse modeling methods (Bénar & Gotman, 2002; Li et al., 2007; Oostenveld & Oostendorp, 2002; Yoshinaga et al., 2008). Subjects with a hemicraniectomy provide a larger window to the cortex—and thus a greater number of electrodes with less spatial smoothing—to use for testing these models. Recent research has also focused on examining individual skull thickness variability on a variety of ERP and time-frequency components (Fordl et al., 2001; Hagemann et al., 2008; Pfefferbaum, 1990). Hemicraniectomy subjects may provide a new way of examining such relationships.

A recent study reported movement-related γ_H activity over scalp EEG (Darvas et al., 2010). γ_H was extracted from the average activity of voxels over premotor and motor cortex using an inverse solution of EEG electrode activity mapped onto the cortical surface. This method allows γ_H activity extraction from a local region of cortex in a manner that may not be possible to do in a single scalp EEG electrode due to smoothing effects, whereas the craniectomy inherently provides a direct window to the cortical surface with decreased smoothing. This is relevant clinically, as the development of long-term, accurate BMI for paralyzed patients is of utmost importance. The hemicraniectomy recording method may prove to be an important bridge between the spatial and spectrotemporal quality of ECoG and the long-term stability of scalp EEG in BMI research. Given the increasing use of hemicraniectomy for neurosurgical purposes, and the ability to test these subjects repeatedly as outpatients, we suggest this model may have applications to a wide variety of cognitive research questions.

Chapter 6

Concluding Remarks

6.1 Summary of Findings

In this thesis I document three main experimental findings. First, I provide the first causal evidence in humans for a dissociable role of the prefrontal cortex and basal ganglia in working memory functions. I show that the prefrontal cortex plays a critical role for intrahemispheric top-down working memory maintenance and attention functions mediated through prefrontal-extrastriate visual cortex interactions. In contrast, the basal ganglia play a more general role in working memory updating. My second finding is that cognitive compensation in response to unilateral prefrontal lesions occurs rapidly and dynamically in response to individual trial demands. Finally, as would be predicted, we demonstrate that this prefrontal cognitive compensation is reliant upon the fidelity of cortico-cortical information transfer from the damaged to the intact hemisphere.

6.2 Personal Thoughts

My goals and interests have changed over the years and I believe this thesis and my Future Directions reflect that. When I began my PhD I was interested in two very different topics: neuropathology and brain machine interfacing. Working with patients provides neuroscientists with unique insights into understanding the brain by looking at what changes

in brain and behavior when certain specific brain regions are damaged. What I first found fascinating when I began my research at Berkeley was the ability to combine these patient-based observations with neuroimaging methods such as EEG which allows us to observe the intricate and complex changes in time and functional networks caused by brain lesions. In my mind brain machine interfaces were an amazing way to combine patient-based research with translatable, useful tools to help those same patients. I want to learn how communication between brain regions gives rise to cognition and how neuroplasticity affects cognition, but I also want to know how brain networks communicate and how what we learn from basic neuroscientific research can benefit patients.

6.3 Future Directions

Recently I have begun collecting electroencephalographic data from patients with implanted subdural electrodes. The unfortunate situation that these patients must confront gives neuroscientists an amazing opportunity to study basic principles underlying the networks subserving cognition. Despite the improved temporal and spatial resolution of these data, like most neuroimaging research many of these methods are inherently correlational. I believe the future of cognitive and systems neuroscience will be based upon examinations into causal relationships between brain and behavior. In my future work I aim to incorporate the imaging and analysis techniques I have acquired in my electrophysiological training as a PhD student with non-invasive methods such as transcranial magnetic stimulation (TMS) and transcranial direct current stimulation (TDCS) to address questions of causality in cognition. By comparing the results of these techniques against findings from patients with focal brain lesions—which also help us address questions of causality—we can begin to truly piece together *how* the brain gives rise to our experience, not just which parts are associated with those experiences.

6.4 Final Thoughts

Translational research is important to me. It's easy to get caught up in the excitement of data collection and analysis and forget that the research I do as a neuroscientist has a goal: to learn how the brain works to help those for whom it does not. I truly count myself as privileged to have been given the opportunity to work and study at the University of California, Berkeley. Occasionally I am reminded that my job is to think, and that I get paid to do what I love the most. But with that carries a responsibility to make the most out of the privileges I have been afforded, and I hope that my training and education allow me to leave the world having done more good than harm.

References

Abraham, K., & Marsan, C. (1958). Patterns of cortical discharges and their relation to routine scalp electroencephalography. *Electroencephalogr. Clin. Neurophysiol.* 10, 447-461.

Alstott, J., Breakspear, M., Hagmann, P., Cammoun, L., Sporns, O., & Friston, K. (2009). Modeling the impact of lesions in the human brain. *PLoS Comput. Biol.* 5, 1-12.

Ashby, F.G., Ell, S.W., Valentin, V.V., & Casale, M.B. (2005). FROST: A distributed neurocomputational model of working memory maintenance. *J. Cogn. Neurosci.* 17, 1728-1743.

Awh, E., Vogel, E., & Oh, S. (2006). Interactions between attention and working memory. *Neuroscience* 139, 201-208.

Bach-y-Rita, P. (1990). Brain plasticity as a basis for recovery of function in humans. *Neuropsychologia* 28, 547-554.

Ball T., Demandt E., Mutschler I., Neitzel E., Mehring C., Vogt K., Aertsen A., & Schulzebonhage A. (2008). Movement related activity in the high gamma range of the human EEG. *NeuroImage* 41, 302-310.

Ball T., Kern M., Mutschler I., Aertsen A., & Schulze-Bonhage A. (2009). Signal quality of simultaneously recorded invasive and non-invasive EEG. *NeuroImage* 46, 708-716.

Barceló, F., Suwazono, S., & Knight, R.T. (2000). Prefrontal modulation of visual processing in humans. *Nat. Neurosci.* 3, 399-403.

Bastiaansen, M.C., Posthuma, D., Groot, P.F., & de Geus, E.J. (2002). Event-related alpha and theta responses in a visuo-spatial working memory task. *Clin. Neurophysiol.* 113, 1882-1893.

Bédard C., Kröger H., & Destexhe A. (2006). Does the 1/*f* frequency scaling of brain signals reflect self-organized critical states? *Phys. Rev. Lett.* 97, 11802.

Bénar C.G., & Gotman J. (2002). Modeling of post-surgical brain and skull defects in the EEG inverse problem with the boundary element method. *Clin. Neurophysiol.* 113, 48-56.

Berger H. (1929). Über das Elektrenkephalogramm des Menchen. *Archives für Psychiatrie*, *87*, 527-570.

Blasi, V., Young, A.C., Tansy, A.P., Petersen, S.E., Snyder, A., & Corbetta, M. (2002). Word retrieval learning modulates right frontal cortex in patients with left frontal damage. *Neuron* 36, 159-170.

Bledowski, C., Rahm, B., & Rowe, J. (2009). What "works" in working memory? Separate systems for selection and updating of critical information. *J. Neurosci.* 29, 13735-13741.

Bressler, S.L. (1995). Large-scale cortical networks and cognition. *Brain Res. Brain Res. Rev.* 20, 288-304.

Brett, M., Johnsrude, I., & Owen, A. (2002). The problem of functional localization in the human brain. *Nat. Rev. Neurosci.* 3, 243-249.

Bruns A. (2004). Fourier-, Hilbert- and wavelet-based signal analysis: are they really different approaches? *J. Neurosci. Methods* 137, 321-332.

Bruns, A. & Eckhorn, R. (2004). Task-related coupling from high- to low-frequency signals among visual cortical areas in human subdural recordings. *Int. J. Psychophysiol.* 51, 97-116.

Canolty, R.T., Edwards, E., Dalal, S.S., Soltani, M., Nagarajan, S.S., Kirsch, H.E., Berger, M.S., Barbaro, N.M., & Knight, R.T. (2006). High gamma power is phase-locked to theta oscillations in human neocortex. *Science* 313, 1626-1628.

Canolty, R.T., Soltani, M., Dalal, S.S., Edwards, E., Dronkers, N., Nagarajan, S.S., Kirsch, H.E., Barbaro, N.M., & Knight, R.T. (2007). Spatiotemporal dynamics of word processing in the human brain. *Front. Neurosci.* 1, 185-196.

Carmichael, S.T., Wei, L., Rovainen, C.M., & Woolsey, T.A. (2001). New patterns of intracortical projections after focal cortical stroke. *Neurobiol. Dis.* 8, 910-922.

Carmichael, S. (2003). Plasticity of cortical projections after stroke. *Neuroscientist* 9, 64-75.

Chao, L.L., & Knight, R.T. (1998). Contribution of human prefrontal cortex to delay performance. *J. Cogn. Neurosci.* 10, 167-177.

Cobb, W., & Sears T. (1960). A study of the transmission of potentials after hemispherectomy. *Electroencephalogr. Clin. Neurophysiol.* 12, 371-833.

Cobb W.A., Guiloff R.J., & Cast J. (1979). Breach rhythm: The EEG related to skull defects. *Electroencephalogr. Clin. Neurophysiol.* 47, 251-271.

Cohen D., & Cuffin B.N. (1991). EEG versus MEG localization accuracy: Theory and experiment. *Brain Topogr.* 4, 95-103.

Cools, R., Ivry, R.B., & D'Esposito, M. (2006). The human striatum is necessary for responding to changes in stimulus relevance. *J. Cogn. Neurosci.* 18, 1973-1983.

Cooper, R., Winter, A., Crow, H., & Walter W. (1965). Comparison of subcortical, cortical and scalp activity using chronically indwelling electrodes in man. *Electroencephalogr. Clin. Neurophysiol.* 18, 217-228.

Corbetta, M., Kincade, M.J., Lewis, C., Snyder, A.Z., & Sapir, A. (2005). Neural basis and recovery of spatial attention deficits in spatial neglect. *Nat. Neurosci.* 8, 1603-1610.

Cramer, S. (2008). Repairing the human brain after stroke: I. Mechanisms of spontaneous recovery. *Ann. Neurol.* 63, 272-287.

Crone, N.E., Miglioretti, D.L., Gordon, B., Sieracki, J.M., Wilson, M.T., Uematsu, S., & Lesser, R.P. (1998a). Functional mapping of human sensorimotor cortex with electrocorticographic spectral analysis. I. Alpha and beta event-related desynchronization. *Brain* 121, 2271-2299.

Crone, N.E., Miglioretti, D.L., Gordon, B., & Lesser, R.P. (1998b). Functional mapping of human sensorimotor cortex with electrocorticographic spectral analysis. II. Event-related synchronization in the gamma band. *Brain* 121, 2301-2315.

Curtis, C.E., & D'Esposito, M. (2003). Persistent activity in the prefrontal cortex during working memory. *Trends Cogn. Sci.* 7, 415-423.

Curtis, C.E., & D'Esposito, M. (2004). The effects of prefrontal lesions on working memory performance and theory. *Cogn. Affect. Behav. Neurosci.* 4, 528-539.

Dalal, S.S., Guggisberg, A., Edwards, E., Sekihara, K., Findlay, A., Canolty, R.T., Berger, M.S., Knight, R.T., Barbaro, N.M., & Kirsch, H. (2008). Five-dimensional neuroimaging: Localization of the time–frequency dynamics of cortical activity. *NeuroImage* 40, 1686-1700.

Darvas, F., Scherer, R., Ojemann, J.G., Rao, R.P., Miller, K.J., & Sorensen L.B. (2010). High gamma mapping using EEG. *NeuroImage* 49, 930-938.

Davis, S.W., Dennis, N.A., Daselaar, S.M., Fleck, M.S., & Cabeza, R. (2008). Que PASA? The posterior-anterior shift in aging. *Cereb. Cortex* 18, 1201-1209.

de Lange, F.P., Jensen, O., Bauer, M., & Toni I. (2008). Interactions between posterior gamma and frontal alpha/beta oscillations during imagined actions. *Front. Hum. Neurosci.* 2, 7.

Delorme, A., & Makeig, S. (2004). EEGLAB: An open source toolbox for analysis of single-trial EEG dynamics including independent component analysis. *J. Neurosci. Methods* 134, 9-21.

DeLucchi, M., Garoutee, B., & Aird, R. (1962). The scalp as an electroencephalographic averager. *Electroencephalogr. Clin. Neurophysiol.* 14, 191-196.

Donders, F.C. (1868). Die Schnelligkeit psychischer Prozesse. *Archiv für Anatomie und Physiologie und wissenschaftliche Medizin*, 657-681.

Draganski, B., Kherif, F., Kloppel, S., Cook, P., Alexander, D., Parker, G., Deichmann, R., Ashburner, J., & Frackowiak, R. (2008). Evidence for segregated and integrative connectivity patterns in the human basal ganglia. *J. Neurosci.* 28, 7143-7152.

Drew, T., & Vogel, E.K. (2008). Neural measures of individual differences in selecting and tracking multiple moving objects. *J. Neurosci.* 28, 4183-4191.

Dunnett, S.B., Meldrum, A., & Muir, J.L. (2005). Frontal-striatal disconnection disrupts cognitive performance of the frontal-type in the rat. *Neuroscience* 135, 1055-1065.

Edwards, E., Soltani, M., Deouell, L. Y., Berger, M., & Knight R. T. (2005). High gamma activity in response to deviant auditory stimuli recorded directly from human cortex. *J. Neurophysiol.* 94, 4269-4280.

Ell, S., Marchant, N., & Ivry, R.B. (2006). Focal putamen lesions impair learning in rule-based, but not information-integration categorization tasks. *Neuropsychologia* 44, 1737-1751.

Frank, M.J., Seeberger, L.C., & O'Reilly, R. (2004). By carrot or by stick: Cognitive reinforcement learning in Parkinsonism. *Science* 306, 1940-1943.

Freeman, W. (2004). Origin, structure, and role of background EEG activity. Part 1. Analytic amplitude. *Clin. Neurophysiol.* 115*,* 2077-2088.

Friedman, H.R., & Goldman-Rakic, P.S. (1994) Coactivation of prefrontal cortex and inferior parietal cortex in working memory tasks revealed by 2DG functional mapping in the rhesus monkey. *J. Neurosci.* 14, 2775-2788.

Fries, P., Reynolds, J.H., Rorie, A.E., & Desimone, R. (2001). Modulation of oscillatory neuronal synchronization by selective visual attention. *Science* 291, 1560-1563.

Friston, K.J., Price, C.J., Fletcher, P., Moore, C., Frackowiak, R.S., & Dolan, R.J. (1996). The trouble with cognitive subtraction. *NeuroImage* 4, 97-104.

Frodl, T., Meisenzahl, E.M., Müller, D., Leinsinger, G., Juckel, G., Hahn, K., Möller, H.J., & Hegerl, U. (2001). The effect of the skull on event-related P300. *Clin. Neurophysiol.* 112, 1773-1776.

Fu, M.J., Daly, J.J., & Çavuşoğlu, M. (2006). A detection scheme for frontalis and temporalis muscle EMG contamination of EEG data. *Conf. Proc. IEEE Eng. Med. Biol. Soc.* 1, 4514-4518.

Fu, S., Zinni, M., Squire, P.N., Kumar, R., Caggiano, D.M., & Parasuraman, R. (2008). When and where perceptual load interacts with voluntary visuospatial attention: an event-related potential and dipole modeling study. *NeuroImage* 39, 1345-1355.

Fuster, J.M., & Alexander, G.E. (1971). Neuron activity related to short-term memory. *Science* 173, 652-654.

Gazzaley, A., Rissman, J., & D'Esposito, M. (2004). Functional connectivity during working memory maintenance. *Cogn. Affect. Behav. Neurosci.* 4, 580-599.

Geisler, C.D., & Gerstein, G.L. (1961). The surface EEG in relation to its sources. *Electroencephalogr. Clin. Neurophysiol.* 13, 927-934.

Gogtay, N., Giedd., J.N., Lusk., L., Hayashi, K.M., Greenstein, D., Vaituzis, A.C., Nugent, T.F., Herman, D.H., Clasen, L.S., Toga, A., Rapoport, J.L., & Thompson, P. (2004). Dynamic mapping of human cortical development during childhood through early adulthood. *Proc. Natl. Acad. Sci. USA* 101, 8174-8179.

Goncharova, I.I., McFarland, D.J., Vaughn, T.M., & Wolpaw, J.R. (2003). EMG contamination of EEG: Spectral and topographical characteristics. *Clin. Neurophysiol.* 114, 1580-1593.

Grahn, J.A, Parkinson, J.A., & Owen, A. (2009). The role of the basal ganglia in learning and memory: neuropsychological studies. *Behav. Brain Res.* 199, 53-60.

Graybiel, A. (2005). The basal ganglia: learning new tricks and loving it. *Curr. Opin. Neurobiol.* 15, 638-644.

Green, D.M., & Swets, J.A. (1966). *Signal Detection Theory and Psychophysics*. New York: Wiley.

Gronau, N., Neta, M., Bar, M. (2008). Integrated contextual representation for objects' identities and their locations. *J. Cogn. Neurosci.* 20, 371-388.

Gusnard, D.A., & Raichle, M.E. (2001). Searching for a baseline: functional imaging and the resting human brain. *Nat. Rev. Neurosci.* 2, 685-694.

Haber, S. (2003). The primate basal ganglia: parallel and integrative networks. *J. Chem. Neuroanat.* 26, 317-330.

Hagemann, D., Hewig, J., Walter, C., & Naumann, E. (2008). Skull thickness and magnitude of EEG alpha activity. *Clin. Neurophysiol.* 119, 1271-1280.

Haider, B., & McCormick, D. (2009). Rapid Neocortical Dynamics: Cellular and Network Mechanisms. *Neuron* 62, 171-189.

Hasegawa, I., Fukushima, T., Ihara, T., & Miyashita, Y. (1998). Callosal window between prefrontal cortices: Cognitive interaction to retrieve long-term memory. *Science* 281, 814-818.

Hayes, A.E., Davidson, M.C., Keele, S.W., & Rafal, R.D. (1998). Toward a functional analysis of the basal ganglia. *J. Cogn. Neurosci.* 10, 178-198.

Hazy, T., Frank, M.J., & O'Reilly, R. (2006) Banishing the homunculus: Making working memory work. *Neuroscience* 139, 105-118.

He, B.J., Snyder, A., Vincent, J.L., Epstein, A., Shulman, G.L., & Corbetta, M. (2007). Breakdown of functional connectivity in frontoparietal networks underlies behavioral deficits in spatial neglect. *Neuron* 53, 905-918.

Histed, M., Pasupathy, A., & Miller, E.K. (2009). Learning substrates in the primate prefrontal cortex and striatum: Sustained activity related to successful actions. *Neuron* 63, 244-253.

Hochberg, L., Serruya, M., Friehs, G., Mukand, J., Saleh, M., Caplan, A., Branner, A., Chen, D., Penn, R., & Donoghue, J. (2006). Neuronal ensemble control of prosthetic devices by a human with tetraplegia. *Nature* 442, 164-171.

Hofmeijer, J., Amelink, G., Algra, A., Van Gijn, J., Macleod, M., Kappelle, L., Van Der Worp, H., & HAMLET investigators. (2006). Hemicraniectomy after middle cerebral artery infarction with life-threatening edema trial (HAMLET). Protocol for a randomised controlled trial of decompressive surgery in space-occupying hemispheric infarction. *Trials* 7, 29.

Huang, A., Tu, Y., Tsai, Y., Chen, Y., Hong, W., Yang, C., Kuo, L., Su, I., Huang, S., & Huang, S. (2008). Decompressive craniectomy as the primary surgical intervention for hemorrhagic contusion. *J. Neurotrauma* 25, 1347-1354.

Jackson, J.H. (1958). A study of convulsions. In: Taylor, J., Ed., *Selected Writings of John Hughlings Jackson*. (Staples: London).

Jensen, O., & Tesche, C.D. (2002). Frontal theta activity in humans increases with memory load in a working memory task. *Eur. J. Neurosci.* 15, 1395-1399.

Johansen-Berg, H., Rushworth, M., Bogdanovic, M.D., Kischka, U., Wimalaratna, S., & Matthews, P.M. (2002). The role of ipsilateral premotor cortex in hand movement after stroke. *Proc. Natl. Acad. Sci . USA* 99, 14518-14523.

Juttler, E., Schwab, S., Schmiedek, P., Unterberg, A., Hennerici, M., Woitzik, J., Witte, S., Jenetzky, E., & Hacke, W. (2007). Decompressive surgery for the treatment of malignant infarction of the middle cerebral artery (DESTINY): A randomized, controlled trial. *Stroke* 38, 2518-2525.

Kimberg, D.Y., & Farah, M.J. (1993). A unified account of cognitive impairments following frontal lobe damage: the role of working memory in complex, organized behavior. *J. Exp. Psychol. Gen.* 122, 411-428.

Klausberger, T., Magill, P., Márton, L.F., Roberts, J.D., Cobden, P.M., Buzsáki, G., & Somogyi, P. (2003). Brain-state- and cell-type-specific firing of hippocampal interneurons in vivo. *Nature* 421, 844-848.

Koessler, L., Maillard, L., Benhadid, A., Vignal, J., Felblinger, J., Vespignani, H., & Braun, M. (2009). Automated cortical projection of EEG sensors: Anatomical correlation via the international 10–10 system. *NeuroImage* 46, 64-72.

Knight, R.T. (2007). Neural networks debunk phrenology. *Science* 316, 1578-1579.

Kolb, B. (1992). Mechanisms underlying recovery from cortical injury: Reflections on progress and directions for the future. In: Rose, F.D. & Johnson, D.A., Eds., *Recovery from Brain Damage*. (Plenum Press: New York).

Lenz, D., Jeschke, M., Schadow, J., Naue, N., Ohl, F., & Herrmann, C. (2008). Human EEG very high frequency oscillations reflect the number of matches with a template in auditory short-term memory. *Brain Res.* 1220, 81-92.

Levy, R., Friedman, H.R., Davachi, L., & Goldman-Rakic, P.S. (1997). Differential activation of the caudate nucleus in primates performing spatial and nonspatial working memory tasks. *J. Neurosci.* 17, 3870-8382.

Lewis, S., Dove, A., Robbins, T., Barker, R., & Owen, A. (2004). Striatal contributions to working memory: A functional magnetic resonance imaging study in humans. *Eur. J. Neurosci.* 19, 755-760.

Li, J., Wang, K., Zhu, S., & He, B. (2007). Effects of holes on EEG forward solutions using a realistic geometry head model. *J. Neural Eng.* 4, 197-204.

Logothetis, N.K., Pauls, J., Augath, M., Trinath, T., & Oeltermann, A. (2001). Neurophysiological investigation of the basis of the fMRI signal. *Nature* 412, 150-157.

Luck, S. J. (2005). *An Introduction to the Event-Related Potential Technique*. (Cambridge: The MIT Press).

Lytton, W.W., Williams, S.T., & Sober, S.J. (1999). Unmasking unmasked: Neural dynamics following stroke. *Prog. Brain Res.* 121, 203-218.

McGeorge, A.J. & Faull, R.L. (1989). The organization of the projection from the cerebral cortex to the striatum in the rat. *Neuroscience* 29, 503-537.

McNab, F., & Klingberg, T. (2008). Prefrontal cortex and basal ganglia control access to working memory. *Nat. Neurosci.* 11, 103-107.

Metting van Rijn A. C., Peper A., & Grimbergen C. A. (1990). High-quality recording of bioelectric events. Part 1. Interference reduction, theory and practice. *Med. Biol. Eng. Comput.* 28, 389-397.

Miller, E.K., Erickson, C.A., & Desimone, R. (1996). Neural mechanisms of visual working memory in prefrontal cortex of the macaque. *J. Neurosci.* 16, 5154-5167.

Miller, E.K., & Cohen, J.D. (2001). An integrative theory of prefrontal cortex function. *Annu. Rev. Neurosci.* 24, 167-202.

Miller, E.K., & Buschman, T.J. (2007). *The Neuroscience of Rule-Guided Behavior* (eds. Bunge, S. & Wallis, J.) 419-440 (Oxford University Press, Oxford).

Miller, K.J., denNijs, M., Shenoy, P., Miller, J.W., Rao, R.P.N., & Ojemann, J.G. (2007). Real-time functional brain mapping using electrocorticography. *NeuroImage* 37, 504-507.

Millett, D. (2001). Hans Berger: From psychic energy to the EEG. *Perspect. Biol. Med.* 44, 522-542.

Mormann, F., Fell, J., Axmacher, N., Weber, B., Lehnertz, K., Elger, C.E., & Fernández, G. (2005). Phase/amplitude reset and theta-gamma interaction in the human medial temporal lobe during a continuous word recognition memory task. *Hippocampus* 15, 890-900.

Moustafa, A.A., Sherman, S., & Frank, M. (2008). A dopaminergic basis for working memory, learning and attentional shifting in Parkinsonism. *Neuropsychologia* 46, 3144-3156.

Müller, N.G., & Knight R.T. (2006). The functional neuroanatomy of working memory: contributions of human brain lesion studies. *Neuroscience* 139, 51-58.

Mukamel, R., Gelbard, H., Arieli, A., Hasson, U., Fried, I., & Malach, R. (2005). Coupling between neuronal firing, field potentials, and FMRI in human auditory cortex. *Science* 309, 951-954.

Neuper, C., Wörtz, M., & Pfurtscheller, G. (2006). ERD/ERS patterns reflecting sensorimotor activation and deactivation. *Prog. Brain Res.* 159, 211-222.

Nudo, R.J. (2007). Postinfarct cortical plasticity and behavioral recovery. *Stroke* 38, 840-845.

Nunez P.L., & Srinivasan, R. (2005). *Electric Fields of the Brain: The Neurophysics of EEG*, 2nd Ed. (New York: Oxford University Press).

Onton, J., Delorme, A., & Makeig, S. (2005). Frontal midline EEG dynamics during working memory. *NeuroImage* 27, 341-356.

Okamoto, M., & Dan, I. (2005). Automated cortical projection of head-surface locations for transcranial functional brain mapping. *NeuroImage* 26, 18-28.

Oostenveld, R., & Oostendorp, T. (2002). Validating the boundary element method for forward and inverse EEG computations in the presence of a hole in the skull. *Hum. Brain Mapp.* 17, 179-192.

O'Reilly, R., & Frank, M.J. (2006). Making working memory work: A computational model of learning in the prefrontal cortex and basal ganglia. *Neural Comput.* 18, 283-328.

Osipova, D., Hermes, D., Jensen, O., & Rustichini, A. (2008). Gamma power is phase-locked to posterior alpha activity. *PLoS ONE* 3, 1-7.

Packard, M., & Knowlton, B. (2002). Learning and memory functions of the basal ganglia. *Annu. Rev. Neurosci.* 25, 563-593.

Pasupathy, A. & Miller, E.K. (2005). Different time courses of learning-related activity in the prefrontal cortex and striatum. *Nature* 433, 873-876.

Pfefferbaum, A. (1990). Model estimates of CSF and skull influences on scalp-recorded ERPs. *Alcohol* 7, 479-482.

Pfurtscheller, G., & Lopes da Silva, F.H. (1999). Event-related EEG/MEG synchronization and desynchronization: Basic principles. *Clin. Neurophysiol.* 110, 1842-1857.

Poldrack, R.A., Clark, J., Paré-Blagoev, E.J., Shohamy, D., Creso Moyano, J., Myers, C.E., & Gluck, M.A. (2010). Interactive memory systems in the human brain. *Nature* 414, 546-550.

Postle, B.R., Awh, E., Jonides, J., Smith, E.E., & D'Esposito, M. (2004). The where and how of attention-based rehearsal in spatial working memory. *Brain Res. Cogn. Brain Res.* 20, 194-205.

Postle, B.R. (2006). Working memory as an emergent property of the mind and brain. *Neuroscience* 139, 23-38.

Pritchard, W. S. (1992). The brain in fractal time: 1/*f*-like power spectrum scaling of the human electroencephalogram. *Int. J. Neurosci.* 66, 119-129.

Raghavachari, S., Kahana, M.J., Rizzuto, D.S., Caplan, J.B., Kirschen, M.P., Bourgeois, B., Madsen, J.R., & Lisman, J.E. (2001). Gating of human theta oscillations by a working memory task. *J. Neurosci.* 21, 3175-3183.

Rao, S.C., Rainer, G., & Miller, E.K. (1997). Integration of what and where in the primate prefrontal cortex. *Science* 276, 821-824.

Ravizza, S.M., & Ivry, R.B. (2001). Comparison of the basal ganglia and cerebellum in shifting attention. *J. Cogn. Neurosci.* 13, 285-297.

Redgrave, P., & Gurney, K. (2006). The short-latency dopamine signal: A role in discovering novel actions? *Nat. Rev. Neurosci.* 7, 967-975.

Romanski, L.M., Tian, J., Fritz, M., Mishkin, P.S., Goldman-Rakic, P.S., & Rauschecker, J.P. (1999). Dual streams of auditory afferents target multiple domains in the primate prefrontal cortex. *Nat. Neurosci.* 2, 1131-1136.

Rorden, C., & Brett, M. (2000). Stereotaxic display of brain lesions. *Behav. Neurol.* 12, 191-200.

Rorden, C., & Karnath, H.O. (2004). Using human brain lesions to infer function: A relic from a past era in the fMRI age? *Nat. Rev. Neurosci.* 5, 813-819.

Rosahl, S.K., & Knight, R.T. (1995). Role of prefrontal cortex in generation of the contingent negative variation. *Cereb. Cortex* 5, 123-134.

Sanai, N., Mirzadeh, Z., & Berger, M. (2008). Functional outcome after language mapping for glioma resection. *N. Engl. J. Med.* 358, 18-27.

Schultz, W. (2002). Getting formal with dopamine and reward. *Neuron* 36, 241-263.

Seger, C.A., & Cincotta C.M. (2006). Dynamics of frontal, striatal, and hippocampal systems during rule learning. *Cereb. Cortex* 16, 1546-1555.

Simon-Thomas, E.R., Brodsky, K., Willing, C., Sinha, R., & Knight, R.T. (2003). Distributed neural activity during object, spatial and integrated processing in humans. *Brain Res. Cogn. Brain Res.* 16, 457-467.

Smith, E., Jonides, J., Koeppe, R., & Awh, E. (1995) Spatial versus object working memory: PET investigations. *J. Cogn. Neurosci.* 7, 337-356.

Solnik, S., DeVita, P., Rider, P., Long, B., & Hortobágyi, T. (2008). Teager-Kaiser Operator improves the accuracy of EMG onset detection independent of signal-to-noise ratio. *Acta Bioeng. Biomech.* 10, 65-68.

Sowell, E.R., Peterson, B.S., Thompson, P., Welcome, S.E., Henkenius, A.L., & Toga, A. (2003). Mapping cortical change across the human life span. *Nat. Neurosci.* 6, 209-215.

Sporns, O., Tononi, G., & Kötter, R. (2005). The human connectome: A structural description of the human brain. *PLoS Comp. Biol.* 1, e42.

Stuss, D.T. & Knight, R.T. (2002). *Principles of Frontal Lobe Function* (Oxford University Press, Oxford).

Todd, J.J., & Marois, R. (2004). Capacity limit of visual short-term memory in human posterior parietal cortex. *Nature* 428, 751-754.

Tomita, H., Ohbayashi, M., Nakahara, K., Hasegawa, I., & Miyashita, Y. (1999). Top-down signal from prefrontal cortex in executive control of memory retrieval. *Nature* 401, 699-703.

Tsuchida, A., & Fellows, L.K. (2009). Lesion evidence that two distinct regions within prefrontal cortex are critical for n-back performance in humans. *J. Cogn. Neurosci.* 21, 2263-2275.

Ungerleider, L.G., & Haxby, J.V. (1994). 'What' and 'where' in the human brain. *Curr. Opin. Neurobiol.* 4, 157-165.

Vahedi, K., Vicaut, E., Mateo, J., Kurtz, A., Orabi, M., Guichard, J., Boutron, C., Couvreur, G., Rouanet, F., Touze, E., Guillon, B., Carpentier, A., Yelnik, A., George, B., Payen, D., & Bousser, M. (2007). Sequential-design, multicenter, randomized, controlled trial of early decompressive craniectomy in malignant middle cerebral artery infarction (DECIMAL Trial). *Stroke* 38, 2506-2517.

Van Vleet, T.M., Heldt, S.A., Pyter, B., Corwin, J.V., & Reep, R.L. (2003). Effects of light deprivation on recovery from neglect and extinction induced by unilateral lesions of the medial agranular cortex and dorsocentral striatum. *Behav. Brain Res.* 138, 165-178.

von Monakow C. (1969). Die lokalisation im grosshirn und der abbau der funktion durch kortikale herde. In: Pribram, K. H. Ed., *Mood, States and Mind.* (Penguin Books: London).

von Stein, A., & Sarnthein, J. (2000). Different frequencies for different scales of cortical integration: From local gamma to long range alpha/theta synchronization. *Int. J. Psychophysiol.* 38, 301-313.

Vogel, E.K., & Machizawa, M.G. (2004). Neural activity predicts individual differences in visual working memory capacity. *Nature* 428, 748-751.

Vogel, E.K., McCollough, A.W., & Machizawa, M.G. (2005). Neural measures reveal individual differences in controlling access to working memory. *Nature* 438, 500-503.

Ward, N.S., Newton, J.M., Swayne, O.B., Lee, L., Frackowiak, R.S., Thompson, A.J., Greenwood, R.J., & Rothwell, J.C. (2007). The relationship between brain activity and peak grip force is modulated by corticospinal system integrity after subcortical stroke. *Eur. J. Neurosci.* 25, 1865-1873.

Whitham, E., Lewis, T., Pope, K., Fitzgibbon, S., Clark, C., Loveless, S., DeLosAngeles, D., Wallace, A., Broberg, M., & Willoughby, J. (2008). Thinking activates EMG in scalp electrical recordings. *Clin. Neurophysiol.* 119, 1166-1175.

Williams, D., & Parsons-Smith, G. (1950). Cortical rhythms not seen in the electroencephalogram. *Brain* 73, 191-202.

Williams, Z., & Eskandar, E. (2006). Selective enhancement of associative learning by microstimulation of the anterior caudate. *Nat. Neurosci.* 9, 562-568.

Wilson FA, Scalaidhe SP, Goldman-Rakic PS (1993) Dissociations of object and spatial processing domain in primate prefrontal cortex. Science 25: 1955-1958.

Wolpaw, J., & McFarland, D.J. (2004). Control of a two-dimensional movement signal by a noninvasive brain-computer interface in humans. *Proc. Natl. Acad. Sci. USA* 101, 17849-17854.

Wundt, W. (1902). *Outlines of Psychology, 2nd Ed.* (Engelmann: Leipzig).

Yago, E., Duarte, A., Wong, T., Barceló, F., & Knight, R.T. (2004). Temporal kinetics of prefrontal modulation of the extrastriate cortex during visual attention. *Cogn. Affect. Behav. Neurosci.* 4, 609-617.

Yang, X., Wen, L., Li, G., Zhan, R., Ma, L., & Liu, W. (2009). Contralateral subdural effusion secondary to decompressive craniectomy performed in patients with severe traumatic brain injury: Incidence, clinical presentations, treatment and outcome. *Med. Princ. Pract.* 18, 16-20.

Yehene, E., Meiran, N., & Soroker, N. (2008). Basal ganglia play a unique role in task switching within the frontal-subcortical circuits: evidence from patients with focal lesions. *J. Cogn. Neurosci.* 20, 1079-1093.

Yeterian, E.H., & Pandya, D.N. (1991). Prefrontostriatal connections in relation to cortical architectonic organization in rhesus monkeys. *J. Comp. Neurol.* 312, 43-67.

Yoshinaga, H., Kobayashi, K., Hoshida, T., Kinugasa, K., & Ohtuska, Y. (2008). Magnetoencephalogram in a postoperative case with a large skull defect. *Pediatr. Neurol.* 39, 48-51.

Yuval-Greenberg, S., Tomer, O., Keren, A.S., Nelken, I., & Deouell, L.Y. (2008). Transient induced gamma-band response in EEG as a manifestation of miniature saccades. *Neuron* 58, 429-441.